



YEDITEPE UNIVERSITY
GRADUATE INSTITUTE OF SOCIAL SCIENCES

**Development of New Forecasting Strategies using Wavelet Transform (WT),
Multiple Wavelet Coherence (MWC) and Multi-Fractal De-Trended Fluctuation
Analysis (MFDFA)**

by
Emrah ORAL

Supervisor
Prof. Dr. Gazanfer UNAL

Submitted to the Graduate Institute of Social Sciences
In partial fulfillment of the requirements for the degree of PhD in Economics
(Financial Economics)


YEDITEPE UNIVERSITY
ISTANBUL, 2018

Approval of the Institute of Social Sciences



Prof. Dr. M. Fazıl GÜLER
Director

I certify that this thesis satisfies all the requirements as a thesis for the degree of Doctor Philosophy (PhD).



Prof. Dr. Veysel Ulusoy
Head of Department

This is to certify that we have read this thesis and that in our opinion it is fully adequate, in scope and quality, as a thesis for the degree of Doctor Philosophy (PhD).



Prof. Dr. Gazanfer Ünal
Supervisor

Examining Committee Members

Prof. Dr. Gazanfer Ünal (Bahçeşehir University)



Prof. Dr. Ömer Yaman Erzurumlu (Bahçeşehir University)



Prof. Dr. Rifat Kamaşak (Bahçeşehir University)



Prof. Dr. Ahmet Özçam (Yeditepe University)



Doç. Dr. Sema Dube (Yeditepe University)

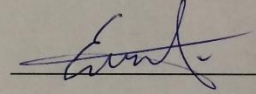


PLAGIARISM

I hereby declare that all information in this document has been obtained and presented in accordance with academic rules and ethical conduct. I also declare that, as required by these rules and conduct, I have fully cited and referenced all material and results that are not original to this work.

23/01/2019

Emrah ORAL

A handwritten signature in blue ink, appearing to read 'Emrah', is written over a horizontal line.

ABSTRACT

Modeling and forecasting has increasingly become very important in analysis of trends in financial markets, particularly in high frequency trades. It is difficult to predict the price return, i.e. profit or loss, due to many unknown variables including social and political unrest, catastrophic events, etc. Hence it can be said that these time series have different characteristics of movement, so called fluctuations. Wavelet analysis, multiple wavelet coherence analysis and especially scale by scale wavelet transform are powerful tools to investigate the series possessing different frequency levels. Multi fractal de-trended fluctuation analysis also reveals the different frequency levels of characteristics. It is realized that there is no generalized forecasting strategy available using these methods together. That is why, as part of this study, a new strategy will be proposed through application on real life data sets to detect highly correlated time series and forecast using vector autoregressive moving average and vector autoregressive fractionally integrated moving average methods in order to compare with real data and quantify the efficiency of forecasting. The thesis is composed of four independent sections. The first section covers a forecasting method using three dimensional multiple wavelet coherence and scale by scale wavelet transformation of precious metals. The second section covers the similar method with western and eastern markets but employs a four dimensional multiple wavelet coherence. The third section covers three dimensional multiple wavelet coherence and its multifractal de-trended fluctuation analysis at the specific scale. The third section utilizes two dimensional wavelet coherence and multifractal de-trended fluctuation analysis of the raw data for a specific determined scale.

ÖZET

Modelleme ve ileri dönük fiyat tahminlerinde finansal marketlerde ki, özellikle yüksek frekanslı al/sat işlemlerinde, eğilimlerin analizinin yapılması artarak daha önemli hale gelmiştir. Fiyatlamaların karla mı yoksa zararla mı sonuçlanacağını tahmin etmek sosyal ve politik çalkantılar, felaketle sonuçlanan olaylar gibi bilinmeyen değişkenler yüzünden çok zordur. Bu yüzden bu ve bunun gibi zaman serileri dalgalanmalar dediğimiz farklı karakteristik hareketlere sahiptirler. Farklı frekans seviyeleri taşıyan zaman serilerini incelemek için wavelet (dalgacık) analizleri, çoklu wavelet uyumluluk analizleri ve özellikle ölçek-ölçek wavelet transformasyonu güçlü araçlardır. Çoklu fraktal meyilden arındırılmış dalgalanma analizleri de farklı frekans seviyelerinde karakteristik özellikleri ortaya çıkarır. Bu iki metodu birlikte kullanan bir genel stratejinin çalışılmadığı fark edildiği için bu çalışmanın bir parçası olarak yeni bir strateji önerilecektir. Bu metot gerçek veri setleri üzerinde yüksek korelasyonlu zaman serileri tespit edilerek uygulanacak ve vektörel özbağlanımlı hareketli ortalama ve vektörel özbağlanımlı fraksiyonlu bütünleşmiş hareketli ortalama yöntemleri ile ileriye dönük fiyat tahminleri gerçek veri ile karşılaştırılarak ve fiyat tahmini verimliliği ölçülerek yapılacaktır. Bu çalışma dört bağımsız bölümden oluşmaktadır. Birinci bölümde değerli metallerin üç boyutlu çoklu dalgacık korelasyonu ve ölçek-ölçek dalgacık dönüşümü belli bir ölçekte kullanılarak ileriye dönük fiyat tahmin yöntemi geliştirilmiştir. İkinci bölümde aynı metot batı ve doğu pazarları için dört boyutlu olarak geliştirilmiştir. Üçüncü kısım üç boyutlu dalgacık korelasyonu ve çoklu fraktal meyilden arındırılmış dalgalanma analizleri belirlenmiş bir ölçek için kullanılmıştır. Son bölüm iki boyutlu dalgacık analizini ve çoklu fraktal meyilden arındırılmış dalgalanma analizini ana veri üzerinde kullanarak sonuçlandırılmıştır.

ACKNOWLEDGEMENTS

First of all, I would like to express my deepest gratitude to my supervisor Prof. Dr. Gazanfer Unal for sharing his endless enthusiasm for financial economics as well as research and for his inestimable support and guidance since the first day of my studies.

I also would like to thank my lecturers for their encouraging comments.

I would like to thank my friends, Tunc Oygur and Alper Kirik for their patience during our study hours, support and great friendship.

I also would like to thank my wife and my family for their understanding and support until the last moment of this work, without whom I would be lost.

TABLE OF CONTENTS

List of Symbols	ix
List of Abbreviations	x
List of Tables	xi
List of Figures	xii
1. Co-Movement of Precious Metals and Forecasting using scale by scale wavelet transform	1
1.1. Introduction	2
1.2. Data and Methodology	5
1.2.1. Data	5
1.2.2. Methodology	6
1.2.2.1. Continuous Wavelet Transform and Inverse CWT	6
1.2.2.2. Three Dimensional Multiple Wavelet Coherence	8
1.2.2.3. Vector Autoregressive Moving Average (VARMA)	9
1.3. Wavelet Analysis	11
1.3.1. Wavelet Coherence	11
1.3.2. Three Dimensional Multiple Wavelet Coherence	14
1.4. Forecasting Results	16
1.5. Conclusion	21
Appendix A. Forecasting Performance of Each Data for 3 Different Time Intervals	23
2. Dynamic Correlation of Eastern and Western Markets and Forecasting: Scale by Scale Wavelet Based Approach	26
2.1. Introduction	27
2.2. Empirical Study	30
2.2.1. Empirical Data	30
2.2.2. Methodology	32
2.2.2.1. A Summary For Continuous Wavelet Transform	32
2.2.2.2. Four Dimensional Multiple Wavelet Coherence	33
2.2.2.3. Vector Autoregressive Moving Average in 4D (VARMA)	35
2.3. Multiple Wavelet Coherence Analysis in 4D	37

2.4. Forecasting Trials, Results and Discussion	41
2.5. Conclusion	46
Appendix A. Inversed Data of Markets and Corresponding Forecasts for the Next 30 Days	48
3. Modeling and Forecasting Multifractal Wavelet Scale: Western Market Vs Eastern Market	54
3.1. Introduction and Literature Review	55
3.2. Data	58
3.3. Methodology	60
3.3.1. Continuous Wavelet Transform (CWT) and Multiple Wavelet Coherence (MWC)	60
3.3.2. Multifractal De-Trended Fluctuation Analysis (MF-DFA)	61
3.3.3. Vector Autoregressive Fractionally Integrated Moving Average (VARFIMA)	63
3.4. Empirical Analysis	65
3.5. Forecasting Results	72
3.6. Discussion and Conclusion	75
Appendix A. Multiple Wavelet Coherence of Real Data and Inversed Data of Each Market with Western Markets	77
Appendix B. Inversed Data and Corresponding Local Hurst Exponents	79
Appendix C. Forecasting Results	82
4. Modeling and Forecasting Time Series of Precious Metals: A New Approach to Multifractal Data	90
4.1. Introduction	91
4.2. Empirical Framework	94
4.2.1. Data	94
4.2.2. Methodology	97
4.2.2.1. Summary for Continuous Wavelet Transform and Multiple Wavelet Coherence	95
4.2.2.2. Multifractal De-Trended Fluctuation Analysis (MF-DFA) ...	98
4.2.2.3. Vector Autoregressive Fractionally Integrated Moving Average (VARFIMA)	100

4.3. Wavelet Coherence and Local Hurst Exponents	102
4.4. Forecasting Results and Analysis	109
4.5. Concluding Remarks	112
Appendix A. Forecasting Results	115
Appendix B. Hurst Exponents for Real and Scale 256 Data	123
Appendix C. Local Hurst Exponents	125
References	126



LIST OF SYMBOLS

C	Complex coherence
Σ	Covariance matrix
I_n	Identity matrix with n by n dimensions
L	Lag operator
H_{loc}	Local Hurst exponent
M	Matrix of all smoothed cross-wavelet spectra
ψ	Mother wavelet transforming function
$p_v^n(i)$	n^{th} order fitting polynomial in the segment order, v
$F_q(s)$	q^{th} order fluctuation function
S_{ij}	Smoothed cross-wavelet spectra
$R_{1(q)}^2$	Square multiple wavelet coherency
$g(z)$	Transfer function
$\varepsilon(t)$	White noise

LIST OF ABBREVIATIONS

AR	Autoregressive
ARFIMA	Autoregressive Fractionally Integrated Moving Average
ARIMA	Autoregressive Integrated Moving Average
ARMA	Autoregressive Moving Average
CWT	Continuous Wavelet Transform
DWT	Discrete Wavelet Transform
H	Hurst Exponent
MA	Moving Average
MLE	Maximum Likelihood Estimation
MF-DFA	Multifractal De-Trended Fluctuation Analysis
VARMA	Vector Autoregressive Moving Average
VARFIMA	Vector Autoregressive Fractionally Integrated Moving Average

LIST OF TABLES

1.1 Statistics of Silver, Gold and Platinum	5
1.2 Correlation of Silver, Gold and Platinum	6
1.3 Correlation of metals within the extracted time series	18
2.1 Statistics of the markets	31
2.2 Correlation of the markets.....	32
2.3 Correlation of inversed daily data of all markets	41
3.1 Correlation values of each market	59
3.2 Correlation Values of Extracted Indexes (Octave 8)	68
3.3 Hurst Exponent of Real and Inversed (Scale 256) Time Series	69
3.4 Minimum and Maximum Local Hurst Exponents at Scale 256	70
3.5 Dates used to forecast market prices	72
4.1 Daily Data of Precious Metals from July 2011 to November 2016	95
4.2 Correlation of gold, silver and platinum	96
4.3 Hurst Exponent of Real and Fluctuation function at scale 256	105
4.4 Minimum and Maximum Values of Local Hurst exponents at scale 256	106
4.5 Dates and couples used to forecast precious metals	110

LIST OF FIGURES

1.1	Prices of Gold, Silver and Platinum from July 2011 to June 2015	5
1.2	Wavelet coherence of Silver and Gold	12
1.3	Wavelet coherence of platinum and silver	13
1.4	Wavelet coherence of platinum and gold	13
1.5	Multiple wavelet coherence of silver with gold and platinum	15
1.6	Multiple wavelet coherence of gold with silver and platinum	15
1.7	Multiple wavelet coherence of platinum with gold and silver	15
1.8	Inversed data of time series 1 starting from October 20 th , 2012 for 222 days ...	17
1.9	Inversed data of time series 2 starting from August 3 rd , 2012 for 601 days	18
1.10	Inversed data of time series 3 starting from March 23 rd , 2013 for 360 days	18
1.11	Forecasting performance of gold data from 3 different time series. ARMA forecast, VARMA forecast, ARMA upper/lower bands, VARMA upper/lower bands, real gold data is shown for the next 30 days	20
1.12	Forecasting performance of silver data from 3 different time series. ARMA forecast, VARMA forecast, ARMA upper/lower bands, VARMA upper/lower bands, real silver data is shown for the next 30 days	23
1.13	Forecasting performance of platinum data from 3 different time series. ARMA forecast, VARMA forecast, ARMA upper/lower Bands, VARMA upper/lower bands, real platinum data is shown for the next 30 days	24
2.1	Western market indexes	30
2.2	Eastern market indexes	30
2.3	Multiple wavelet coherence of Nikkei with SP500, FTSE and DAX	38
2.4	Multiple wavelet coherence of Taiex with SP500, FTSE and DAX	39

2.5	Multiple wavelet coherence of Kospi with SP500, FTSE and DAX	39
2.6	Inversed Daily Data of All Markets at Octave Value of 8	40
2.7	Inversed data of markets starting from September 29 th , 2012 for 207 days and forecast of Nikkei for the next 30 days	44
2.8	Inversed data of markets starting from March 22 nd , 2012 for 331 days and forecast of Nikkei for the next 30 days	45
2.9	Inversed data of markets starting from June 12 th , 2010 for 297 days and forecast of Nikkei for the next 30 days	46
2.10	Inversed data of markets starting from March 22 nd , 2012 for 316 days and forecast of Taiex for the next 30 days	48
2.11	Inversed data of markets starting from May 13 th , 2010 for 333 days and forecast of Taiex for the next 30 days	49
2.12	Inversed data of markets starting from September 20 th , 2010 for 413 days and forecast of Taiex for the next 30 days	50
2.13	Inversed data of markets starting from November 9 th , 2010 for 289 days and forecast of Kospi for the next 30 days	51
2.14	Inversed data of markets starting from June 21 st , 2012 for 318 days and forecast of Kospi for the next 30 days	52
2.15	Inversed data of markets starting from July 7 th , 2011 for 295 days and forecast of Kospi for the next 30 days	53
3.1	Real values of each stock market	59
3.2	Multiple wavelet coherence of Nikkei with SP500, FTSE and DAX	66
3.3	Extracted values of indexes (scale 256)	67

3.4 Wavelet coherence of inversed time series between Nikkei and each western market at Scale 256	68
3.5 Nikkei Inverse Data (A-top) and Corresponding Local Hurst Exponents at Scale 256 (B-bottom)	70
3.6 The time series used to calculate local Hurst Exponents at scale 256	71
3.7 Nikkei with FTSE Forecasting Results for the next 30-days data taken from December 24, 2010 for 706 days	73
3.8 Taiex with DAX Forecasting Results for the next 30-days data taken from November 14, 2009 for 1001 days	74
3.9 Kospi with SP500 Forecasting Results for the next 30-days data taken from November 19, 2011 for 478 days	74
3.10 Multiple wavelet coherence of Taiex with SP500, FTSE and DAX	77
3.11 Wavelet coherence of inversed time series between Taiex and each western markets at Scale 256	77
3.12 Multiple wavelet coherence of Kospi with SP500, FTSE and DAX	78
3.13 Wavelet coherence of inversed time series between Kospi and each western markets at Scale 256	78
3.14 Taiex Inverse Data and Corresponding Local Hurst Exponents at Scale 256 ..	79
3.15 Kospi Inverse Data and Corresponding Local Hurst Exponents at Scale 256 ..	79
3.16 SP500 Inverse Data and Corresponding Local Hurst Exponents at Scale 256 ..	80
3.17 FTSE Inverse Data and Corresponding Local Hurst Exponents at Scale 256 ..	80
3.18 DAX Inverse Data and Corresponding Local Hurst Exponents at Scale 256 ..	81
3.19 Nikkei with SP500 Forecasting Results for the next 30-days data taken from December 19, 2009 for 1275 days	82

3.20 Nikkei with SP500 Forecasting Results for the next 30-days data taken from December 24, 2010 for 215 days	82
3.21 Nikkei with FTSE Forecasting Results for the next 30-days data taken from December 24, 2010 for 199 days	83
3.22 Nikkei with DAX Forecasting Results for the next 30-days data taken from November 19, 2009 for 999 days	83
3.23 Nikkei with DAX Forecasting Results for the next 30-days data taken from November 19, 2009 for 1199 days	84
3.24 Taiex with SP500 Forecasting Results for the next 30-days data taken from March 29, 2010 for 385 days	84
3.25 Taiex with SP500 Forecasting Results for the next 30-days data taken from December 19, 2009 for 803 days	85
3.26 Taiex with FTSE Forecasting Results for the next 30-days data taken from March 29, 2010 for 372 days	85
3.27 Taiex with FTSE Forecasting Results for the next 30-days data taken from December 19, 2009 for 772 days	86
3.28 Taiex with DAX Forecasting Results for the next 30-days data taken from November 14, 2009 for 501 days	86
3.29 Kospi with SP500 Forecasting Results for the next 30-days data taken from October 15, 2010 for 776 days	87
3.30 Kospi with FTSE Forecasting Results for the next 30-days data taken from July 07, 2010 for 576 days	87
3.31 Kospi with FTSE Forecasting Results for the next 30-days data taken from March 29, 2010 for 776 days	88

3.32 Kospi with DAX Forecasting Results for the next 30-days data taken from December 19, 2009 for 1176 days	88
3.33 Kospi with DAX Forecasting Results for the next 30-days data taken from December 19, 2009 for 875 days	89
4.1 The daily prices of gold, silver and platinum starting from July, 2011 to November, 2016	95
4.2 Multiple wavelet coherence of gold with silver and platinum	103
4.3 Multiple wavelet coherence of silver with gold and platinum	104
4.4 Multiple wavelet coherence of platinum with gold and silver	105
4.5 Gold Local Hurst Exponents at Scale 256-day period	107
4.6 Silver local Hurst exponents at Scale 256-day period	107
4.7 Platinum local Hurst exponents at scale 256-day period	108
4.8 Fraction function at scale 256	109
4.9 Gold and platinum data at Scale 256 from February 25 th , 2011 to January 11 th , 2012	111
4.10 Forecasting for gold with platinum starting from January 11, 2012 for the next 30 days	111
4.11 Forecasting for platinum with gold starting from January 11, 2012 for the next 30 days	112
4.12 Gold and platinum data at Scale 256 from December 19 th , 2011 to April 18 th , 2012	115
4.13 Forecasting for gold with platinum starting from April 18 th , 2012 for the next 30 days	115

4.14 Forecasting for platinum with gold starting from April 18 th , 2012 for the next 30 days	116
4.15 Gold and silver data at Scale 256 from 25 th February 2011 to January 6 th , 2012	116
4.16 Forecasting for gold with silver starting from January 6 th , 2012 for the next 30 days	117
4.17 Forecasting for silver with gold starting from January 6 th , 2012 for the next 30 days	117
4.18 Gold and silver data at Scale 256 from March 6 th , 2010 to May 18 th , 2012	118
4.19 Forecasting for gold with silver starting from May 18 th , 2012 for the next 30 days	118
4.20 Forecasting for silver with gold starting from May 18 th , 2012 for the next 30 days	119
4.21 Silver and platinum data at Scale 256 from April 19 th , 2010 to July 21 st , 2012	119
4.22 Forecasting for silver with platinum starting from July 21 st , 2012 for the next 30 days	120
4.23 Forecasting for platinum with silver starting from July 21 st , 2012 for the next 30 days	120
4.24 Silver and platinum data at Scale 256 from February 25 th , 2011 to January 11 th , 2012	121
4.25 Forecasting for silver with platinum starting from January 11 th , 2012 for the next 30 days	121
4.26 Forecasting for platinum with silver starting from January 11 th , 2012 for the next 30 days	122

4.27 Log-log plot of platinum real data ($H=1.4714$)	123
4.28 Log-log plot of platinum data at scale 256 ($H=1.3237$)	123
4.29 Log-log plot of silver real data ($H=1.4927$)	123
4.30 Log-log plot of silver data at scale 256 ($H=1.4515$)	124
4.31 Silver local Hurst exponents at Scale 256-day period	125
4.32 Platinum local Hurst exponents at scale 256-day period	125



CHAPTER 1

CO-MOVEMENT OF PREVIOUS METALS AND FORECASTING USING SCALE BY SCALE WAVELET TRANSFORM

Summary

In this chapter, a new approach is proposed to improve forecasting performances. We analyze the co-movement of precious metals (daily data of gold, silver and platinum starting from July, 2011) using multiple wavelet coherence and determine the movement dependencies on frequency–time space. The data is split into frequencies using scale by scale continuous wavelet transform. All three time-series retaining the same frequency scale are (i) selected, (ii) inversed and (iii) forecasted using multivariate model, Vector Auto Regressive Moving Average (VARMA). We conclude that the efficiency of VARMA forecasting is substantially increased because of same frequency highly correlated time series obtained by using scale by scale wavelet transform. Moreover, the direction of price shift (increasing/decreasing trend) is prospected to an adequately distinguishable degree.

1.1. Introduction

Economic time series are composed of different agents operating with different objectives over different terms. Therefore, it progresses on various frequencies. Investigating financial time series is one of the primary concerns of financial engineering. Nonetheless, all of the engineering, investigation and examination in financial world eventually boil down to one common goal, predicting the price on the next day. That is why scrutinizing time series has always been of high importance and numerous methods are developed and available in the literature such as Doan, T., Littermann, R. and Sims, C. (1984), Litterman, R. B. (1985), Stock, J. H. and Watson, M. W. (1999), Stock, J. H. and Watson, M. W. (2002), Lutkepohl, H (2004), De Mol, C., Giannone, D. and Reichlin, L. (2006), Athanasopoulos, G. and Vahid, F. (2008), Carriero, A., Kapetanios, G. and Marcellino, M. (2008), Kahraman and Unal (2012), Barunik, J, E Kocenda and L Vacha (2013), Simionescu, M (2013), Kahraman and Unal (2016).

Fourier transform is one of the methods to understand the time series with different frequencies. Unfortunately, since Fourier Transform losses the time information, it cannot be used with non-stationary financial data to analyze time and frequency of the financial time series simultaneously. Hence, other methods have been developed. Using wavelet analysis has become a common tool to analyze the time series. Wavelet transforms expand time series into time-frequency space and can therefore find localized intermittent periodicities, eliminating the weaknesses in Fourier transform (Gulerce and Unal, 2015). This method has started to find place in economic and financial applications in recent years.

Torrence and Compo (1998), and Grinsted et al. (2004) provided a software package for cross-wavelet transform and wavelet coherence analysis in order to

effectively and efficiently examine common and coherent signals in multiple time series. Partial wavelet coherence and multiple wavelet coherence have wide applications in studies of geophysical systems and marine studies. We will utilize the similar methods to analyze the coherence of commodity price of precious metals; gold, silver and platinum. According to Ng, E. K., & Chan, J. C. (2012), partial wavelet coherence helps identify the resulting wavelet transform coherence (WTC) between two time-series after eliminating the influence of their common dependence. Multiple wavelet coherence will show the effect of two factors together on the commodity itself which is the fundamental difference from multiple correlations.

The wavelet transform will be utilized to extract the specific time-frequency data out of highly-correlated period, which is determined by the outcome of the multiple wavelet coherence analysis. As Yilmaz and Unal (2016) stated, analysis of wavelet coherence allows observing many exciting interrelationships in time–frequency space in a much detailed way than other methods. Once this relation is well discovered, it may be used to model the data for forecasting purposes and it is the assumption that this will enhance the performance of modeling as well as forecasting to a new level of accuracy.

Forecasting time series of financial assets is a trait of financial engineering and very important for many investors and speculators all around the world. One important asset in the world market is gold as well as other precious metals; silver and platinum. These precious metals have very high heteroskedastic, nonlinear as well as unit root behavior just like any other financial assets. These characteristics make it very challenging to forecast the future of these metal prices.

As a result of different efforts to improve the forecasting performance, multivariate models have been offered instead of univariate models. The vector

ARMA model is employed for forecasting the correlated (interrelated) time series and for investigating the dynamic impact of random disturbances on the system of variables. The VARMA is a dynamic system of equations that examine the impacts of fluctuations (shocks) or correlations (interactions) between financial variables.

VARMA is proposed to improve the forecasting results with higher precision by using more information through a combination of multiple highly correlated data. Multivariate ARMA models were first introduced by Quenouille in 1957 and then improved later on after the successful application of univariate models by Box-Jenkins in 1970s. Later on it has been improved by Dunsmuir & Hannan (1976), Hannan (1981), and Akaike (1988). One of the main problems with multivariate ARMA models is that they perform better with small numbers of variables. As the number of the variables increase, it creates a problem called dimension effect. Penalty function and factor models are two methods suggested overcoming the problem where VARMA models do possess these properties. It is shown that VARMA models do give better fit results because of having low mean squared errors compared to univariate models hence resulting in good forecasting performances.

Section 2 contains the data and methodology used in this chapter. Basics of continuous wavelet transform, multiple wavelet coherence and VARMA are introduced as a summary review. In section 3, we analyze the commodity prices of precious metals; gold, silver and platinum, using wavelet transform as well as multiple wavelet coherence and understand their movement dependencies on time-frequency space. After their co-movement period is determined for different time intervals, the data is split into pieces of corresponding frequency and time domain by using continuous wavelet transform. The same frequency domain of each series is extracted and inversed. Then, we use VARMA model to forecast. In section 4, the

forecast results are analyzed and compared with respect to the univariate ARMA model. In section 5, the chapter is concluded with the discussion of results. In Appendix, the forecasting results for silver and platinum are presented.

1.2. Data & Methodology

1.2.1. Data

The commodity prices of silver, gold and platinum are taken from Yahoo Finances! starting from July 2011 to June 2015 which is composed of approximately 1400 daily data. The price values are plotted in figure 1.

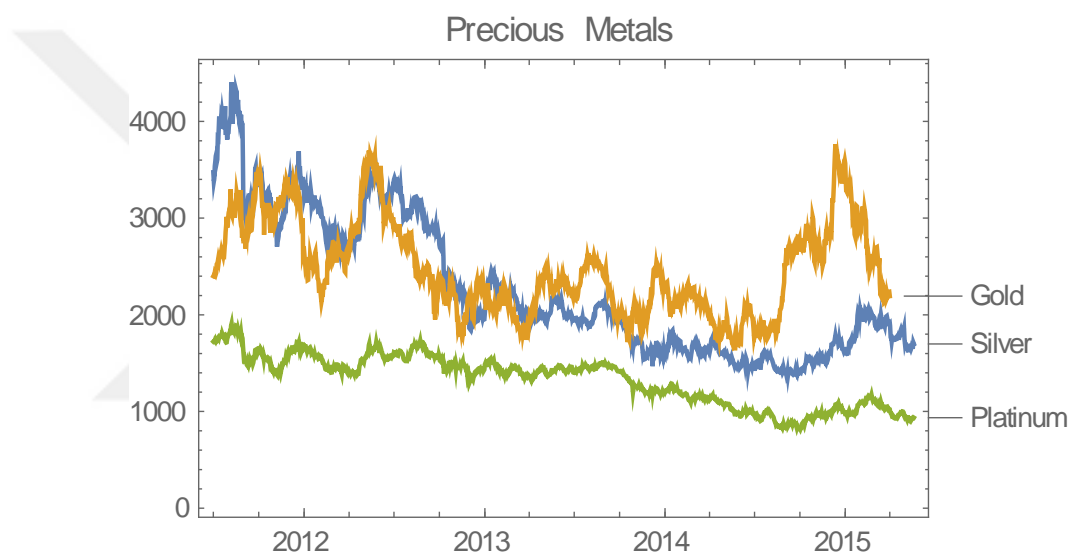


Figure 1.1. *Prices of Gold, Silver and Platinum from July 2011 to June 2015*

The statistical analysis of the data in Table 1 shows that platinum is the one with the lowest standard deviation throughout the time period. Silver prices display high fluctuation with respect to other two metals with a considered value of volatility. The corresponding correlation data of the metals can be found below in Table 2. Gold displays higher correlation with silver with respect to its relationship with platinum. However, the correlation between silver and platinum is the highest at 85%.

Table 1.1

Statistics of silver, gold and platinum

	Mean	Median	Std. Dev.	Skewness	Kurtosis
Silver	2272.43	1992.74	723.334	0.7720	2.4518
Gold	2478.67	2384.68	482.096	0.5140	2.4090
Platinum	1327.16	1410.00	260.958	-0.2204	1.9512

Table 1.2.

Correlation of silver, gold and platinum

	Silver	Gold	Platinum
Silver	1		
Gold	0.6409	1	
Platinum	0.8514	0.3979	1

In light of this section, we will reveal the relationship between these metals and find out the leading price and the nature of their co-movement through analysis of wavelet coherence. Then we will utilize wavelet transform to see if a certain specific range of frequency in the data within the high correlation period would help enhance the performance of forecasting.

1.2.2. Methodology

1.2.2.1. Continuous wavelet transform and inverse CWT.

An excellent introduction of wavelet and application into the economics and finance has been provided by Gencay (2002). Many other applications afterwards may be found in Fay (2009), Aguiar-Conraria and Soares (2011), Gellegati (2011), Barunik, Kocenda and Vacha (2013) and Aguiar-Conraria and Soares (2014). The wavelet transform uses a localized function with finite support of decomposition – a wavelet. Discrete and continuous wavelet transforms are two fundamental transforms out of many different transform methods. As stated by Grinsted, A., Moore, J. C., & Jevrejeva, S. (2004), continuous wavelet transform (CWT) is mainly preferred for

feature extraction purposes. Hence, we use CWT to extract the frequency-time information. Given a time series, continuous wavelet transform is defined as (1)

$$CWT_x^\psi(s, \tau) = \langle X, \rightarrow \psi(s, \tau) \rangle = \frac{1}{\sqrt{s}} \int_{-\infty}^{+\infty} X(t) \psi^* \left(\frac{t-\tau}{s} \right) dt \quad (1)$$

Where " τ " and " s " are the translation and the scale parameters, respectively. " ψ " is the mother wavelet and it is the transforming function. The term translation corresponds with the time information in the transform domain and scale parameter is the frequency of the information. The scale parameter is similar to the scale used in maps. High scales means a global view whereas low scales mean a more specific and detailed view. Therefore, wavelet transform provides information on time and frequency domain by mapping the time series into τ and s parameters. But one must note that scale and frequency have inverse relationship. As the scale decreases (increases), the frequency increases (decreases). As a result, the periodical span of the time information decreases (increases) as well.

Since the wavelet transform is decomposing a time series into different energy levels, the inverse of the transform must satisfy the law of conservation of energy.

Hence it must satisfy equation (2),

$$\int_{-\infty}^{+\infty} |x(t)|^2 dt = \frac{1}{c_\psi} \int_{-\infty}^{+\infty} \int_{-\infty}^{+\infty} |W_x(\tau, s)|^2 \frac{d\tau ds}{s^2} \quad (2)$$

In turn, it makes it possible to reconstruct the time series data by the formula (3),

$$x(t) = \frac{2}{c_\psi} \int_{-\infty}^{+\infty} \left[\int_{-\infty}^{+\infty} W_x(\tau, s) \psi_{\tau, s}(t) d\tau \right] \frac{ds}{s^2} \quad (3)$$

In the continuous wavelet transform, the scaling parameter s is given by equal-tempered scale calculated by the equality in (4),

$$s_{oct, voc} = \alpha 2^{oct-1} 2^{voc/nvoc} \quad (4)$$

Where “oct” is the octave number, “voc” the voice number, and “ α ” the smallest wavelet scale. The octaves are used as a conversion factor of scales, and consequently the frequencies. Hence, from the figures, we may point out the same frequency interval for each time series and inverse the data with the same frequency value as desired.

1.2.2.2. Three dimensional multiple wavelet coherence.

Multiple wavelet coherence is an extension of bivariate case of wavelet coherence. When calculation of coherency and phase differences are concerned, the correlation of the interesting variable X_1 and X_2 with other variables is taken into account. The squared multiple wavelet coherency between X_1 and all other series X_2, \dots, X_p is defined as (5)

$$R_{1(23\dots p)}^2 = R_{1(q)}^2 = 1 - \frac{M^d}{S_{11}M_{11}^d} \quad (5)$$

Where M is the $p \times p$ matrix of all smoothed cross-wavelet spectra (denoted by S_{ij})

$$S_{ij} = S(W_{X_i X_j}) \left(S_{ij} = S_{ij}^*, S_{ij} = S(|W_{X_i}|^2) \right)$$

$$M = \begin{bmatrix} S_{11} & S_{12} & \dots & S_{1p} \\ S_{21} & S_{22} & \dots & S_{2p} \\ \vdots & \vdots & \ddots & \vdots \\ S_{p1} & S_{p2} & \dots & S_{pp} \end{bmatrix} \quad (6)$$

Complex coherence denoted by C is the $p \times p$ matrix of all smoothed complex wavelet coherencies as shown in equation (7),

$$\rho_{ij} = \frac{S(W_{ij})}{\sqrt{S(|W_i|^2)S(|W_j|^2)}} \text{ and } \rho_{ij} = \rho_{ji}^*$$

$$C = \begin{bmatrix} 1 & \rho_{12} & \dots & \rho_{1p} \\ \rho_{21} & 1 & \dots & \rho_{2p} \\ \vdots & \vdots & \ddots & \vdots \\ \rho_{p1} & \rho_{p2} & \dots & 1 \end{bmatrix} \quad (7)$$

$$R_{1(q)}^2 = 1 - \frac{C^d}{C_{11}^d}$$

In our case of three time series, the cofactor of the complex coherence matrix is equal to (8) and the squared multiple wavelet coherencies become (9)

$$C_{11}^d = \begin{vmatrix} 1 & \rho_{23} \\ \rho_{32} & 1 \end{vmatrix} = 1 - \rho_{23}\rho_{32} = 1 - R_{23}^2$$

$$C^d = 1 - R_{23}^2 - R_{12}^2 - R_{13}^2 + \rho_{12}\rho_{23}\rho_{31} + \rho_{13}\rho_{21}\rho_{32}$$

$$C^d = 1 - R_{23}^2 - R_{12}^2 - R_{13}^2 + 2R(\rho_{12}\rho_{23}\rho_{31})$$

$$C^d = 1 - R_{23}^2 - R_{12}^2 - R_{13}^2 + 2R(\rho_{12}\rho_{23}\rho_{13}^*) \quad (8)$$

$$R_{1(23)}^2 = 1 - \frac{1 - R_{23}^2 - R_{12}^2 - R_{13}^2 + 2R(\rho_{12}\rho_{23}\rho_{13}^*)}{1 - R_{23}^2}$$

$$R_{1(23)}^2 = \frac{R_{12}^2 + R_{13}^2 - 2R(\rho_{12}\rho_{23}\rho_{13}^*)}{1 - R_{23}^2} \quad (9)$$

To calculate the partial wavelet coherence, the equations become

$$\rho_{123} = -\frac{C_{21}^d}{\sqrt{C_{11}^d C_{22}^d}}$$

$$C_{11}^d = 1 - R_{23}^2, C_{22}^d = 1 - R_{12}^2$$

$$C_{21}^d = (-1)^{1+2} \begin{vmatrix} \rho_{12} & \rho_{13} \\ \rho_{32} & 1 \end{vmatrix} = -(\rho_{12} - \rho_{13}\rho_{32}) = -(\rho_{12} - \rho_{13}\rho_{23}^*)$$

Hence,

$$\rho_{123} = \frac{\rho_{12} - \rho_{23}\rho_{13}^*}{\sqrt{(1 - R_{13}^2)(1 - R_{23}^2)}}$$

1.2.2.3. Vector autoregressive moving average (VARMA)

The ARMA (p, q) process is described by the difference equation (10)

$$(a_0 - a_1L_{(t,-1)} - \dots - a_pL_{(t,-p)})y(t) = c + (b_0 - b_1L_{(t,-1)} - \dots - b_pL_{(t,-p)})\varepsilon(t) \quad (10)$$

Where $y(t)$ is the sequence of n elements, $\varepsilon(t)$ is white noise, L the shift operator and the constant c is taken to be zero if not specified. An n dimensional vector ARMA process should have real coefficient matrices a_i and b_j of dimensions $n \times n$, real vector c of length n , a disturbance vector of n elements determined by serially uncorrelated white noise processes. Hence, the covariance matrix Σ should be symmetric positive definite of dimensions $n \times n$. The vector ARMA process with zero constant has transfer function $g(z^{-1})$,

$$g(z) = (a_0 - a_1z - \dots - a_pz^p)^{-1} \cdot (b_0 - b_1z - \dots - b_qz^q)$$

Where a_0 and b_0 are the $n \times n$ identity matrices. The equation (10) can now be written in summary notation as

$$A(L)y(t) = M(L)\varepsilon(t) \quad (11)$$

Where L is the lag operator and $A(z) = A_0 + A_1z + \dots + A_pz^p$ and $M(z) = M_0 + M_1z + \dots + M_qz^q$ are matrix values polynomials. A multivariate process of this nature is commonly described as a VARMA process. The equation (11) can be rewritten as

$$y(t) = M(L)\{A^{-1}(L)\varepsilon(t)\} = M(L)\xi(t) \quad (12)$$

This suggest a two-step procedure begins with the calculation of (13) and (14),

$$\xi(t) = \varepsilon(t) - \{A_1\xi_{t-1} + \dots + A_r\xi_{t-r}\} \quad (13)$$

$$y(t) = M_0\xi_t + M_1\xi_{t-1} + \dots + M_r\xi_{t-r+1} \quad (14)$$

Where r is equal to p or q whichever is the highest, if p is not equal to q . Then either $A_i=0$ for $i=p+1, \dots, q$ or $M_i=0$ for $i=q+1, \dots, p$.

Since,

$$\xi_r(t) = \xi_{(t-r+1)}$$

$$\text{and } \xi_r(t) = \xi_{r-1}(t-1)$$

$$\text{, then } \xi_{(t-r+1)} = \xi_{r-1}(t-1) \quad (15)$$

Which turn equation (14) into (16),

$$y(t) = M_0\xi_1(t) + M_1\xi_2(t) + \dots + M_{r-1}\xi_r(t) \quad (16)$$

It is apparent that even low order of processes, such a vector system would produce a large dimension of matrices in the calculation. However it also shows that VARMA model can be reduced in a straightforward way to a set of n interrelated ARMA models. Rewriting equation (12),

$$y(t) = M(L) \frac{1}{|A(L)|} A^*(L) \varepsilon(t) \quad (17)$$

Where $|A(L)|$ is the scalar-valued determinant of $A(L)$ and $A^*(L)$ is the adjoint matrix. The process becomes

$$|A(L)|y(t) = M(L)A^*(L)\varepsilon(t) \quad (18)$$

A system of n ARMA processes with the common lag operator, L.

1.3. Wavelet Analysis

There are two types of wavelet transform, continuous and discrete wavelet transform. The discrete wavelet transform is a compact representation of the data and is particularly useful for noise reduction and data compression whereas the continuous wavelet transform is better for feature extraction purposes as Grinsted, A., Moore, J. C., & Jevrejeva, S. (2004) stated. In our study, continuous wavelet transform as well as wavelet coherence will be employed. One must note that wavelet coherence is a measure of two continuous-wavelet transforms to find significant coherence even though the common power is low (Grinsted, A., Moore, J. C., & Jevrejeva, S. (2004)).

1.3.1. Wavelet coherence

The wavelet coherence plot brings out a figure with time on the x axis and frequency of period value on the y axis. The lower frequency values give higher scale values or periods of co-movement. In the right hand side, the bar indicates the power of the coherence. The yellow color means higher power and moving into blue color

means lower coherence between the terms. The thin faded section around edges indicates the cone of influence area. It is due to low efficient results obtained by the wavelet transform at the edges of the time series data. The areas that are contoured with black line indicate 5% significance level against red noise. The blue (cold) regions represent no time and frequency dependence at the 5% significance level. The arrows indicate the relation between two time series in phase. Arrows pointing to the right means positive dependence and to the left means a negative relationship. If the arrow is pointing up, the first series leading the second in the analysis and the down pointing arrows indicates the second series as leading item in that time and frequency region.

As we look at the wavelet coherence of silver and gold in figure 2, the coherence scalogram demonstrates very high interaction. There is always a relation in almost every frequency during the time interval of the samples. However this seems to be weakening around 16-32 day period and 64-128 day periods around the last two years. There is very high correlation in all periods of 64-512 day from January 2012 up to June 2014. The high relationship of phase movement on 128 and 256-512 day period continuous at all times.

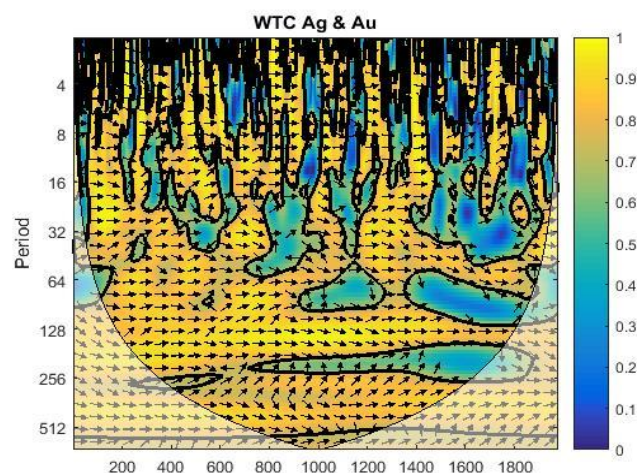


Figure 1.2. *Wavelet coherence of silver and gold*

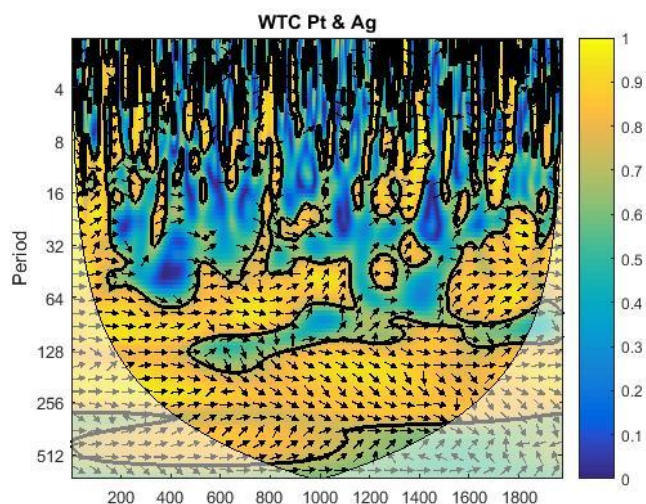


Figure 1.3. *Wavelet coherence of platinum and silver*

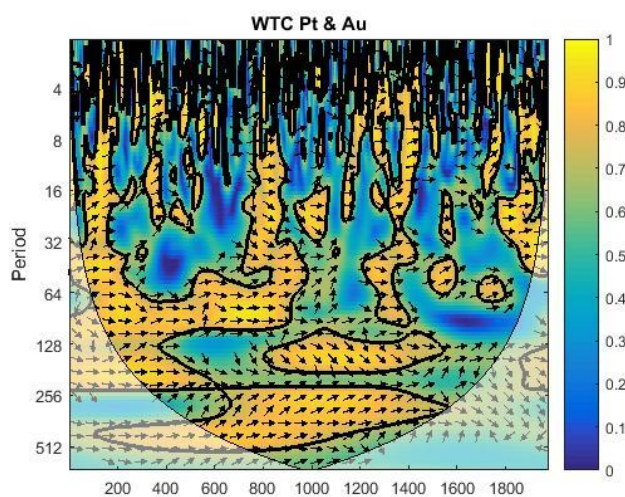


Figure 1.4. *Wavelet coherence of platinum and silver*

We find out the similar results of coherence around 128-512 day period when we examine the wavelet coherence of platinum and silver as shown in figure 3. In contrast with our results of high positive correlation between platinum and silver, the plot displays weaker levels of co-movement when compared with the silver and gold coherence plot. Platinum and silver displays almost no co-movement at the high frequencies. There is only local phase relation observed around 32 day period within the last year and around 64 day period between July, 2011 and 2014.

As expected, platinum and gold shown in Fig. 4 display minimum correlation with each other. There are some local regions in phase relation with high significance but the two metals generally do not display inter relation with each other. There are still co-movement regions which can be found around 64, 128, and 128-512 day periods from time to time. But there is no continuous relationship between two metals.

1.3.2. Three Dimensional Multiple wavelet coherence

Multiple wavelet coherence will show the effect of two factors together on the commodity itself. As we include the two commodities into the equation and run a multiple wavelet coherence analysis, the relationship between the three precious metals become much stronger. As you can see below in Figure 5 thru Figure 7, once the effect of gold and platinum is incorporated with the silver prices, one can tell that these metals are in phase relationship at all frequency levels at all times. As shown in figure 6, it provides similar outcomes for gold as well except that the relation is not as strong at all frequency levels as we get closer to our current time zone.

Figure 7 illustrates that, with multiple wavelet coherence, the relation of the metals and how they affect each other can be explained better. As shown in figure 7 below, the relation around 128-512 day period became much clear and it can be observed throughout the time interval. Also, there are fewer regions without phase relationship, shown in blue areas, compared to single wavelet coherence of platinum with either gold or silver alone.

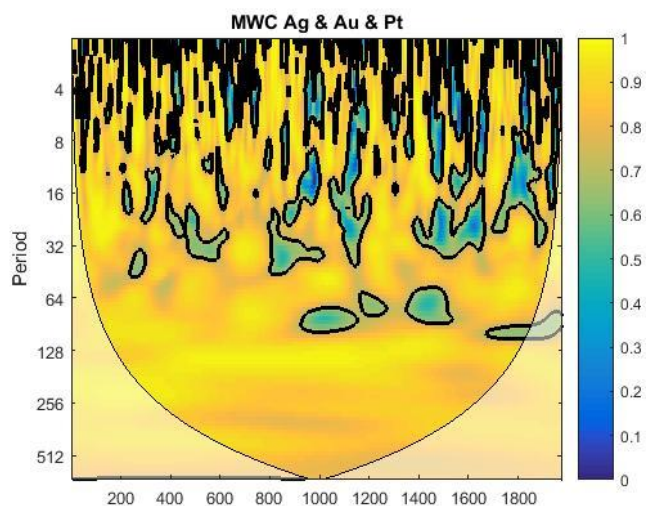


Figure 1.5. Multiple wavelet coherence of silver with gold and platinum

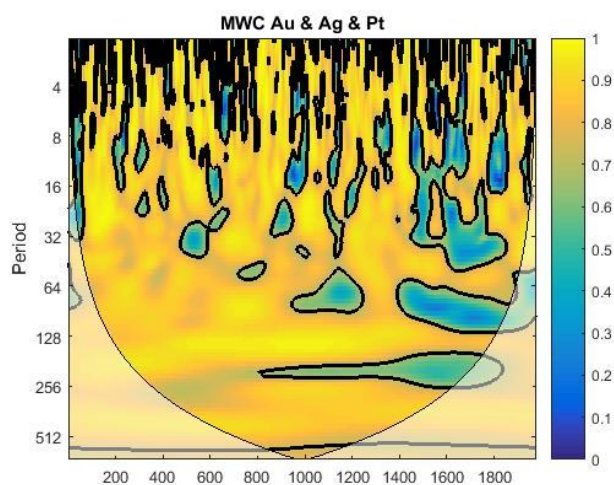


Figure 1.6. Multiple wavelet coherence of gold with silver and platinum

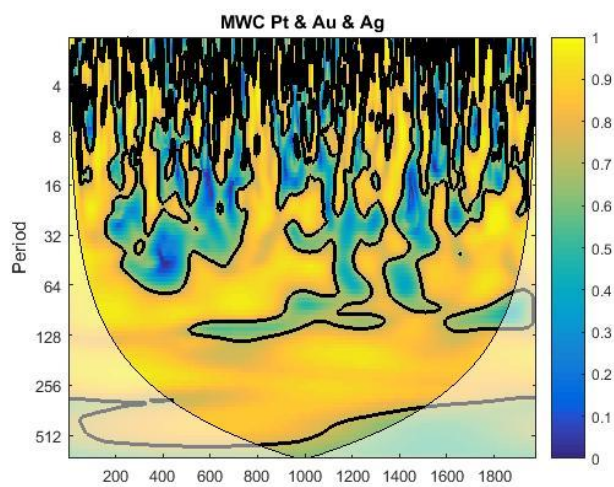


Figure 1.7. *Multiple wavelet coherence of platinum with gold and silver*

Hence these results help us understand the co-movement regions where there is high correlation. As a result, one can conclude that there is strong relationship around 128-256 day periods at all times. This corresponds with octave number 8 in the continuous wavelet transform. We will extract the data at this specific frequency where we observe high correlation in the time axis. The data between these periods (frequencies) will be used to model the time series and then their forecasting performances are compared accordingly.

1.4. Forecasting Results

As it is stated earlier, the main objective of this study is to demonstrate multivariate ARMA models have better forecasting results compared to other univariate models used. Furthermore, it is to show that extracting the data with the same frequency value by using wavelet transform will enhance the forecasting results due to new highly-correlated time-series obtained.

One of the main problems with VARMA is that it provides better results when small number of variables used. To overcome this problem so called dimension effect, some suggestions and solutions were presented by Dias and Kapetanios (2014) such as using a penalty function, variable selection or a shrinkage rule in order to select or diminish appropriate coefficients to become zero or using a Factor Models. Both models help reduce the dimensionality problems and VARMA do carry properties of both methods.

By using highly correlated data in a multivariate model, the data moving with similar frequency values will lead to a decrease in the values of the variance matrices. We have pointed out the high correlation regions by the multiple wavelet coherence analysis and the data within this period is selected from three different starting points

with different intervals of time series. The first data starts from October 20th 2012 with the length of 222 days, the second data starts from August 3, 2012 with the length of 601 days and the third set of data is extracted from March 23rd, 2013 with the length of 360 days. Once the time intervals are determined, continuous wavelet transform is utilized to transform the data into time and frequency space. After that, the corresponding frequency of the data is extracted by employing inverse continuous wavelet transform. As we have indicated previously that all of the three precious metals display high coherence around 128-256 day period which is equal to octave value of 8 in the scalogram. As a result, we get a new time series of metals within the same time interval with the same frequency value.

The values of the inversed time series data for three different periods are shown in Figs 8-10, respectively. One can easily notice the co-movement within each time series even though they are extracted from different sections of the time series data.

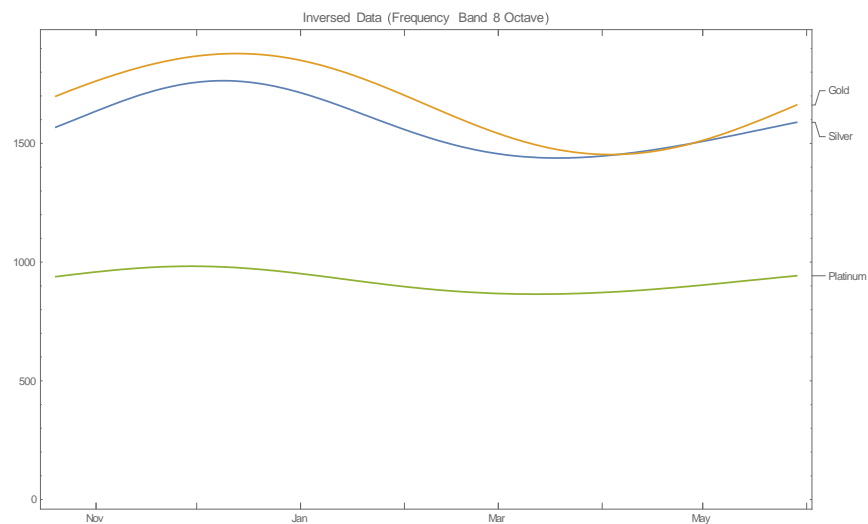


Figure 1.8. *Inversed data of time series 1 starting from October 20th, 2012 for*

222 days

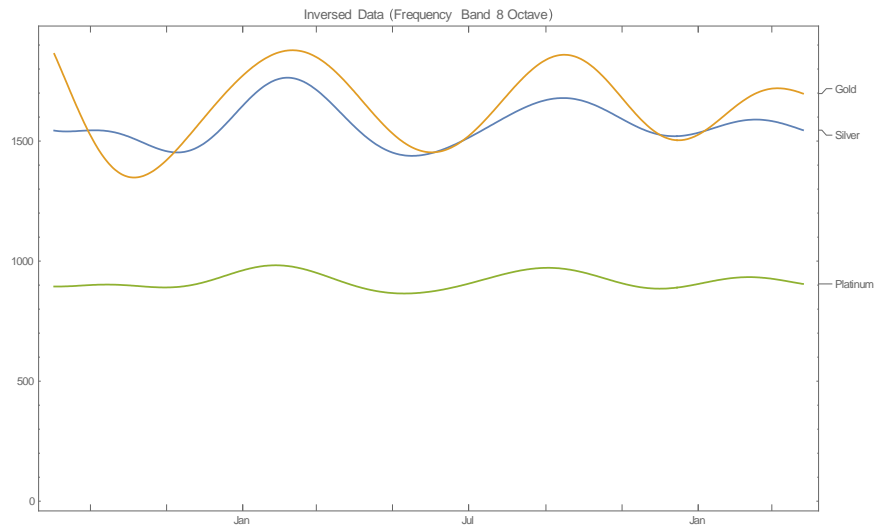


Figure 1.9. *Inversed data of time series 2 starting from August 3rd, 2012 for 601 days*

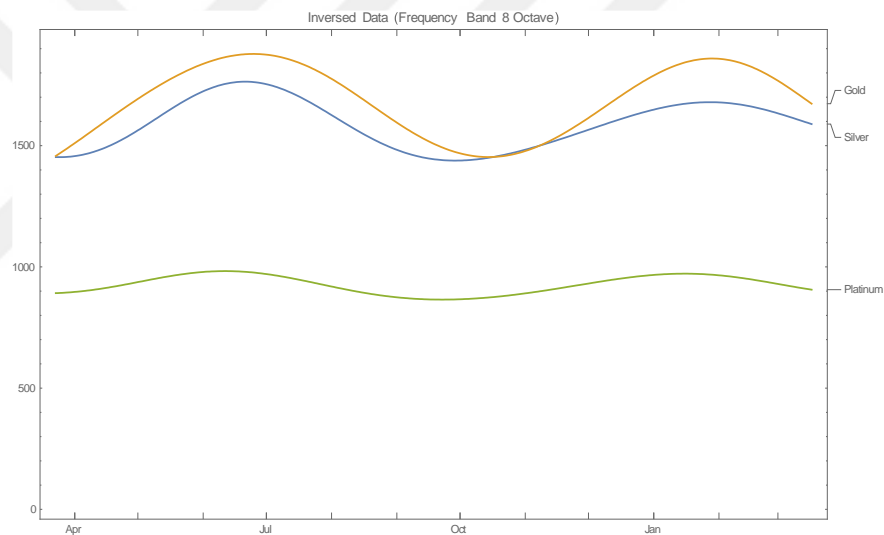


Figure 1.10. *Inversed data of time series 3 starting from March 23rd, 2013 for 360 days*

The correlation of the extracted data is now increased remarkably as it is shown in the Table 3. The co-movement of the interval time series chosen is very much in phase relation with each other.

Table 1.3.

Correlation of metals within the extracted time series

Data 1	Data 2	Data 3
--------	--------	--------

	Silver	Gold	Silver	Gold	Silver	Gold
Gold	0.9624		0.8658		0.9615	
Platinum	0.9450	0.8989	0.9169	0.7991	0.9255	0.8866

After that, the model parameters have been selected based on the AIC criterion and the three time series data are forecasted with ARMA (1, 1) model. ARMA (1, 1) model is applied to each metal of the chosen interval without any extraction procedure. On the other hand, the VARMA (1, 1) model is applied to the data extracted and then forecasted. The forecasting results later on are moved upward by the difference of the final value of the data frame chosen and the first forecast value calculated. Lastly, it is plotted accordingly.

As it can be seen from the results of gold forecasting in Figure 11, the forecasting data is projected in a much narrower interval once the data coherence is discovered and applied into the model. The forecasting follows the direction of the change of the price data in a much closer order as well. This is due to the behavior of the extracted data and high correlation between each vector of time series.

It is important to note that the forecasting data of a VARMA model provides a vector of upper and lower bands in a narrower fashion due to the low covariance values obtained in the matrices. Moreover, as a natural result of multivariate modeling, the covariance matrix gives out a vector of three arrays for each of the lower and upper bands calculated. We have simplified the results by selecting the minimum of the upper boundary and the maximum of the lower boundary values as they are plotted.

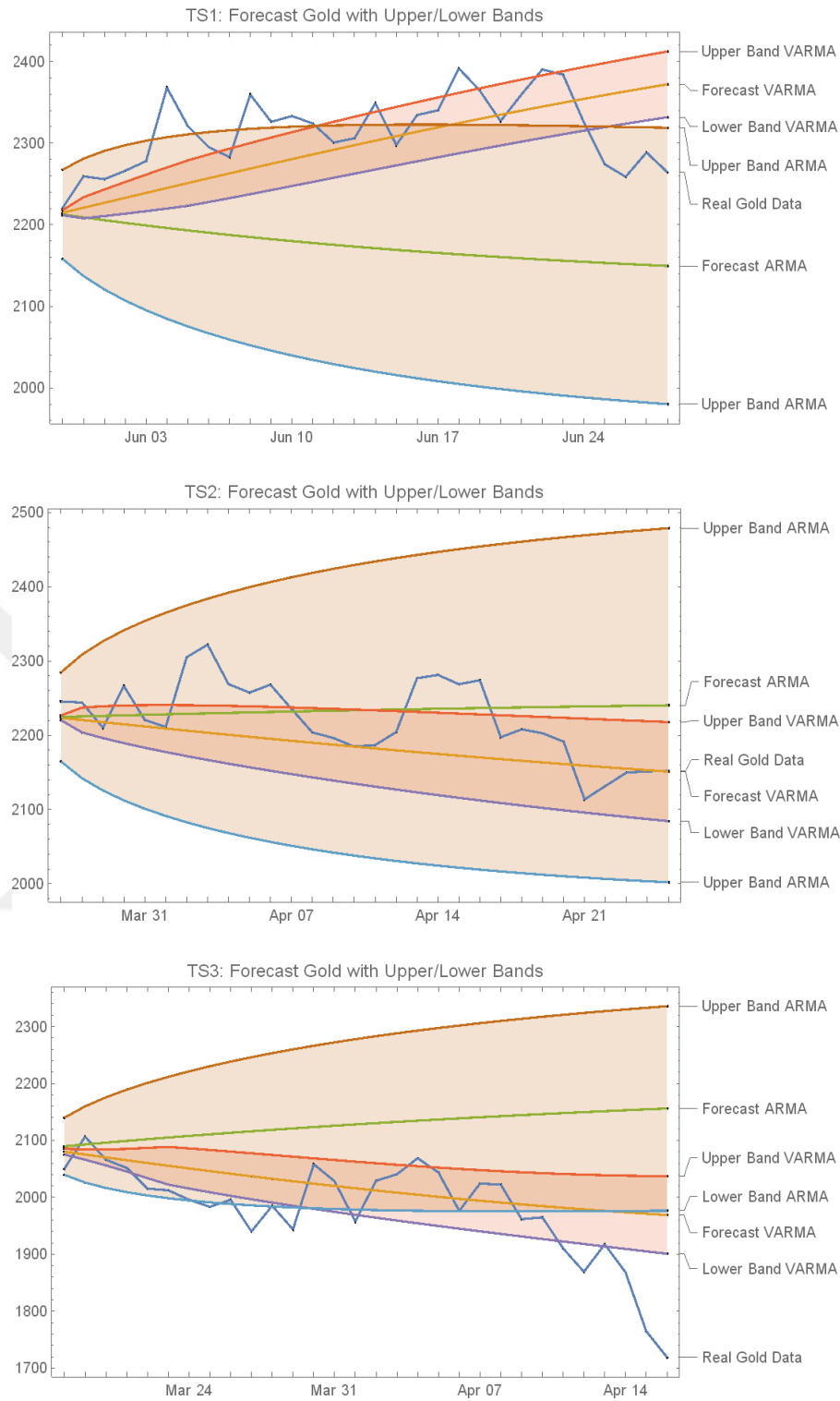


Figure 1.11. Forecasting performance of gold data from 3 different time series.

ARMA forecast, VARMA forecast, ARMA upper/lower bands, VARMA upper/lower bands, real gold data is shown for the next 30 days

As shown in the figures, the forecasting precision of the model is very much increased by using the VARMA model and the model demonstrates significant accuracy on the initial days of the forecasting. The corresponding results for silver (Figure 12) and platinum (Figure 13) may be found in the Appendix section.

1.5. Conclusion

It is shown that even though the precious metals are not highly correlated quantitatively, the detailed phase relation between the models can easily be explored using multiple wavelet coherence analysis. It can be said that the three metals are highly correlated at low frequencies, meaning in longer periods throughout the time.

It may also be concluded that the forecasting performance of a model is improved by using the VARMA model of correlated time series data. This directly corresponds with the results obtained by Pena and Sanchez (2007) that the performances of multivariate ARMA models are relatively better with respect to univariate models. It is also shown that the consistency in forecasting is obtained regardless of the size of the data set. Adequate results have been obtained with both small size (220 days) data sets as well as larger size (600 days) data sets which correspond with the results of Dias and Kapetanios (2011).

Furthermore, it is shown that the correlated data can be extracted by using scale by scale wavelet transform and used to increase the efficiency of forecasting. Two advantages may be underlined. Firstly, it increases the accuracy of the forecasting range in terms of mean squared errors and provide narrow band of upper and lower limits. Secondly, it increases the efficiency of the prediction of the price shift (increase (↑) or decrease (↓)) in the near future because of the highly correlated data that possess the same frequency characteristic of the movement.

In all, wavelet transform would allow investors to extract data with same periodical movement out of different assets. Thus, VARMA forecasting with higher accuracy can be made possible approximately for all times, once the data in co-movement is successfully determined. Subsequently, the use of scale by scale wavelet transforms increases the efficiency of VARMA forecasting significantly.



Appendix A. Forecasting performance of each data for 3 different time intervals

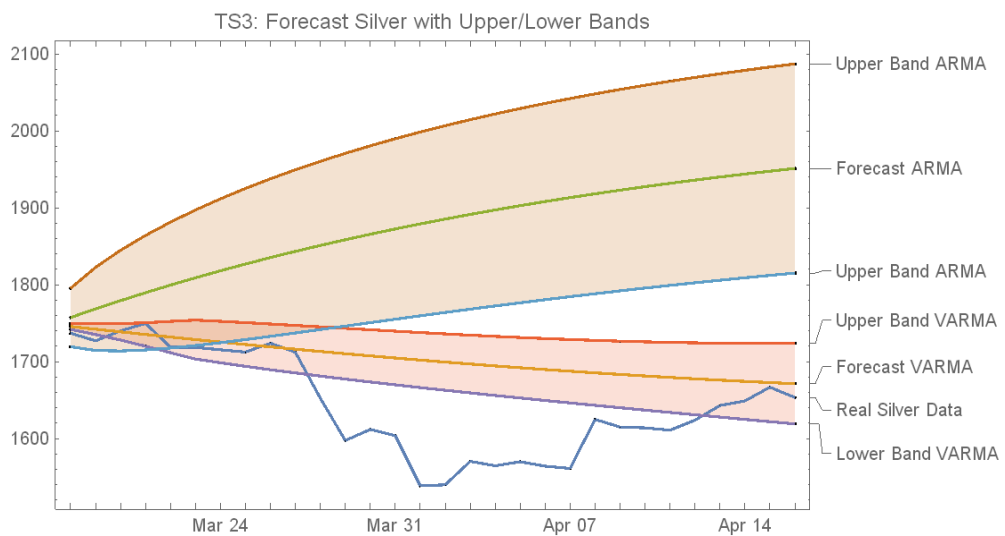
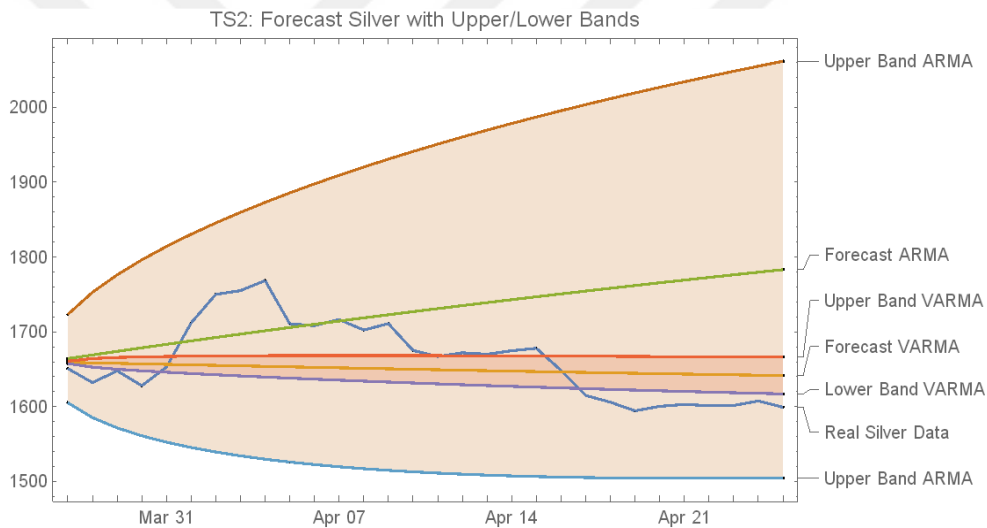
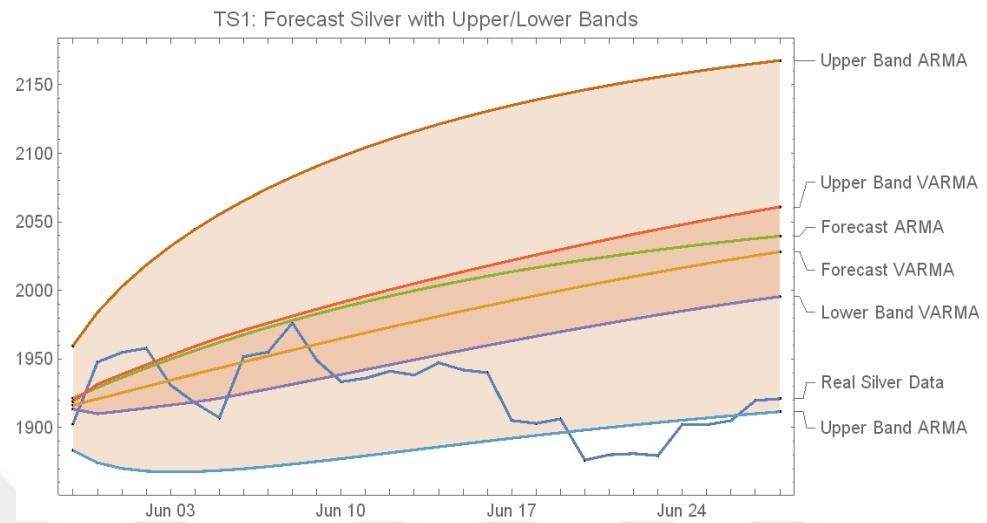
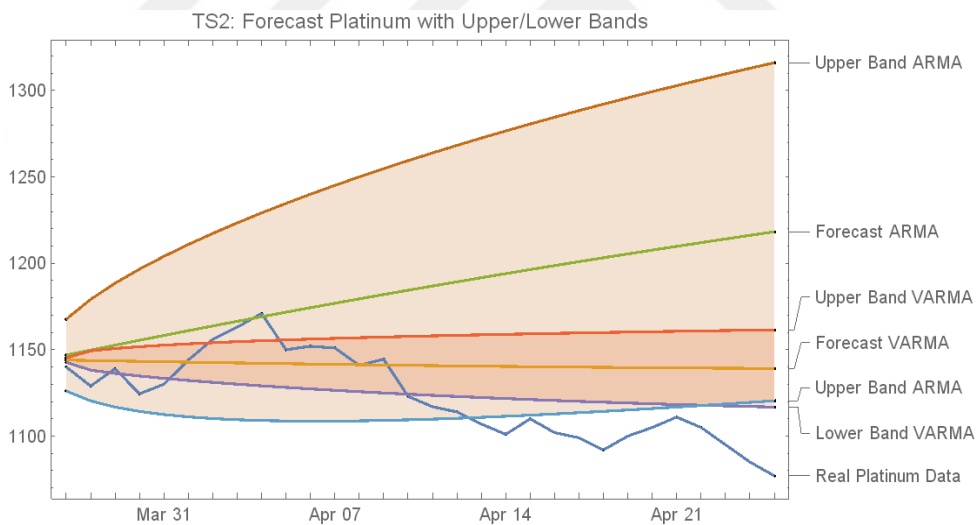
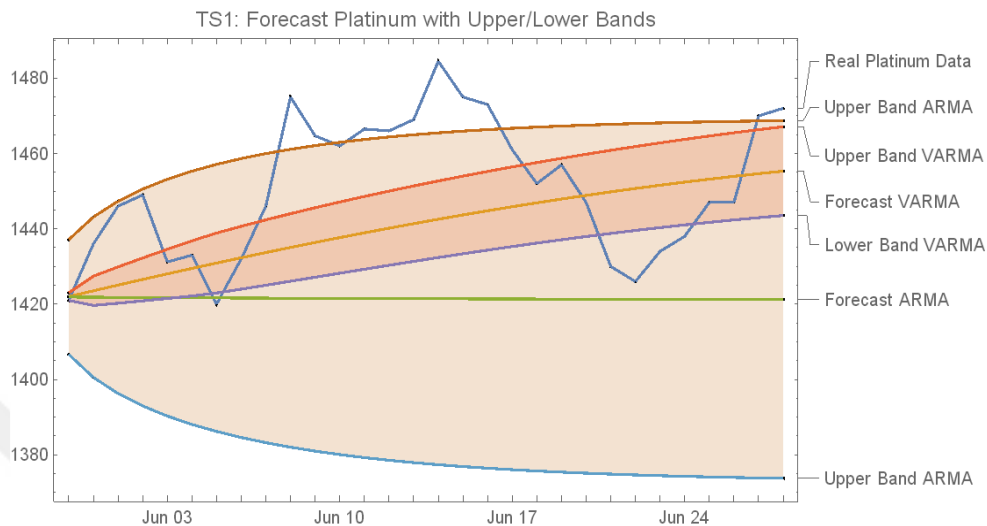


Figure 1.12. Forecasting performance of silver data from 3 different time series.

ARMA forecast, VARMA forecast, ARMA upper/lower bands, VARMA upper/lower bands, real silver data is shown for the next 30 days



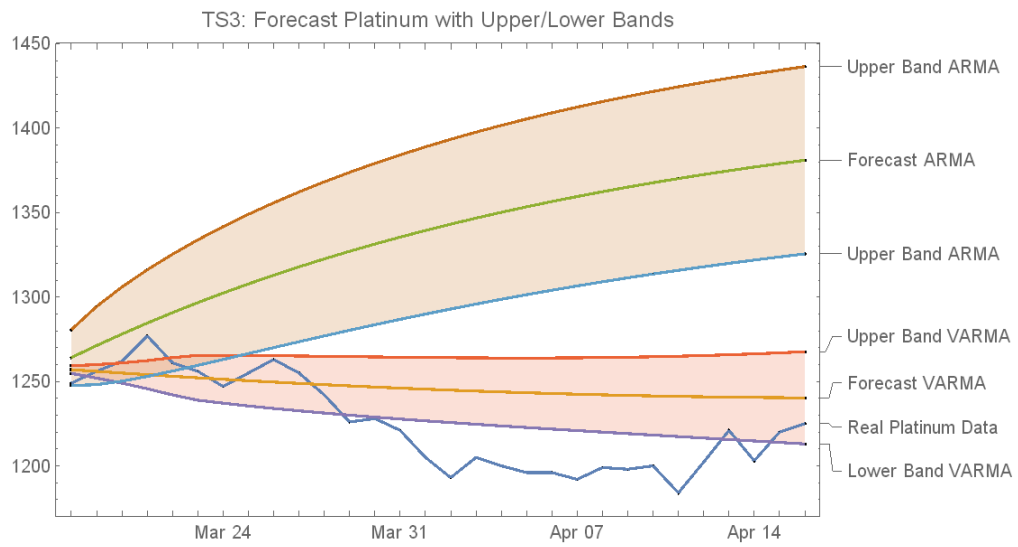


Figure 1.13. *Forecasting performance of platinum data from 3 different time series. ARMA forecast, VARMA forecast, ARMA upper/lower Bands, VARMA upper/lower bands, real platinum data is shown for the next 30 days*

CHAPTER 2

DYNAMIC CORRELATION OF EASTERN AND WESTERN MARKETS AND FORECASTING: SCALE BY SCALE WAVELET BASED APPROACH

Summary

In this chapter, dynamic four-dimensional (4D) correlation of eastern and western markets is analyzed. A wavelet based scale by scale analysis method has been introduced to model and forecast stock market data for strongly correlated time intervals. The daily data of stock markets of SP500, FTSE and DAX (western markets) and NIKKEI, TAIEX and KOSPI (eastern markets) are obtained from 2009 to the end of 2016 and their co-movement dependencies on frequency-time space using four-dimensional (4D) multiple wavelet coherence (MWC) are determined. Once the data is detached into levels of different frequencies using scale by scale continuous wavelet transform, all of the time series possessing the same frequency scale are selected, inversed and forecasted using multivariate model, Vector Autoregressive Moving Average (VARMA). It is concluded that the efficiency of forecasting is increased substantially using the same frequency highly correlated time series obtained by scale by scale wavelet transform. Moreover, the increasing or decreasing trend of prospected price shift is foreseen fairly well.

2.1. Introduction

Financial time series acts on different frequencies since different investors may be seen to influence the price series of the assets on different scales and periods. Hence, it requires a thorough check of financial time series both in time and frequency space.

Fourier transform was one of the methods to study the time series data but it loses the time information as it looks deep into the frequency values of the series therefore it could not be used successfully to study the non-stationary financial time series data. Instead, a new method, wavelet analysis, have been developed which does not depend on the assumption of stationarity (Burrus, Gopinath and Guo (1998)). The wavelet approach is model-free and permits a time series to be decomposed into different frequency components without losing time information (Revoredo and Miguel (2014)). As elaborated by Gulerce and Unal (2016), wavelet transform expands time series into time–frequency space and can therefore find localized intermittent periodicities, eliminating the weaknesses in Fourier transform.

Since the influential work of Gencay (2002), wavelet tools have been extensively used in analyzing financial times series in many studies such as Aguiar-Conraria and Soares (2011), Barunik, Kocenda and Vacha (2013) and Aguiar-Conraria and Soares (2014). As Haven (2012) stated multi-scale analysis, estimation of unknown parameters, and removal of noise from raw data series may be counted as the three principal application of wavelet methods in finance and economics. Examples of multi scale analysis may be found by McCarthy and Orlov (2012) and Graham, Kiviaho and Nikkinen (2013) where the continuous wavelet transform and the wavelet coherence are specifically used in financial applications to determine correlation estimates across different time series and frequencies.

There have been many investigations studying the dynamic relation of different markets. Janakiramanan and Lamba (1998) and Cha and Cheung (1998) investigate the interrelation between Asia-Pacific equity markets and the US using vector autoregression (VAR) models, concluding that the US has a significant influence on these markets as well as strong interrelationships within the Asia-Pacific region. Rua and Nunes (2009) applied wavelet analysis to investigate the correlations between Germany and the US, two major developed markets, on an extensive stock market level. Graham, Kiviaho and Nikkinen (2012) continue to the analysis of emerging stock markets across the world and Graham and Nikkinen (2011) specifically compare the Finnish stock market with other markets world-wide.

Torrance and Compo (1998) and Grinsted et al. (2004) provided a software package for wavelet coherence analysis in order to effectively and efficiently examine common and coherent signals in multiple time series. The same methodology will be utilized to study the correlation of Asian Markets (NIKKEI, TAIEX and KOSPI) with respect to developed markets (SP500, FTSE and DAX). Multiple wavelet coherence will show the effect of three markets from the developed countries on each of the Asian market itself which is the fundamental difference from multiple correlations.

We will produce in phase movement of markets using multiple wavelet coherence. Then using continuous wavelet transform, the specific time and frequency domain will be filtered out of the time series. We are aware that analysis of multiple wavelet coherence allows observing many exciting interrelationships in time–frequency space in a much detailed way than other methods (Yilmaz and Unal (2016)). This clean relation of highly correlated time series may be used to model the data for forecasting purposes. This is the assumption of the chapter that it will improve the performance of modeling as well as forecasting to a new level of accuracy.

Predicting the market price on the next day, forecasting, has always been the hardest challenge for all investors and speculators in the financial world around the globe due to high heteroskedastic, nonlinear as well as unit root behavior that all markets possess. In an effort to improve forecasting performances, many different methods have been offered. One of the methods is to use multivariate models instead of univariate ones. Multivariate models were first introduced by Quenouille (1957) and later improved by Akaike (1974), Dunsmuir and Hannan (1976), and Hannan (1981). The VARMA model is employed for forecasting the correlated (interrelated) time series and for investigating the dynamic impact of random disturbances on the system of variables. The VARMA is a dynamic system of equations that examine the impacts of fluctuations (shocks) or correlations (interactions) between financial variables (Oral and Unal (2017)). It is proposed to improve the forecasting results with higher precision by using more information through a combination of multiple highly correlated data. It is shown that VARMA models do give better fit results because of having low mean squared errors compared to univariate models hence resulting in good forecasting performances (Oral and Unal (2017)).

Section 2 contains the data and methodology used in this chapter. Basics of continuous wavelet transform (CWT), multiple wavelet coherence and VARMA are introduced as a summary review. In section 3, using multiple wavelet coherence, we analyze the markets interrelations and reveal their movement dependencies on time-frequency space. Once the specific time and frequency interval is decided, VARMA model is used to forecast indexes. Section 4 will compare and discuss multivariate ARMA model with respect to univariate ARMA model and display the forecasting results. In section 5, the chapter will be concluded with the discussion of results. In Appendix, the forecasting results of TAIEX and KOSPI stock markets are presented.

2.2. Empirical Study

2.2.1. Empirical Data

The stock index of SP500, FTSE, DAX, NIKKEI, TAEIX and KOSPI are taken from Yahoo Finances! starting from March, 2009 to December, 2016. It is composed of 1930 daily data per market. Fig. 1 displays the US (SP500), UK (FTSE) and German (DAX) stock markets and Fig. 2 displays the Japan (NIKKEI), Taiwan (TAEIX) and South Korea (KOSPI) stock market indexes.

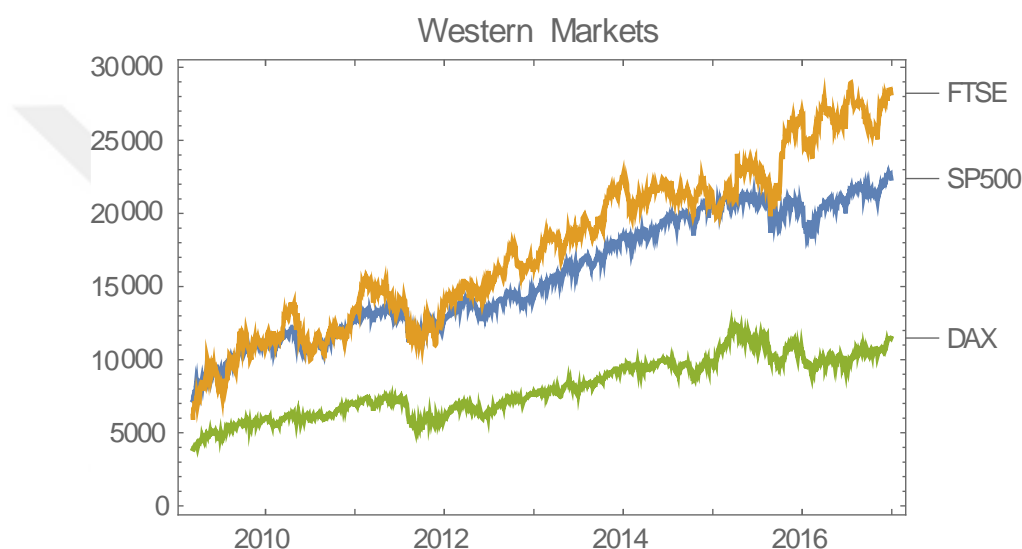


Figure 2.1. *Western Market Indexes*

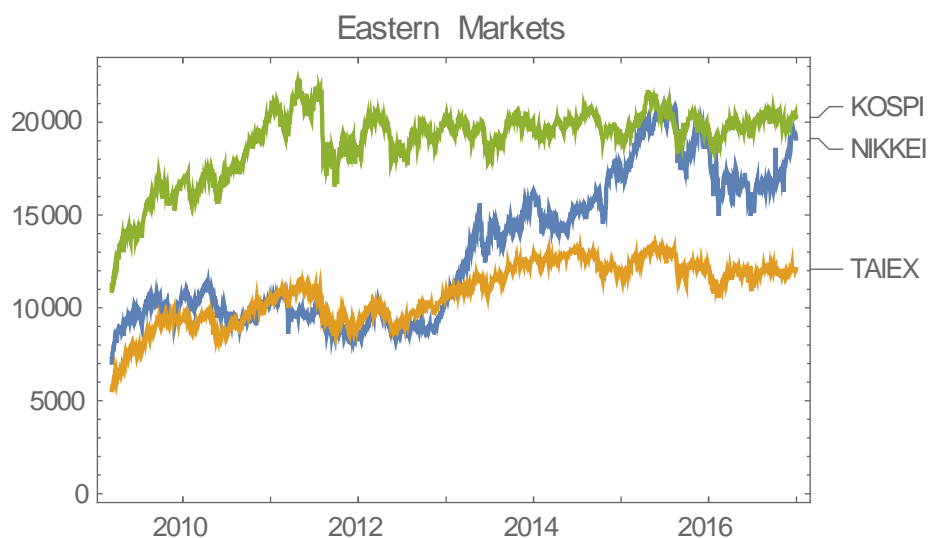


Figure 2.2. *Eastern Market Indexes*

The statistical analysis of the markets may be found in Table 1. According to these results, five markets out of six displays more flat than normal distribution (platykurtic) with kurtosis values less than 3 and Kospi is demonstrating more peaked than normal distribution (leptokurtic) with kurtosis values more than 3. Four of the markets are positively skewed with respect to the normal distribution; however Taiwanese and South Korean stock market indexes are negatively skewed where the mass of the distribution is concentrated on the right side of the mean.

Table 2.1.

Statistics of the Markets

	Mean	Median	St. Dev	Kurtosis	Skewness
SP500	15624.60	14641.00	4019.24	1.6055	0.0295
FTSE	17506.10	17404.10	5470.83	1.9346	0.1345
DAX	7933.90	7502.27	1968.09	1.9303	0.2041
NIKKEI	13014.70	11348.20	3801.02	1.7416	0.4055
TAIEX	10786.00	10946.60	1598.57	2.5694	-0.4556
KOSPI	18963.70	19552.80	1857.84	5.3912	-1.5253

The correlation of the markets is shown in Table 2. All of the markets except South Korea have correlation value more than 90% with SP500 stock market. The value of correlation between stock markets of Japan, Taiwan and South Korea are quite close to each other with US and German stock markets. UK stock market has slightly less correlation in comparison with the rest. It is surprising to see that South Korea has the highest correlation with the Taiwanese stock market rather than any other markets in the Asian region or in the west. KOSPI displays higher parallel

movement with SP500, FTSE and DAX compared to NIKKEI, a very closer market in the region.

Table 2.2.

Correlation of the Markets

	SP500	FTSE	DAX	NIKKEI	TAIEX	KOSPI
SP500	1	0.9689	0.9593	0.9178	0.9117	0.6675
FTSE	0.9689	1	0.9181	0.8604	0.8589	0.6476
DAX	0.9593	0.9181	1	0.9233	0.9102	0.6659
NIKKEI	0.9178	0.8604	0.9233	1	0.8302	0.4743
TAIEX	0.9117	0.8589	0.9102	0.8302	1	0.7775
KOSPI	0.6675	0.6476	0.6659	0.4743	0.7775	1

In consideration of these, we will analyze the co-movement characteristics of these markets using wavelet transform and multiple wavelet coherence. And then we will try to determine a certain frequency value that will help enhance the forecasting performance and compare the results accordingly.

2.2.2. Methodology

2.2.2.1. A summary for continuous wavelet transform

An excellent way of wavelet application in finance and economics has been introduced by Gencay (2002). Other application afterwards have been utilized by Aguiar-Conraria and Soares (2011), Barunik, Kocenda and Vacha (2013) and Aguiar-Conraria and Soares (2013), Yilmaz and Unal (2017). A wavelet is a localized function with finite support of decomposition. There are many different wavelet transform methods. Out of many, discrete and continuous wavelet transforms are two fundamental ones where continuous wavelet transform (CWT) is mainly preferred for

feature extraction purposes as Grinsted, Moore and Jevrejeva (2004) stated.

Therefore, we use CWT to extract the frequency-time information of the data. Given a times series, continuous wavelet transform is defined as (1)

$$CWT_x^\psi(s, \tau) = \langle X, \psi(s, \tau) \rangle = \frac{1}{\sqrt{s}} \int_{-\infty}^{+\infty} X(t) \psi^* \left(\frac{t-\tau}{s} \right) dt \quad (1)$$

Where " τ " is the translation which corresponds with the time information and " s " is the scale parameter which corresponds with the frequency information in the transform domain. " ψ " is the transforming function also known as the mother wavelet. Similar to the scale used in maps, high scale value means a global view and low scale value means a more specific and detailed view. Henceforth, by mapping the time series into τ and s parameters, wavelet transform provides information on time and frequency domain but one must note that there is an inverse relationship exist between scale and frequency. As the scale increases (decreases), the periodical span of the time information increases (decreases) but the frequency decreases (increases). Since the wavelet transform is, by some means, a matter of decomposing a time series into different energy levels, the inverse of the transform must also satisfy the law of conservation of energy. Hence it must satisfy equation (2),

$$\int_{-\infty}^{+\infty} |x(t)|^2 dt = \frac{1}{c_\psi} \int_{-\infty}^{+\infty} \int_{-\infty}^{+\infty} |W_x(\tau, s)|^2 \frac{d\tau ds}{s^2} \quad (2)$$

In turn, it makes it possible to reconstruct the time series data by the formula (3),

$$x(t) = \frac{2}{c_\psi} \int_{-\infty}^{+\infty} \left[\int_{-\infty}^{+\infty} W_x(\tau, s) \psi_{\tau, s}(t) d\tau \right] \frac{ds}{s^2} \quad (3)$$

In the continuous wavelet transform, the scaling parameter s is given by equal-tempered scale calculated by the equality in (4),

$$s_{oct, voc} = \alpha 2^{oct-1} 2^{voc/nvoc} \quad (4)$$

Where "oct" is the octave number which is used as a conversion factor of scales, consequently the frequencies, "voc" is the voice number, and " α " is the smallest

wavelet scale. Hence, from the figures, we may point out the same frequency interval for each time series and inverse the data with the same frequency value as desired.

2.2.2.2. Four dimensional multiple wavelet coherence.

Bivariate case of wavelet coherence may be extended into multivariate wavelet coherence as the number of series increase. The correlation of interesting variables X_1 and X_2 with other variables is taken into account as the calculation of coherency and phase differences are the matter of concern. The squared multiple wavelet coherency between X_1 and all other series X_2, \dots, X_p is defined as (5)

$$R_{1(23\dots p)}^2 = R_{1(q)}^2 = 1 - \frac{M^d}{S_{11}M_{11}^d} \quad (5)$$

Where M is the $p \times p$ matrix of all smoothed cross-wavelet spectra (denoted by S_{ij})

$$S_{ij} = S(W_{X_i X_j}) \left(S_{ij} = S_{ij}^*, S_{ij} = S(|W_{X_i}|^2) \right)$$

$$M = \begin{bmatrix} S_{11} & S_{12} & \dots & S_{1p} \\ S_{21} & S_{22} & \dots & S_{2p} \\ \vdots & \vdots & \ddots & \vdots \\ S_{p1} & S_{p2} & \dots & S_{pp} \end{bmatrix} \quad (6)$$

The $p \times p$ matrix of all smoothed complex wavelet coherencies is complex coherence denoted by C as shown in equation (7),

$$\rho_{ij} = \frac{S(W_{ij})}{\sqrt{S(|W_i|^2)S(|W_j|^2)}} \text{ and } \rho_{ij} = \rho_{ji}^*$$

$$C = \begin{bmatrix} 1 & \rho_{12} & \dots & \rho_{1p} \\ \rho_{21} & 1 & \dots & \rho_{2p} \\ \vdots & \vdots & \ddots & \vdots \\ \rho_{p1} & \rho_{p2} & \dots & 1 \end{bmatrix} \quad (7)$$

$$R_{1(q)}^2 = 1 - \frac{C^d}{C_{11}^d}$$

In our case of four time series, the cofactor of the complex coherence matrix is equal to (8)

$$C_{11}^d = \begin{vmatrix} 1 & \rho_{23} & \rho_{24} \\ \rho_{32} & 1 & \rho_{34} \\ \rho_{42} & \rho_{43} & 1 \end{vmatrix}$$

$$\begin{aligned} &= 1 - \rho_{23}\rho_{32} - \rho_{24}\rho_{42} + \rho_{23}\rho_{34}\rho_{42} + \rho_{24}\rho_{32}\rho_{43} - \rho_{34}\rho_{43} \\ &= 1 - R_{23}^2 - R_{24}^2 - R_{34}^2 + 2R(\rho_{23}\rho_{34}\rho_{24}^*) \end{aligned}$$

$$C^d = C_{11}^d - \rho_{12}C_{12}^d + \rho_{13}C_{13}^d - \rho_{14}C_{14}^d \quad (8)$$

Eq. 8 can be expressed in details as following.

$$\begin{aligned} C^d &= 1 - \rho_{12}\rho_{21} - \rho_{13}\rho_{31} - \rho_{24}\rho_{42} - \rho_{23}\rho_{32} - \rho_{14}\rho_{41} - \rho_{34}\rho_{43} + \rho_{12}\rho_{23}\rho_{31} \\ &\quad + \rho_{13}\rho_{21}\rho_{32} + \rho_{12}\rho_{24}\rho_{41} + \rho_{14}\rho_{23}\rho_{32}\rho_{41} - \rho_{13}\rho_{24}\rho_{32}\rho_{41} \\ &\quad + \rho_{13}\rho_{24}\rho_{41} - \rho_{12}\rho_{23}\rho_{34}\rho_{41} + \rho_{14}\rho_{21}\rho_{42} - \rho_{14}\rho_{23}\rho_{31}\rho_{42} \\ &\quad + \rho_{13}\rho_{24}\rho_{31}\rho_{42} - \rho_{13}\rho_{22}\rho_{34}\rho_{42} + \rho_{23}\rho_{34}\rho_{42} + \rho_{14}\rho_{31}\rho_{43} \\ &\quad - \rho_{12}\rho_{24}\rho_{31}\rho_{43} - \rho_{14}\rho_{21}\rho_{32}\rho_{43} + \rho_{24}\rho_{32}\rho_{43} + \rho_{12}\rho_{21}\rho_{34}\rho_{43} \end{aligned}$$

Or it can be written as the following,

$$\begin{aligned} C^d &= 1 - R_{12}^2 - R_{13}^2 - R_{23}^2 - R_{14}^2 - R_{24}^2 - R_{34}^2 + \rho_{12}\rho_{23}\rho_{31} + \rho_{13}\rho_{21}\rho_{32} \\ &\quad + \rho_{12}\rho_{24}\rho_{41} + \rho_{14}\rho_{21}\rho_{42} + \rho_{23}\rho_{34}\rho_{42} + \rho_{24}\rho_{32}\rho_{43} + \rho_{14}\rho_{31}\rho_{43} \\ &\quad + \rho_{13}\rho_{24}\rho_{41} + \rho_{14}\rho_{23}\rho_{32}\rho_{41} - \rho_{13}\rho_{24}\rho_{32}\rho_{41} - \rho_{12}\rho_{23}\rho_{34}\rho_{41} \\ &\quad - \rho_{14}\rho_{23}\rho_{31}\rho_{42} + \rho_{13}\rho_{24}\rho_{31}\rho_{42} - \rho_{13}\rho_{22}\rho_{34}\rho_{42} - \rho_{12}\rho_{24}\rho_{31}\rho_{43} \\ &\quad - \rho_{14}\rho_{21}\rho_{32}\rho_{43} + \rho_{12}\rho_{21}\rho_{34}\rho_{43} \end{aligned}$$

And the squared multiple wavelet coherencies become (9).

$$R_{1(234)}^2 = 1 - \frac{C^d}{C_{11}^d} \quad (9)$$

2.2.2.3. Vector autoregressive moving average (VARMA).

Synchronization of multiple time series is very important in understanding the efficiency increase of multivariate time series analysis. As Tsay stated, dynamic relations between variables can be identified better with vector autoregressive moving average models. Using highly correlated data series, as the dimension of the model increases, the VARMA model not only considers the historical data of each series but

also other interrelated variables in between the series. Hence, it leads to more accurate results compared to scalar counter models as Lutkepohl and Poskitt (1996) stated.

The difference equation in (10) describes the The ARMA (p, q) process

$$(a_0 - a_1L_{(t,-1)} - \dots - a_pL_{(t,-p)})y(t) = c + (b_0 - b_1L_{(t,-1)} - \dots - b_qL_{(t,-q)})\varepsilon(t) \quad (10)$$

Where $y(t)$, $\varepsilon(t)$, L and c are the sequence of n elements, the white noise, the shift operator and the constant, respectively. The constant c is equal to zero unless otherwise specified. An n dimensional vector ARMA process should have real coefficient matrices a_i and b_j of dimensions $n \times n$, real vector c of length n , a disturbance vector of n elements determined by serially uncorrelated white noise processes. Hence, the covariance matrix Σ should be symmetric positive definite of dimensions $n \times n$. The vector ARMA process with zero constant has transfer function $g(z^{-1})$,

$$g(z) = (a_0 - a_1z - \dots - a_pz^p)^{-1} \cdot (b_0 - b_1z - \dots - b_qz^q)$$

Where a_0 and b_0 are the $n \times n$ identity matrices. The equation (10) can now be written in summary notation as

$$A(L)y(t) = M(L)\varepsilon(t) \quad (11)$$

Where L is the lag operator and $A(z)=A_0+A_1z+\dots+A_pz^p$ and $M(z)=M_0+M_1z+\dots+M_qz^q$ are matrix values polynomials. A multivariate process of this nature is commonly described as a VARMA process. The equation (11) can be rewritten as (12)

$$y(t) = M(L)\{A^{-1}(L)\varepsilon(t)\} = M(L)\xi(t) \quad (12)$$

This suggest a two-step procedure begins with the calculation of (13) and (14),

$$\xi(t) = \varepsilon(t) - \{A_1\xi_{t-1} + \dots + A_r\xi_{t-r}\} \quad (13)$$

$$y(t) = M_0\xi_t + M_1\xi_{t-1} + \dots + M_r\xi_{t-r+1} \quad (14)$$

Where r is the highest value of p or q when p is not equal to q . This indicates that either A_i is equal to 0 for every i greater than $p+1$ but less than q or M_i is equal to 0 every i greater than $q+1$ but less than p .

Since,

$$\begin{aligned}\xi_r(t) &= \xi_{(t-r+1)} \\ \text{and } \xi_r(t) &= \xi_{r-1}(t-1) \\ , \text{ then } \xi_{(t-r+1)} &= \xi_{r-1}(t-1)\end{aligned}\quad (15)$$

Which turn equation (14) into (16),

$$y(t) = M_0 \xi_1(t) + M_1 \xi_2(t) + \dots + M_{r-1} \xi_r(t) \quad (16)$$

It can be clearly realized that such a vector system would produce a large dimension of matrices in the calculation even at low order of processes. However it also shows that VARMA model can be reduced in a straightforward way to a set of n interrelated ARMA models. Rewriting equation (12),

$$y(t) = M(L) \frac{1}{|A(L)|} A^*(L) \varepsilon(t) \quad (17)$$

Where $|A(L)|$ is the scalar-valued determinant of $A(L)$ and $A^*(L)$ is the adjoint matrix. The process becomes

$$|A(L)|y(t) = M(L)A^*(L)\varepsilon(t) \quad (18)$$

where a system of n dimensional ARMA process is defined with the common lag operator, L .

2.3. Multiple Wavelet Coherence Analysis in 4D

Multiple wavelet coherence brings out a plot that depends on a careful interpretation. On the x-axis you will find the time information and y-axis will indicate the frequency. The lower frequency means higher scale or vice versa. In the right, the power of the coherence is displayed. The warmer yellow colors mean higher correlation where 1 indicates the highest correlation and colder blue colors mean low

correlation where 0 indicates no correlation. The areas with black contour indicate the time-frequency regions with statistical significance at 5% significance level against red noise. The faded area falls onto the outside of the cone of influence (COI) which is due to the errors caused by the discontinuities in the wavelet transform. As Yilmaz and Unal (2016) stated, the continuous wavelet transform may return wrong estimation on the edges since the shape of the wavelet might exceed the length of the data.

When we examine the multiple wavelet coherence plots, as shown in Fig. 3-5, of three Asian markets NIKKEI, TAIEX and KOSPI with SP500, FTSE and DAX, we realize that there is very high interrelation between all of the markets almost at all times. All markets display no correlation around 64 and 128 day periods between March of 2013 and October of 2014. The same can be stated around 32 and 64 day periods between August of 2015 and June of 2016. All of the markets are highly and fully correlated between 128-512 day periods at all times.

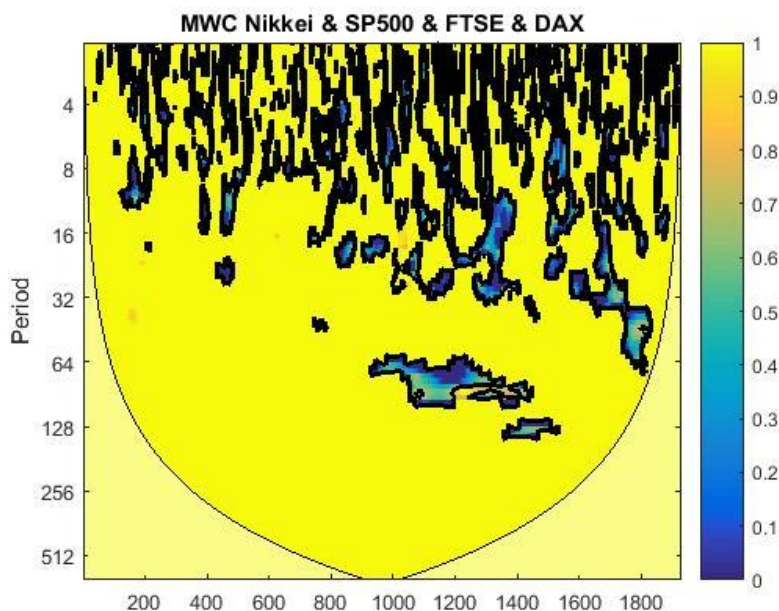


Figure 2.3. Multiple wavelet coherence of Nikkei with SP500, FTSE and DAX

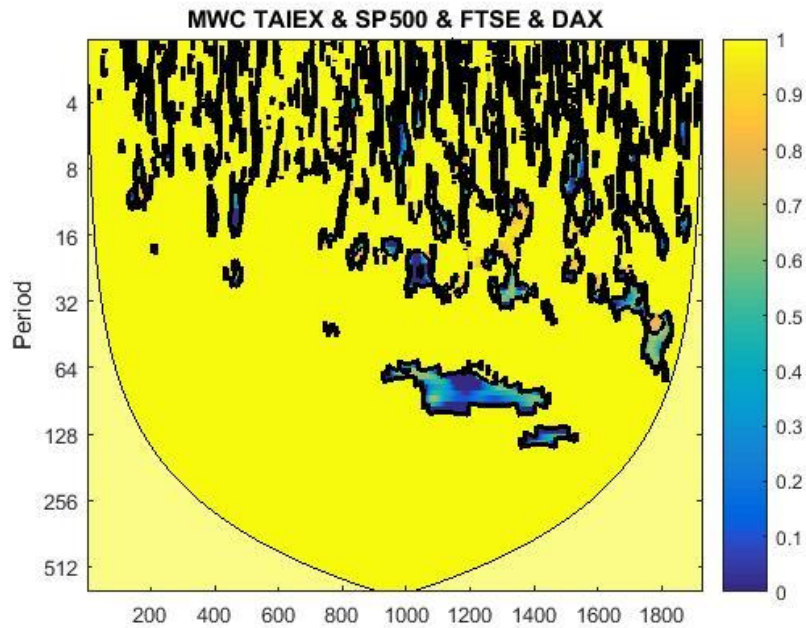


Figure 2.4. Multiple wavelet coherence of Taiex with SP500, FTSE and DAX

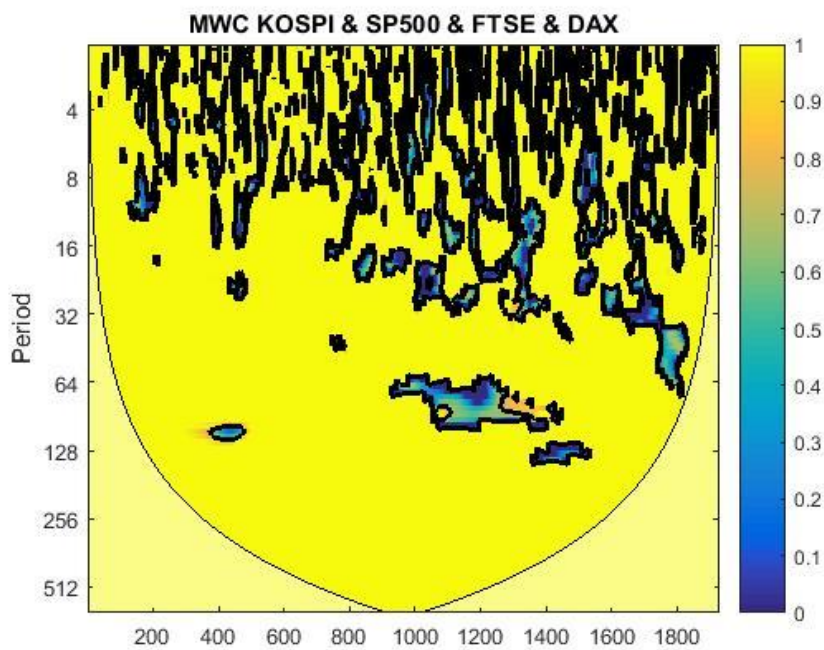


Figure 2.5. Multiple wavelet coherence of Kospi with SP500, FTSE and DAX

It is also intriguing to see that the high coherence is also true for South Korean stock market, even though the classical correlation calculations did not provide high correlation value compared to the other two Asian stock markets. Similar difference

between multiple wavelet coherence and correlation calculations is observed by Oral and Unal (2017) indicating better performance out of wavelet coherency analysis.

Multiple wavelet coherence helps us understand where the correlation is the highest on frequency and time space. According to these results, one may easily conclude that 256 day period at all-time intervals give the best coherent data which corresponds to octave value of 8 in the continuous wavelet transform. We extract the data at this specific period (frequency) and use it for the forecasting purposes.

The extracted and inversed data of all markets at octave value of 8 are plotted in Fig. 6. Now it is clearly possible to see even in bare eyes how all data is in coherence and moving together. This is also in line with the findings of Hyde et al (2007) that there is strong evidence to suggest that markets display common trends over the long term.

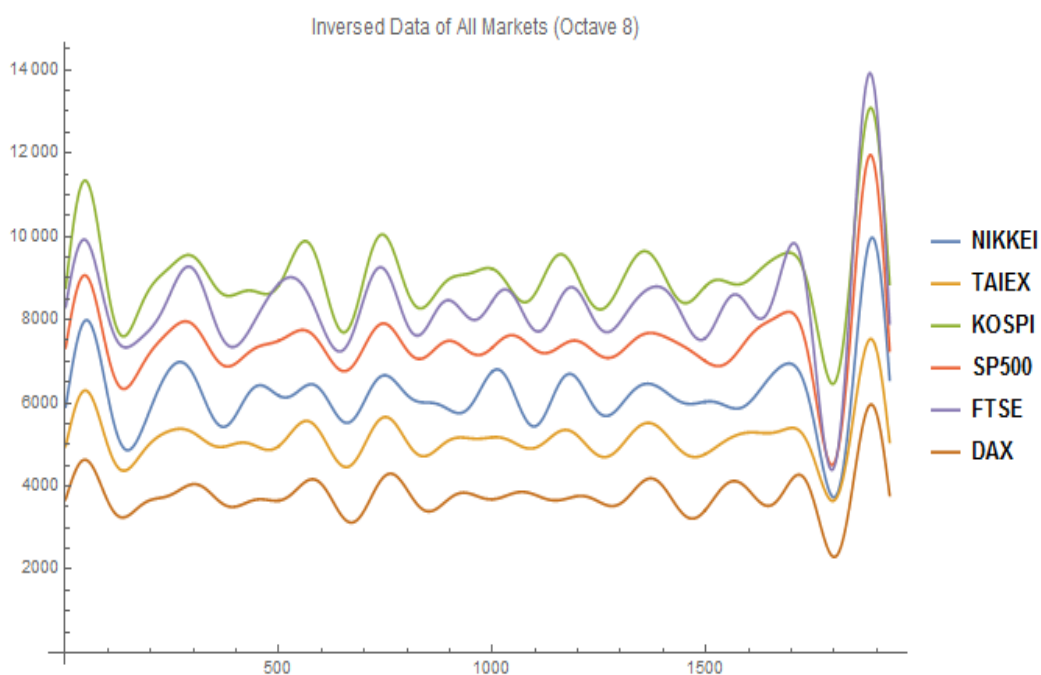


Figure 2.6. *Inversed Daily Data of All Markets at Octave Value of 8*

The correlation of the inversed data has now substantially increased including the South Korean stock market as shown in Table 3. Now we obtain a set of time series data where all markets are highly correlated with each other at all times.

Table 2.3.

Correlation of Inversed Daily Data of All Markets

	SP500	FTSE	DAX	NIKKEI	TAIEX	KOSPI
SP500	1	0.9691	0.9133	0.9514	0.9556	0.9398
FTSE	0.9691	1	0.9138	0.9309	0.9361	0.9259
DAX	0.9133	0.9138	1	0.8862	0.9503	0.9196
NIKKEI	0.9514	0.9309	0.8862	1	0.9398	0.9368
TAIEX	0.9556	0.9361	0.9503	0.9398	1	0.9859
KOSPI	0.9398	0.9259	0.9196	0.9368	0.9859	1

Since continuous wavelet transform returns errors on the edges due to the wavelet size exceeding the length of the data, we utilize the daily data from October of 2010 up to August of 2015 in order to avoid possible discrepancies.

2.4. Forecasting Trials, Results and Discussion

As stated earlier, the fundamental purpose of the finance market is to predict the price in the future. Hence employing efficient forecasting methods is very crucial. In this chapter, we are presenting this new approach where vector auto regressive moving average is combined with scale by scale continuous wavelet transform.

Each of the Asian market is correlated with SP500, FTSE and DAX. The data are selected from three different time intervals for each market and can be listed as following.

- NIKKEI stock market data are selected starting

- from September 29th, 2012 for 207 days (Fig. 7),
 - from March 22nd, 2012 for 331 days (Fig. 8), and
 - from June 12th, 2010 for 297 days (Fig. 9).
- TAIEX Stock market data are selected starting
 - from March 22nd, 2012 for 316 days (Fig. A.1),
 - from May 13th, 2010 for 333 days (Fig. A.2), and
 - from September 20th, 2010 for 413 days (Fig. A.3).
 - KOSPI stock market data are selected starting
 - from November 9th, 2010 for 289 days (Fig. A.4),
 - from June 21st, 2012 for 318 days (Fig. A.5) and
 - from July 7th, 2011 for 295 days (Fig. A.6).

They are split into frequencies scale by scale using continuous wavelet transform and the data corresponding with octave value 8, which equals to 256 day period, are selected to be inverted.

By doing so, we obtain time series data with the same frequency value moving along the same time frame. Hence, we have two different type of data set within the same interval for each period selected. One of them is the raw data as it is recorded daily and forecasted on its own. The other one is processed with continuous wavelet transform, inverted at a predetermined scale and then forecasted using vector auto regressive moving average.

It is important to note that the data extracted has set of values less than the original value due to the nature of continuous wavelet transform. In order to compensate the forecasting difference in data, it is moved upward by the difference of the last value of the original data set and the first value of the forecasting result. Additionally, VARMA provides upper and lower boundaries as the number of

variables. Hence, we get 4 upper and 4 lower band vectors as a result. In this chapter, we filter the minimum values of the upper boundary and the maximum values of the lower boundary vectors and display them in our results.

One must also remember that using highly correlated data set is crucial; otherwise the forecasting results come out of charts. As it can be seen from the results of NIKKEI forecasting, VARMA, provides a narrower range of prediction with respect to univariate model of ARMA. This is due to the low variance value reached in the model which helps increase the precision of the forecasting. It can also be said that initial days of the VARMA forecasting are more successful as opposed to univariate model of ARMA model.

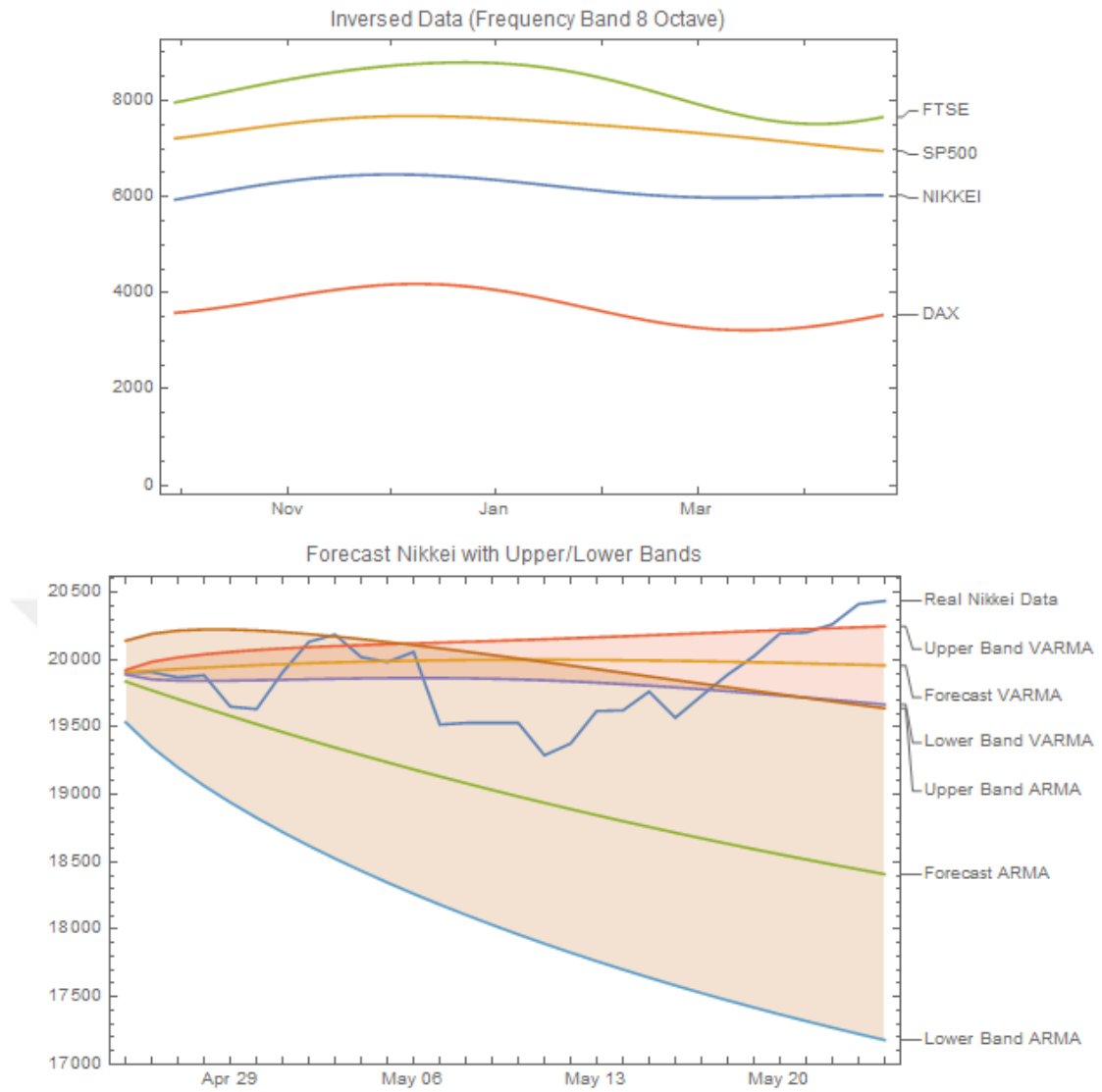


Figure 2.7. *Inversed data of markets starting from September 29th, 2012 for 207 days and forecast of Nikkei for the next 30 days*

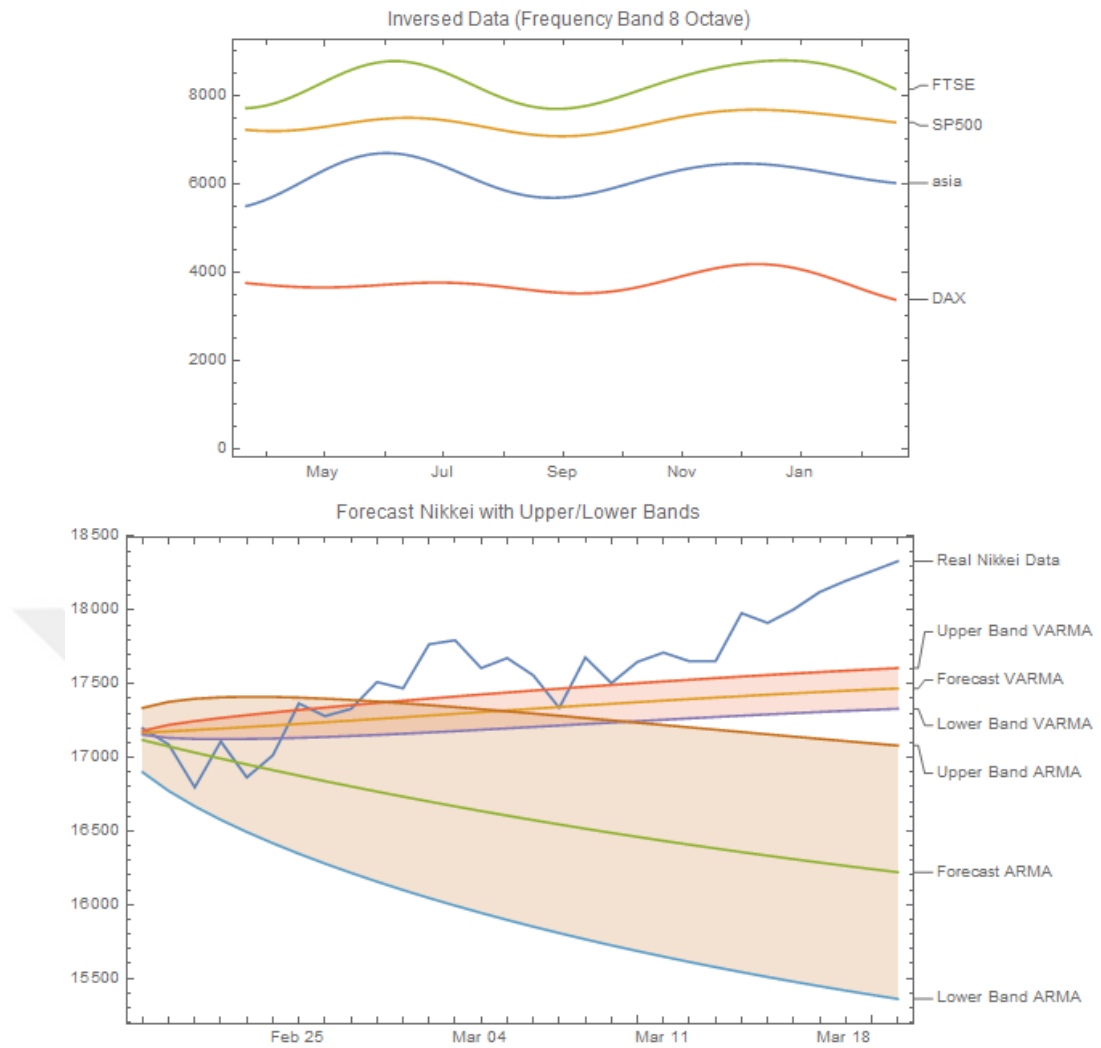


Figure 2.8. *Inversed data of markets starting from March 22nd, 2012 for 331 days and forecast of Nikkei for the next 30 days*

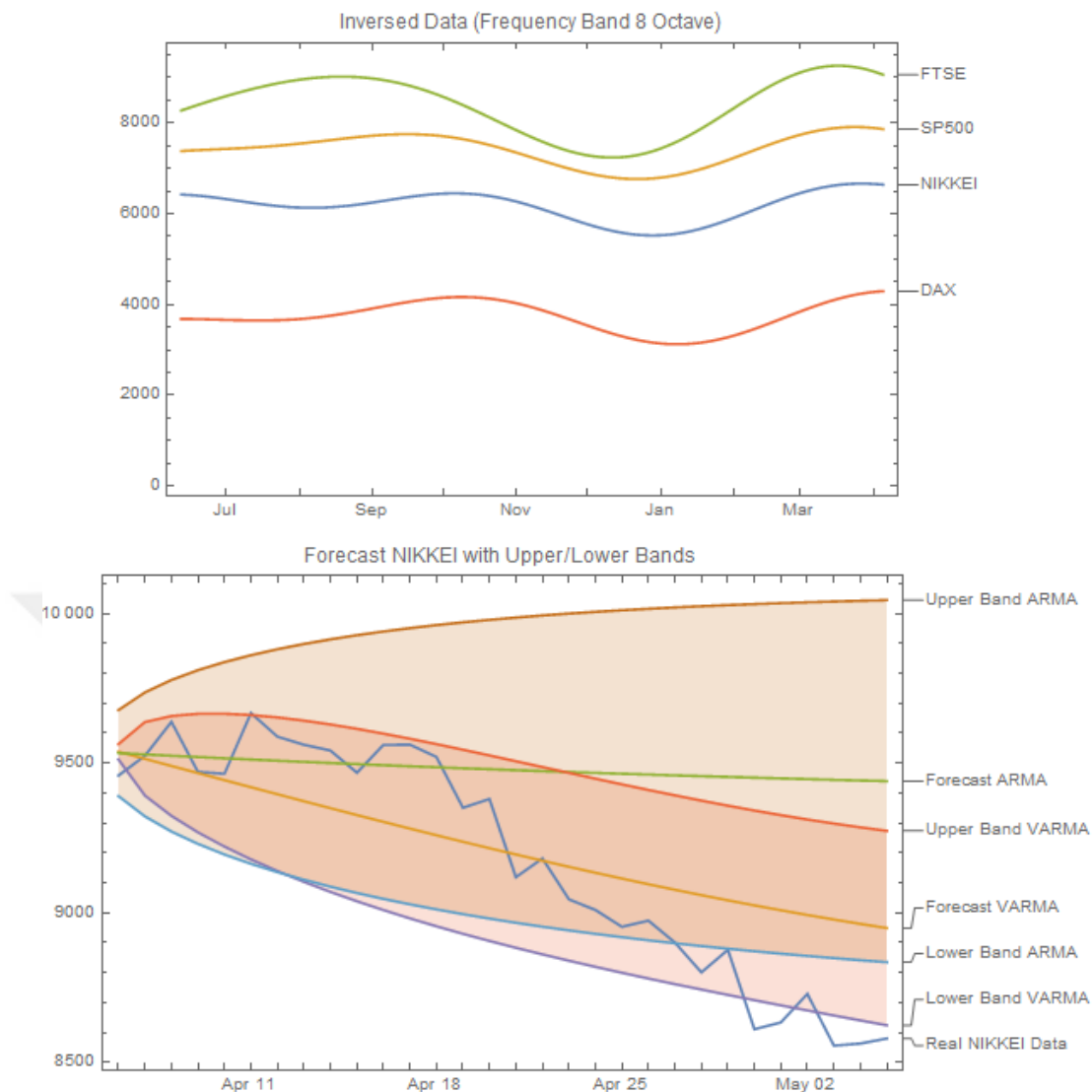


Figure 2.9. *Inversed data of markets starting from June 12th, 2010 for 297 days and forecast of Nikkei for the next 30 days*

2.5. Conclusion

It is seen that South Korea always has the highest correlation with the Taiwanese stock market. Taiwan follows the stock market movement in the developed countries closer with respect to other Asian markets. It can also be stated that Asian markets are more correlated with the markets of the developed countries than with each other from their own regions. This also coincides with the findings of Janakiraman and Lamba (1998) and Cha and Cheung (1998). Nevertheless, one can

conclude that the multiple wavelet coherence provides better and visual justification of in-phase relation in different data sets. The correlation between any data set may be explored more meticulously. We have seen that all three markets are highly correlated in low frequencies (longer periods) throughout the time frame.

Using VARMA model of highly correlated time series amply increases the performance of the forecasting. This directly coincides with the results obtained by Peña and Sanchez (2007) that the performances of multivariate ARMA models are relatively better with respect to univariate models. Furthermore, we were able to provide consistent results both with small size and larger size data set which agrees with the findings of Dias and Kapetanios (2011) that consistency in VARMA forecasting may be obtained regardless of the size of the data set.

In line with the findings of Oral and Unal (2017), multiple wavelet transform and continuous wavelet transform may be used to dissect the data scale by scale, obtain highly correlated data sets and use them to increase the efficiency of forecasting performance. By doing so, low mean squared errors are calculated which results with a narrow band of upper and lower limit. Moreover price movement trend is better predicted in terms of direction, increasing or decreasing course. As a result, using scale by scale wavelet transform allows any investor to pick time series data with higher correlation. This would allow VARMA forecasting perform with higher accuracy once the correlated data is determined as correct and accurate as possible. In conclusion, VARMA forecasting performance is increased remarkably by the use of scale by scale wavelet transform.

Appendix A. Inversed Data of Markets and Corresponding Forecasts for the Next 30 Days

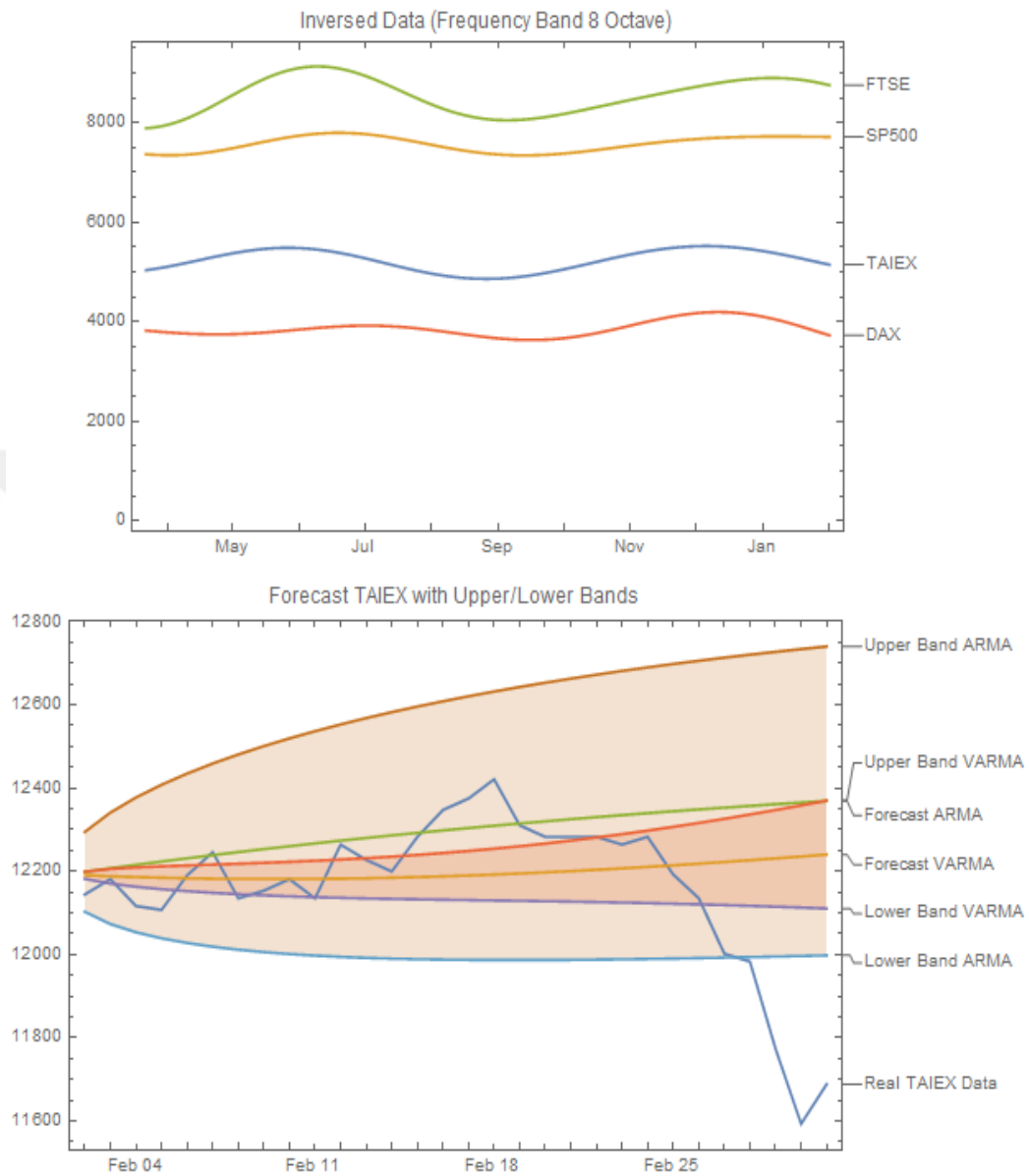


Figure 2.10. *Inversed data of markets starting from March 22nd, 2012 for 316 days and forecast of Taiex for the next 30 days*

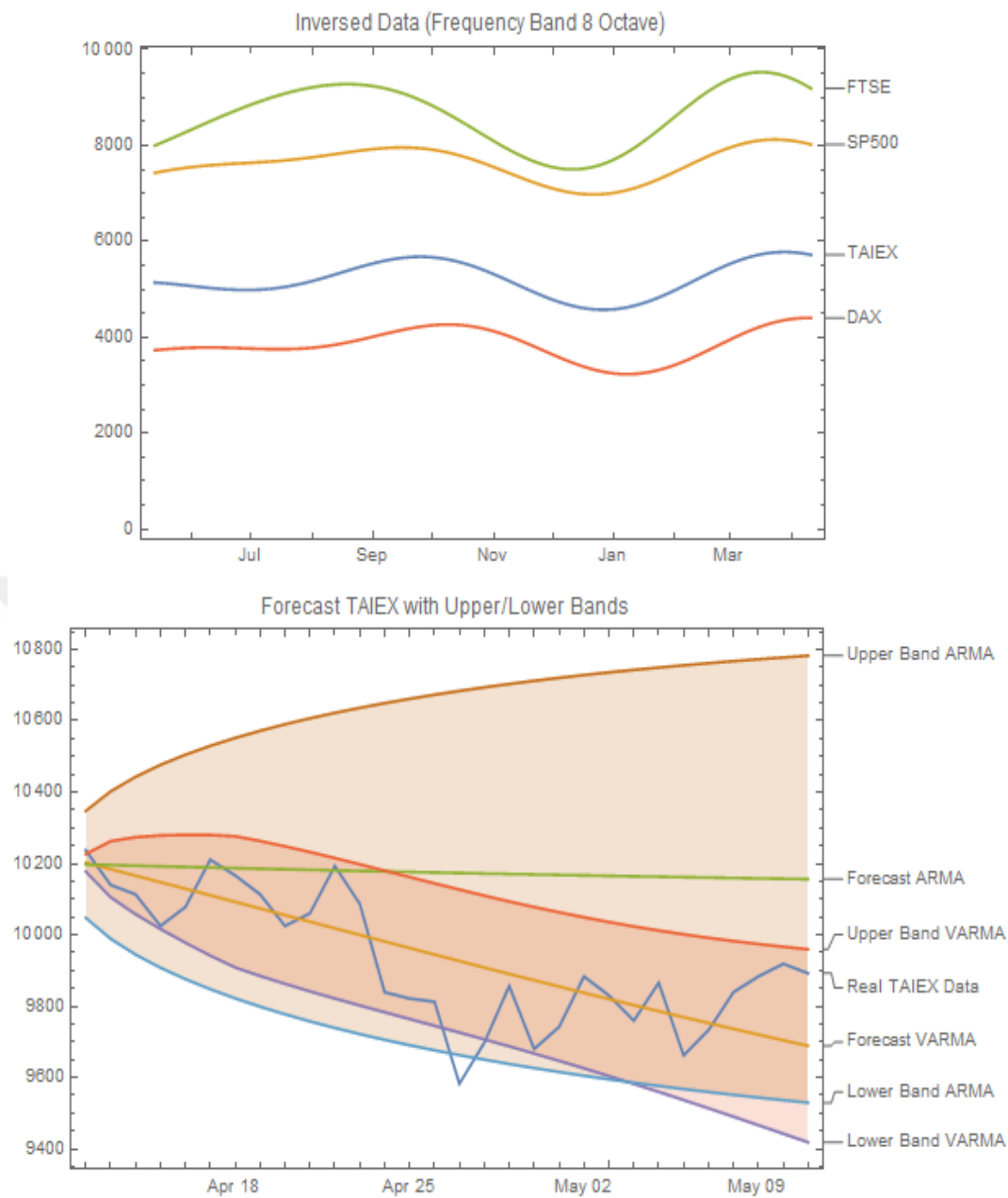


Figure 2.11. *Inversed data of markets starting from May 13th, 2010 for 333 days and forecast of Taiex for the next 30 days*

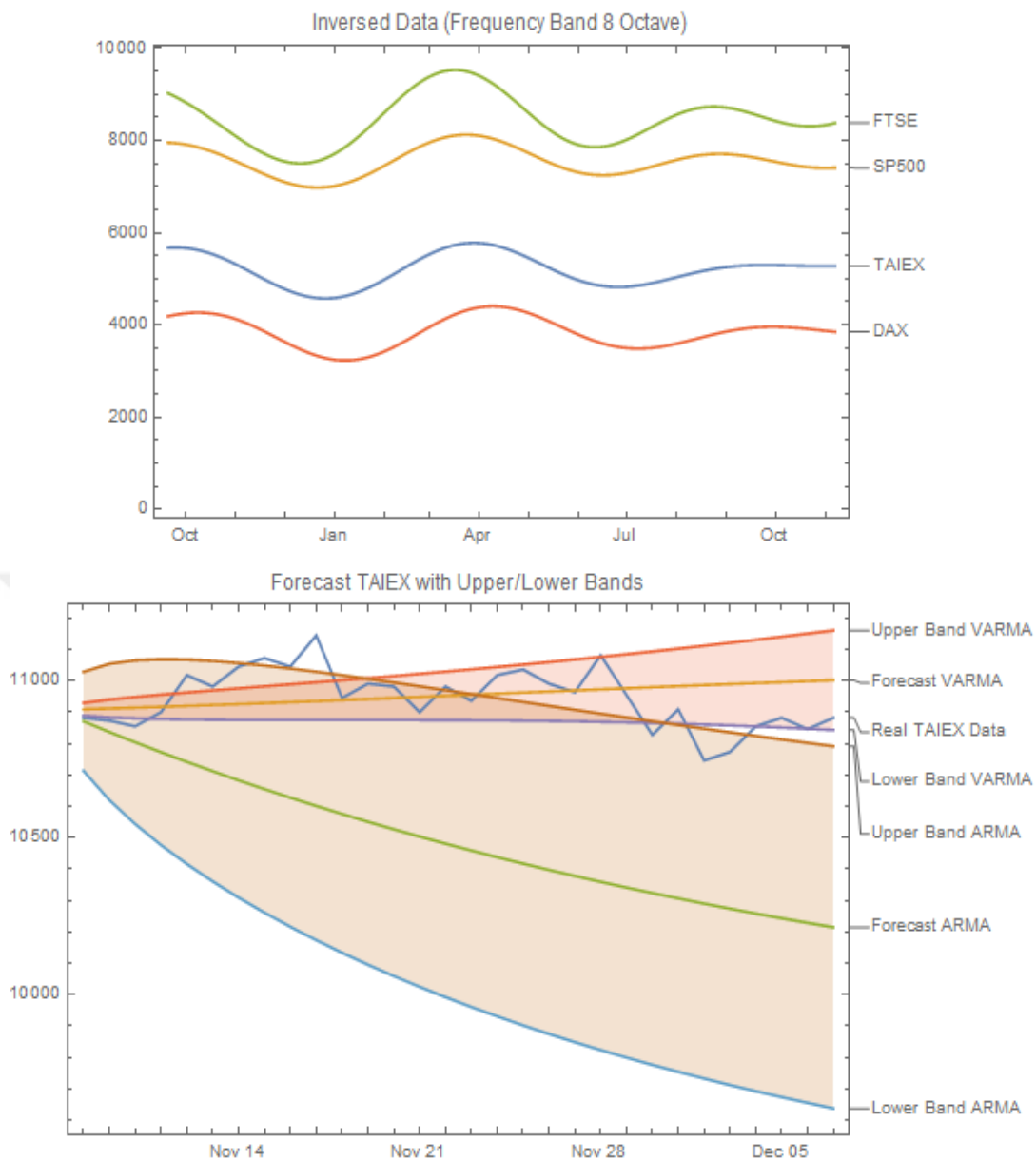


Figure 2.12. *Inversed data of markets starting from September 20th, 2010 for 413 days and forecast of Taiex for the next 30 days*

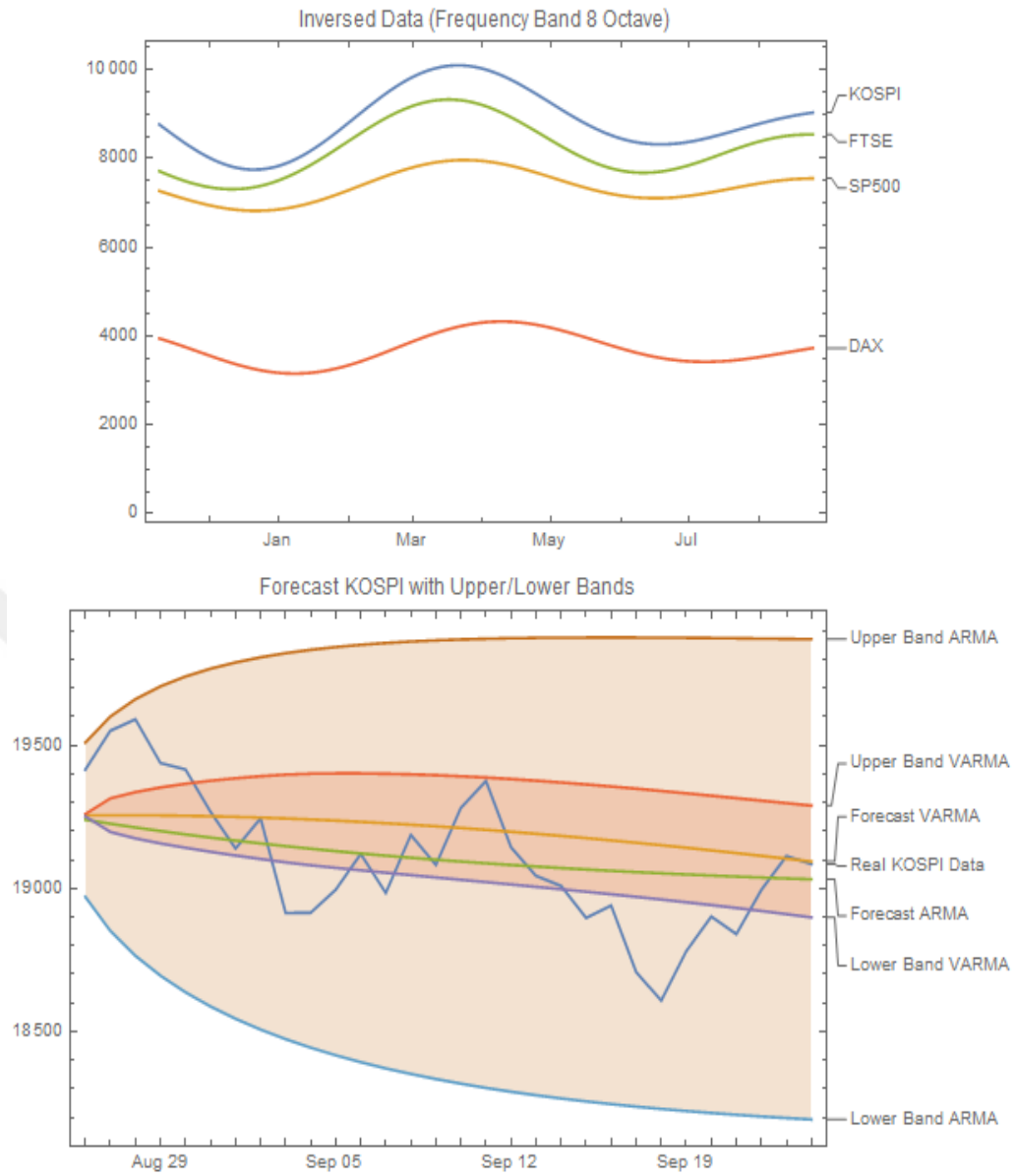


Figure 2.13. *Inversed data of markets starting from November 9th, 2010 for 289 days and forecast of KOSPI for the next 30 days*

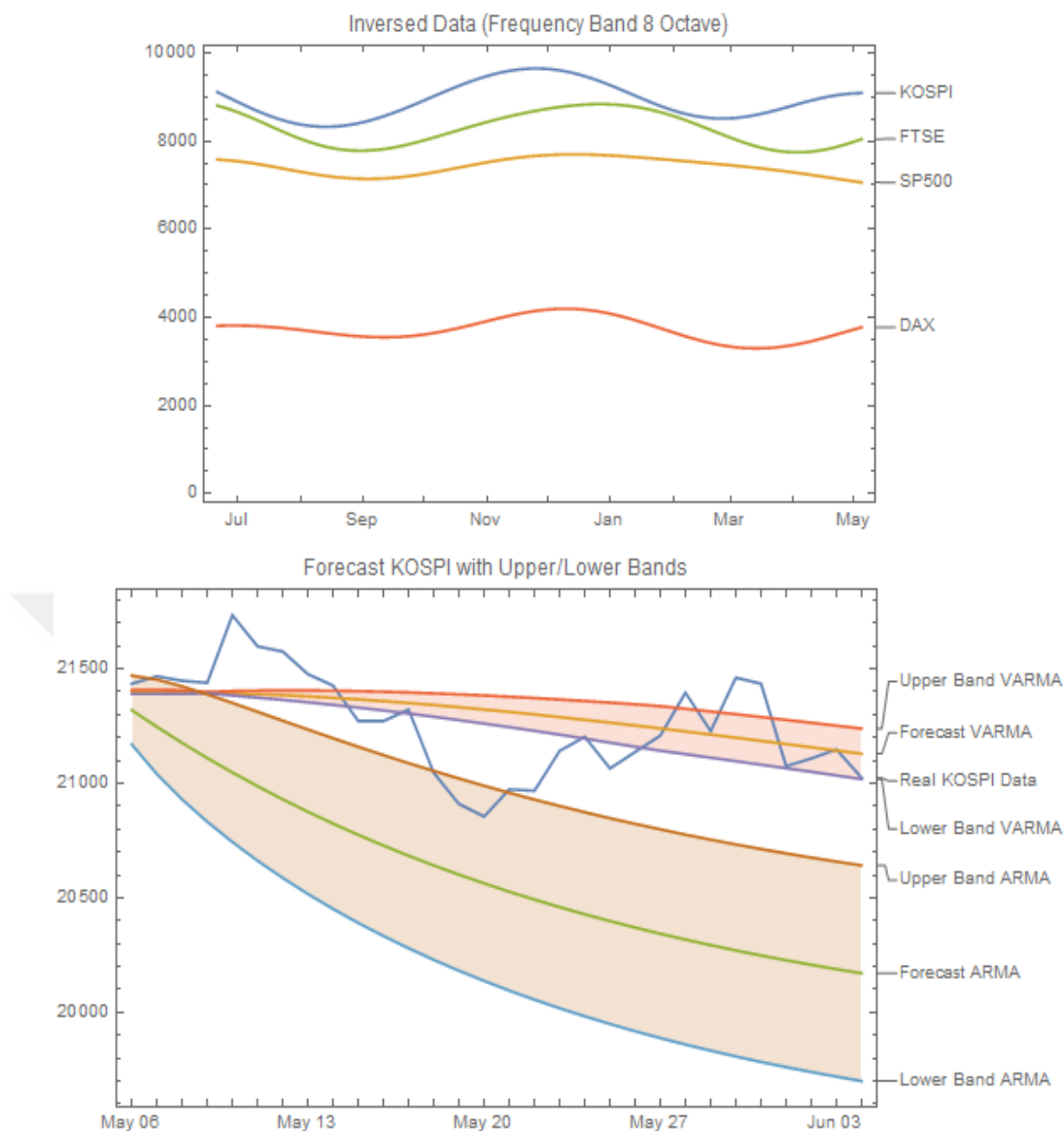


Figure 2.14. *Inversed data of markets starting from June 21st, 2012 for 318 days and forecast of Kospi for the next 30 days*

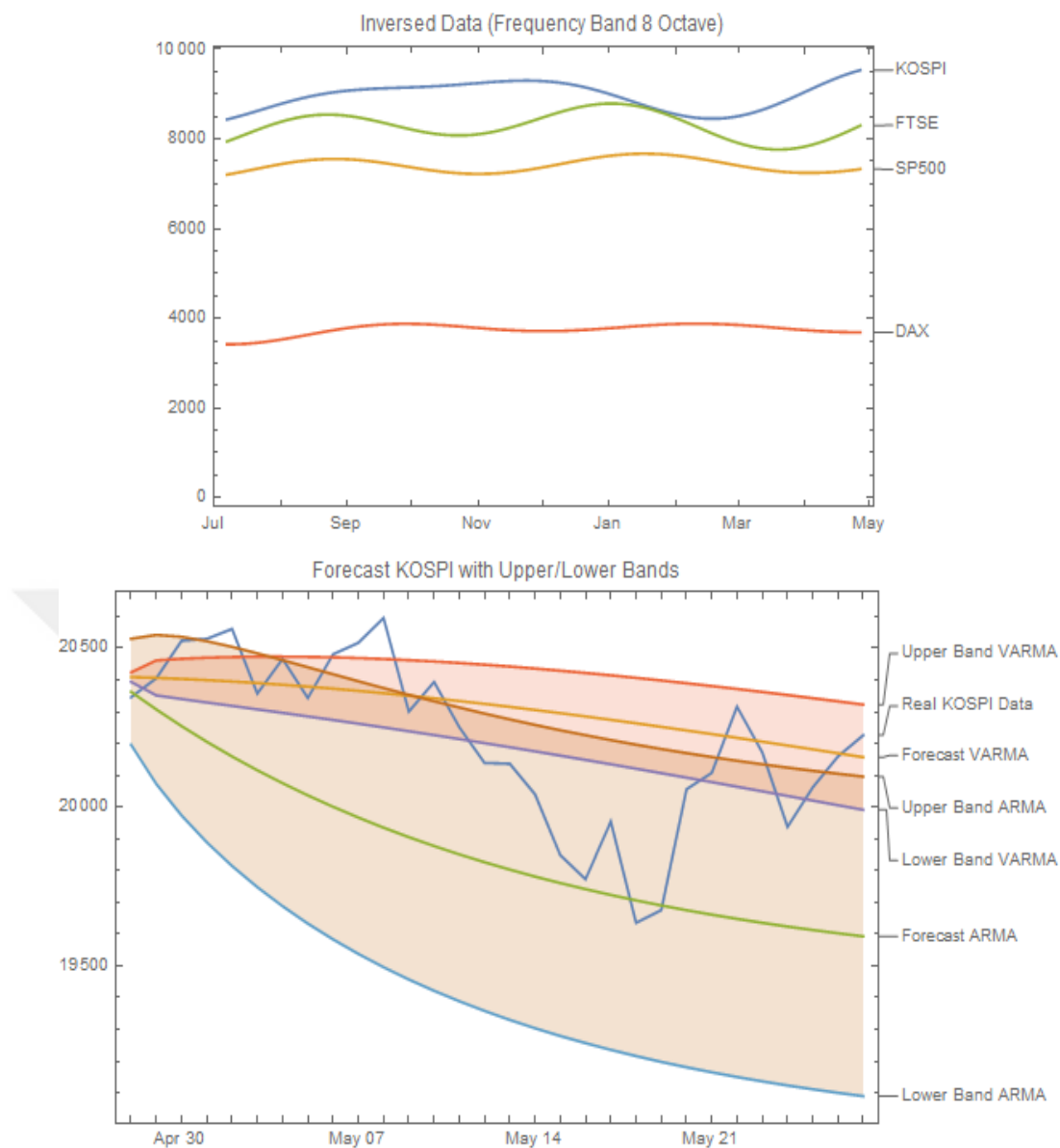


Figure 2.15. *Inversed data of markets starting from July 7th, 2011 for 295 days and forecast of KOSPI for the next 30 days*

CHAPTER 3

MODELING AND FORECASTING MULTIFRACTAL WAVELET SCALE: WESTERN MARKET vs EASTERN MARKET

Summary

This leading primary study is about modeling multifractal wavelet scale time series data using multiple wavelet coherence (MWC), continuous wavelet transform (CWT) and multifractal de-trended fluctuation analysis (MFDFA) and forecasting with vector autoregressive fractionally integrated moving average (VARFIMA) model. The data is acquired from Yahoo Finances!, which is composed of 1671 daily stock market of eastern (NIKKEI, TAIEX, KOSPI) and western (SP500, FTSE, DAX) markets. Once the co-movement dependencies on time-frequency space are determined with multiple wavelet coherence, the coherent data is extracted out of raw data at a certain scale by using continuous wavelet transform. The multifractal behavior of the extracted series is verified by multifractal de-trended fluctuation analysis and its local Hurst exponents have been calculated obtaining root mean square of residuals at each scale. This inter-calculated fluctuation function time series have been re-scaled and used to estimate the process with vector autoregressive fractionally integrated moving average (VARFIMA) model and forecasted accordingly. The results have shown that the direction of price change is determined without difficulty and the efficiency of forecasting have been substantially increased using highly correlated multifractal wavelet scale time series data.

3.1. Introduction and Literature Review

Economics is a man-made science. Since the invention of money, there has been a struggle in pricing. This struggle has increased enormously within the last century. The advanced technological developments today have brought it up to another dimension where it becomes an integrated matter of social sciences, technology and engineering at the same time. Hence there are many factors, persons, and goals affecting the price each day which causes it to move in fluctuations on many occasions dealing with different stress levels and shocks. That is why studying the price of any item in the market requires a particularized analysis that allows one to spot minute changes in different periods as well as scales.

There are many tools serving this purpose like Fourier transform. However, Fourier transform loses the time information as it looks deep into the frequency information of the data. We need to best utilize a method like wavelet analysis that does not need stationarity (Burrus et al., 1998) in the time series and does not lose the time information as it is able to go deep into the frequency information at different scales (Reboredo and Rivera-Castro, 2014). Wavelet analysis is one of the methods that are capable of keeping the time and frequency information at the same time, finding localized intermittent periodicities, and eliminating the weaknesses in Fourier transform as pointed by Gulerce and Unal (2016).

Wavelet analysis is another method in analyzing financial time series. Aguiar-Conraria and Soares (2011, 2014), McCarthy and Orlov (2012), Graham et al. (2013) and Barunik et al. (2013) have been using the leading work of Gencay (2002) in analyzing financial time series to determine correlation estimates across different time and periods in their studies. Multi-scale analysis is stated as one of the main applications of wavelet methods in finance and economics by Haven. (2012).

There have been many investigations exploring the relation of different markets using these tools. The Finnish stock market has been compared with other markets worldwide by Graham and Nikkinen (2011). The emerging stock markets across the world were analyzed by Graham et al. (2012). Rua and Nunes (2009) analyzed two major developed markets, US and Germany, engaging wavelet analysis to explore co-movement dependencies. Using multivariate autoregressive model, in phase movement of Asia-Pacific equity markets and the US has been investigated by Janakiramanan and Lamba (1998) and Cha and Cheung (1998). Loh (2013) investigated the co-movement of 13 Asia-Pacific stock market returns with that of European and US Stock market returns using wavelet coherence methods.

Kantelhardt et al. (2002) has proposed multifractal de-trended fluctuation analysis (MF-DFA) as an alternative method in scrutinizing financial time series. It is also accepted as a strong and dynamic technique due to its ability to detect multifractal behavior in non-stationary time series. Tas and Unal (2013) made a comparative study of multifractal detrended fluctuation analysis to detect multifractal character of natural gas daily returns. Benbachir and Alaoui (2011) performed the multifractal de-trended fluctuation analysis method to investigate the multifractal properties of the Moroccan Dirham with respect to the US Dollars. Thompson and Wilson (2014) performs an in-depth analysis of GE stocks and contrasting the results with those obtained using multifractal de-trended fluctuation analysis and using conventional time series models.

A software package for wavelet coherence analysis is provided by Torrence and Compo (1998) and Grinsted et al. (2004) in order to be able to examine in-phase movement, frequent and consistent signals in multiple time series. Moreover, a Matlab tool for multifractal de-trended fluctuation analysis has been introduced by

Ihlen (2012). Both of the methodologies will be used to study the inter relation of Asian Markets (Japan, Taiwan and South Korea) in comparison to developed markets (US, UK and Germany) and their multifractal behavior. Multiple wavelet coherence will display the inter relation of each eastern market with western markets and multifractal detrended fluctuation analysis will be used not only to confirm their multifractal behavior but also to access multifractal time series of these markets at the specific scale.

By the use of continuous wavelet transform, a specific time and scale interval retaining long range dependence will be extracted out of the time series. This will allow observing many exciting interrelationships in time-frequency space in a much detailed way than other methods as stated by Yilmaz and Unal (2016). The multifractal behavior of these series may be validated by the help of Matlab tool. The same tool may be used to obtain a brand-new series out of local Hurst exponent calculations. It is this section`s assumption that these new series will result in better forecasting performance using vector autoregressive fractionally integrated moving average (VARFIMA) model with respect to autoregressive fractionally integrated moving average (ARFIMA) model.

All markets do possess highly heteroskedastic, non-linear and unit root behaviors due to different speculators, hedgers, investors, traders playing role with different goals on different terms and specifications. This makes it harder to estimate the price on the next day. Hence improving the forecasting performance of different methods has been one of the primary goals of financial engineering. Both univariate and multivariate models have been offered in the past. Quenouille has introduced the first multivariate model in 1957 which is later improved by Akaike (1974), Dunsmuir and Hannan (1976) and Hannan (1981). Oral and Unal (2017) underline that multivariate

models are a dynamic system of equations that examine the impacts of fluctuations (shocks) or correlations (interactions) between financial variables. Using more information out of multiple highly correlated data provides forecasting results with higher precision and multivariate models provide better results because of having low mean-squared errors compared to univariate models.

In following, data and methodology will be covered in section 2. Fundamental formulations of continuous wavelet transform and multiple wavelet coherence, basics of multifractal detrended fluctuation analysis and vector autoregressive fractionally integrated moving average will be introduced as a summary review. In section 3, multiple wavelet coherence will be utilized to reveal the inter relation of the markets and their movement dependencies on time-frequency space. Once the highly correlated time and scale interval is determined, the multifractal behavior of the time series will be validated. Out of inversed data set, a new set of data used in calculation of local Hurst exponents will be procured. In section 4, the forecasting results will be compared and discussed between multivariate and univariate models. Section 5 will conclude with the discussion of the results. In appendix A, 4D multiple wavelet coherence and 2D wavelet coherence results of eastern markets with each western markets will be presented. Appendix B will give local Hurst exponents at scale 256 for all markets along with the inversed data set and appendix C will display two forecasting results of each market couples, totaling 18 trials of forecasts.

3.2. Data

The data is acquired from Yahoo Finances!, which is composed of stock market indexes from eastern markets of Japan (NIKKEI), Taiwan (TAIEX), South Korea (KOSPI), and western markets of United States (SP500), United Kingdom

(FTSE) and Germany (DAX). It is composed of 1671 daily records of each market starting from March 10, 2009 as shown in Fig. 1.

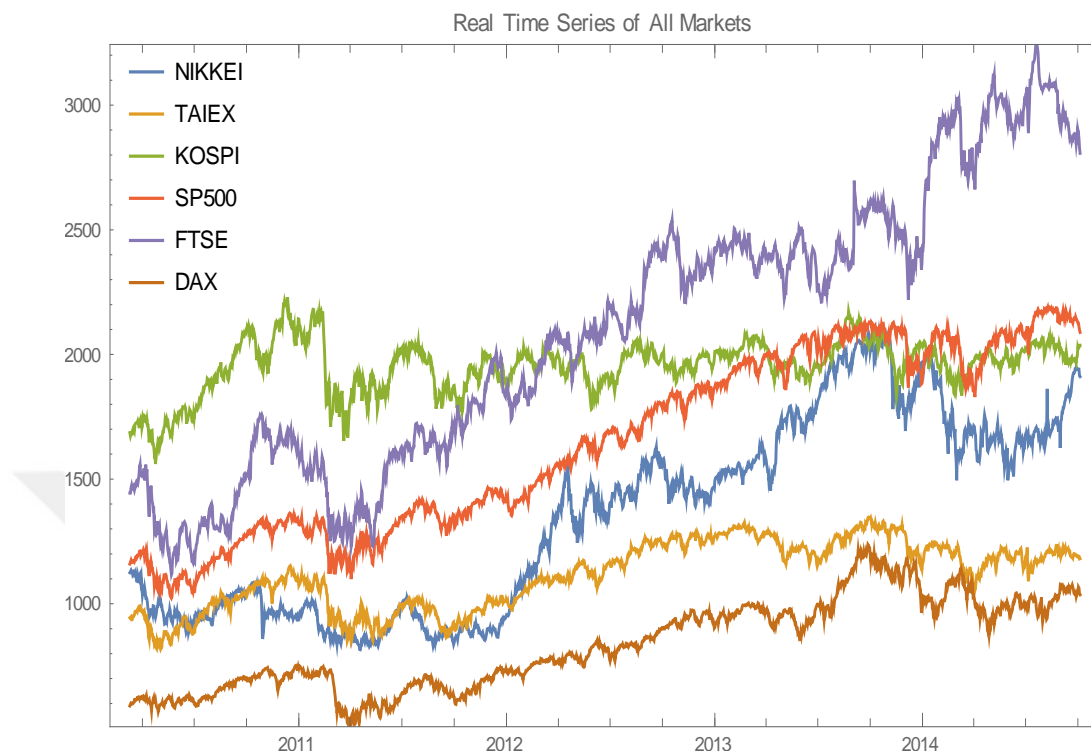


Figure 3.1. *Real Values of Each Stock Market*

As shown in Table 1, SP500, FTSE and DAX are highly correlated with each other and NIKKEI and TAIEX with the least correlation value of 83% and higher. On the other hand, KOSPI seems to have developed other factors influencing its market trend and does not demonstrate high correlation with the rest of the markets neither with markets in the east nor with markets in the west. South Korea has the least correlation with Japanese Market with the value of less than 50% and the highest correlation with Taiwanese market with the value of 78%.

Table 3.1.

Correlation Values of Each Market

	SP500	FTSE	DAX	NIKKEI	TAIEX	KOSPI
SP500	1	0.9689	0.9593	0.9178	0.9117	0.6675

FTSE	0.9689	1	0.9181	0.8604	0.8589	0.6476
DAX	0.9593	0.9181	1	0.9233	0.9102	0.6659
NIKKEI	0.9178	0.8604	0.9233	1	0.8302	0.4743
TAIEX	0.9117	0.8589	0.9102	0.8302	1	0.7775
KOSPI	0.6675	0.6476	0.6659	0.4743	0.7775	1

The data will be analyzed using wavelet transform and multiple wavelet coherence in order to detect a series of data possessing a higher correlation with each other. It is our assumption that this data will display multi fractal behavior. Once the multi fractal behavior is verified, we will look into the local Hurst exponents' series at the same scale detected by the wavelet coherence and use it to improve forecasting performances and compare the results with the traditional methods.

3.3. Methodology

3.3.1. Continuous Wavelet Transform (CWT) and Multiple Wavelet Coherence (MWC)

Gencay (2002) has introduced a new tool of wavelet application in finance and economics. More applications have been employed later by many researchers such as Aguiar-Conraria and Soares (2014), Barunik et al. (2013), Yilmaz and Unal (2016) and Oral and Unal (2017). Two essential wavelet methods are discrete and continuous wavelet transforms. However, Grinsted et al. (2004) states that CWT is used more for feature extraction purposes hence CWT is used to examine the frequency and time information of the time series. CWT is defined as in equation (1),

$$CWT_x^\psi(s, \tau) = \langle X, \psi(s, \tau) \rangle = \frac{1}{\sqrt{s}} \int_{-\infty}^{+\infty} X(t) \psi^* \left(\frac{t-\tau}{s} \right) dt \quad (1)$$

Where " ψ " the transforming is function also known as the mother wavelet, " τ " is the translation which corresponds with the time information and " s " is the scale

parameter which corresponds with the frequency information in the transform domain.

Additionally, bivariate case of wavelet coherence may be extended into multivariate models where four dimensional multiple wavelet coherence may be defined as in equation (2),

$$\begin{aligned}
C^d = & 1 - R_{12}^2 - R_{13}^2 - R_{23}^2 - R_{14}^2 - R_{24}^2 - R_{34}^2 + \rho_{12}\rho_{23}\rho_{31} + \rho_{13}\rho_{21}\rho_{32} + \\
& \rho_{12}\rho_{24}\rho_{41} + \rho_{14}\rho_{21}\rho_{42} + \rho_{23}\rho_{34}\rho_{42} + \rho_{24}\rho_{32}\rho_{43} + \rho_{14}\rho_{31}\rho_{43} + \rho_{13}\rho_{24}\rho_{41} + \\
& \rho_{14}\rho_{23}\rho_{32}\rho_{41} - \rho_{13}\rho_{24}\rho_{32}\rho_{41} - \rho_{12}\rho_{23}\rho_{34}\rho_{41} - \rho_{14}\rho_{23}\rho_{31}\rho_{42} + \rho_{13}\rho_{24}\rho_{31}\rho_{42} - \\
& \rho_{13}\rho_{22}\rho_{34}\rho_{42} - \rho_{12}\rho_{24}\rho_{31}\rho_{43} - \rho_{14}\rho_{21}\rho_{32}\rho_{43} + \rho_{12}\rho_{21}\rho_{34}\rho_{43}
\end{aligned} \tag{2}$$

Where C denotes complex coherence, R^2_{ij} is squared multiple wavelet coherencies. For details of these methods, the reader may look into the articles, “dynamic correlation of eastern and western markets and forecasting: Scale-by-scale wavelet-based approach (Oral and Unal, 2017)” and “co-movement of precious metals and forecasting using scale by scale wavelet transform (Oral and Unal, 2017).”

3.3.2. Multifractal De-Trended Fluctuation Analysis (MF-DFA).

Fractal structures and behavior are found in all financial time series data. Multi fractal analysis identifies the deviations in fractal structure within time periods with large and small fluctuations (Ihlen 2012). The MF-DFA method is a robust and powerful technique which is proposed by Kantelhardt et al. (2002) with the main advantage of allowing multifractal behavior detection in non-stationary time series. The time series data $X(t)$ is assumed to be self-similar with Hurst exponent $H \geq 0$. For any $c > 0$ we have

$$X(ct) = c^H X(ct) \tag{3}$$

Where a process with $H < 0.5$ exhibits anti-persistence with short range dependence which means that an increase in the process is high likely to be followed by decrease

in the next time segment and vice versa. When $H > 0.5$, the time series exhibits persistence with long range dependence which means that successive non-overlapping time segment is more likely to have the same sign.

The MF-DFA consists of five steps. Let $X(t)$ be a time series of length N . First of all, the accumulated profile $y(i)$ of the time series $X(t)$ for $i=1, \dots, N$ is determined.

$$y(i) = \sum_{i=1}^N [X(i) - \bar{x}] \quad (4)$$

Where \bar{x} denotes the mean of the time series $X(t)$. Later, we divide the profile $y(i)$ into non-overlapping segments of equal length scale s , $N_s = \text{int}(N/s)$ rounding the number to the nearest integer, $\text{int}()$. In order to include a short part of the end of the profile, the same procedure starting from the end of the profile is repeated, giving $2N_s$ segments.

Each of the $2N_s$ segments are estimated with a local trend by fitting a polynomial to the data. Then, the variances are calculated by two formulas in terms of segment v . For each segment $v = 1, \dots, N_s$:

$$F^s(v, s) = \frac{1}{s} \sum_{i=1}^s [y((v-1)s + i) - p_v^n(i)]^2 \quad (5)$$

And for the reverse selection of each segment $v = N_s+1, \dots, 2N_s$:

$$F^s(v, s) = \frac{1}{s} \sum_{i=1}^s [y((N-v-N_s)s + i) - p_v^n(i)]^2 \quad (6)$$

Where $p_v^n(i)$ is the n^{th} order fitting polynomial in the segment order, v . Linear, quadratic, cubic or higher order polynomials can be used for $n > 3$. Next, the variances over all segments will be averaged in order to obtain q^{th} order fluctuation functions which is defined as equation (7) for $q \neq 0$:

$$F_q(s) = \left[\frac{1}{2N_s} \sum_{v=1}^{2N_s} [F^2(v, s)]^{q/2} \right]^{1/q} \quad (7)$$

And if for $q=0$, the equation is evaluated as in equation (8)

$$F_0(s) = \exp \left[\frac{1}{2N_s} \sum_{v=1}^{2N_s} \ln [F^2(v, s)] \right] \quad (8)$$

The main purpose of the MF-DFA function is to determine the behavior of the q -dependent fluctuations $F_q(s)$ with regard to the time scale s , for various values of q . For different values of time scales s , the equations 5 thru 8 should be run repeatedly in order to be able to analyze the multi-scaling behavior of the fluctuation functions $F_q(s)$. This will be obtained by estimating the slope of log-log plots of $F_q(s)$ with respect to s for different values of q , such as -3, -2, -1, 0, 1, 2, 3. If long-range power-law correlation as fractal proprieties is analyzed, fluctuation function $F_q(s)$ will behave as the following power-law scaling

$$F_q(s) \sim s^{h(q)} \quad (9)$$

For different values of q , $h(q)$ is regressed on the time series $F_q(s)$. if $h(q)$ is a constant value for all values of q , then the time series is said to be monofractal. Contrarily, if $h(q)$ is a steadily decreasing function of q then the time series is said to be multifractal. For positive (negative) values of q , the Hurst exponents $h(q)$ describe the scaling properties of large (small) fluctuations. As Ihlen (2012) stated the small (larger) local Hurst exponents in the periods of the multifractal time series with local fluctuation of large (small) magnitudes reflects the noise (random walk) like structure of the local fluctuations. It is therefore consistent with the generalized Hurst exponents for negative and positive q 's, respectively. Nevertheless, the local Hurst exponent is able to recognize structural changes within time series instantly. This is the main advantage with respect to generalized Hurst exponent.

3.3.3. Vector Autoregressive Fractionally Integrated Moving Average (VARFIMA)

Vector autoregressive fractionally integrated moving average (VARFIMA) models allows us to simultaneously address the long-run effects as well as the short and long term dynamics characterized by the AR, MA and the fractional differencing

parameters (Tsay, 2012). It has been a useful tool for many time series observations, including Sowell (1989) and Dueker and Startz (1998), Box-Steffensmeier and Tomlinson (2000), Clarke and Lebo (2003) and Durr et al. (1997). The ARFIMA(p,d,q) process can be described by the difference equation in (10)

$$(1 - a_1 E_{|t_n-1|} - \dots - a_p E_{|t_n-p|})(1 - E_{|t_n-1|})^d y(t) = (1 + b_1 E_{|t_n-1|} + \dots + b_q E_{|t_n-p|})e(t) \quad (10)$$

where $y(t)$ is the state output, $e(t)$ is the white noise input, and E is the shift operator. An n-dimensional vector ARFIMA process should have real coefficients matrices a_i , and b_j of dimensions $n \times n$, real integrating parameter d_i such that $-0.5 < d < 0.5$, and the covariance matrix Σ should be symmetric positive definite of dimensions n by n . The vector ARFIMA process has transfer matrix $g(z^{-1})$ where $g(z)$ function can be defined as (11)

$$g(z) = \left((I_n - a_1 z - \dots - a_p z^p) \cdot (I_n - z)^d \right)^{-1} (I_n + b_1 z + \dots + b_q z^q) \quad (11)$$

where I_n is the n by n identity matrix. Equation (11) can now be written in summary notation as

$$A(E)(I - E)^d y(t) = M(E)\varepsilon(t) \quad (12)$$

Where E is the lag operator and $A(z) = (A_0 - A_1 z - \dots - A_p z^p) \cdot (A_0 - z)^d$ and $M(z) = M_0 + M_1 z + \dots + M_q z^q$. Equation (12) can be written as follows:

$$y(t) = M(E)\{A^{-1}(E)(I - E)^{-d}\varepsilon(t)\} = M(E)\xi(t) \quad (13)$$

This means a two-step of calculation for $\xi(t)$ first and then for $y(t)$.

From here, we see that VARFIMA model can be reduced in a straightforward way to a set of n interrelated ARFIMA models. Hence, when we rewrite equation (12), we get

$$y(t) = M(E) \frac{1}{|A(E)|(I-E)^d} A^*(E)\varepsilon(t) \quad (14)$$

Where $|A(E)|$ is the scalar valued determinant of $A(E)$ and $A^*(E)$ is the adjoint matrix. The process becomes

$$|A(E)|(I - E)^d y(t) = M(E)A^*(E)\varepsilon(t) \quad (15)$$

where a system of n-dimensional ARFIMA process is defined with the common lag operator, E and co-integration fraction, d .

3.4. Empirical Analysis

Wavelet coherence displays the time series information in frequency and time space. The x axis displays the time information and the y axis displays the frequency information. The frequency and period/scale information are the same but inversely proportional. The low frequency means higher scale/period of the information or vice versa. As the scale gets higher, the longer periods of data set is taken into account. The warmer yellow colors in the figure indicate higher correlation area. The cooler blue colors mean no correlation during the time and frequency period. The power of correlation is shown in the column on the right where 1(one) indicates highest correlation and 0 (zero) indicates no correlation. The black lines display the statistical significance at 5% level against the red noise in the time-frequency space on the graph. The faded area is due to the discontinuities in the wavelet function since the shape of the wavelet may exceed the length of the data (Unal and Yilmaz, 2016). This area may return wrong estimations and is accepted at the outside of the cone of influence (COI).

Wavelet coherency is a great tool to understand where the correlation is higher in time and frequency space. As shown in Figure 2, there are blue regions found with less significance between 2 to 128 day periods. On the other hand, Nikkei is found to be correlated with each western market between 128 and 256 day periods at all times. Four dimensional multiple wavelet coherence results for other markets are shown in

Fig. A1 and A3 in the appendix section where they all move in coherence on 256 day period at all times.

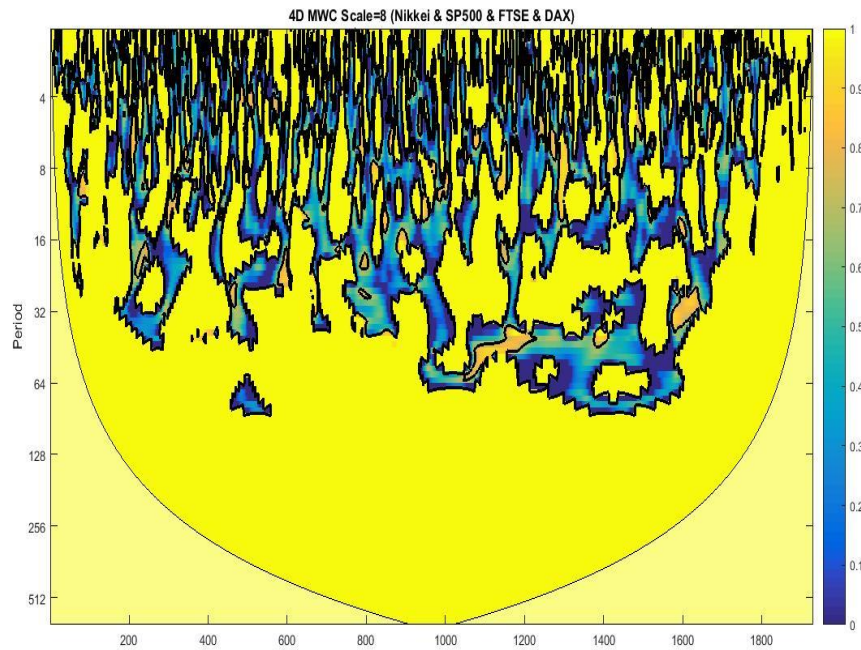


Figure 3.2. *Multiple wavelet coherence of Nikkei with SP500, FTSE and DAX*

According to these results, we were able to point out that all time-series of each market are highly correlated around 256 day period, which corresponds to octave value of 8 (scale 256) in the wavelet transform. Hence we inversed the data at this specific scale neglecting the other scales and obtained the following time series as shown in Fig. 2.

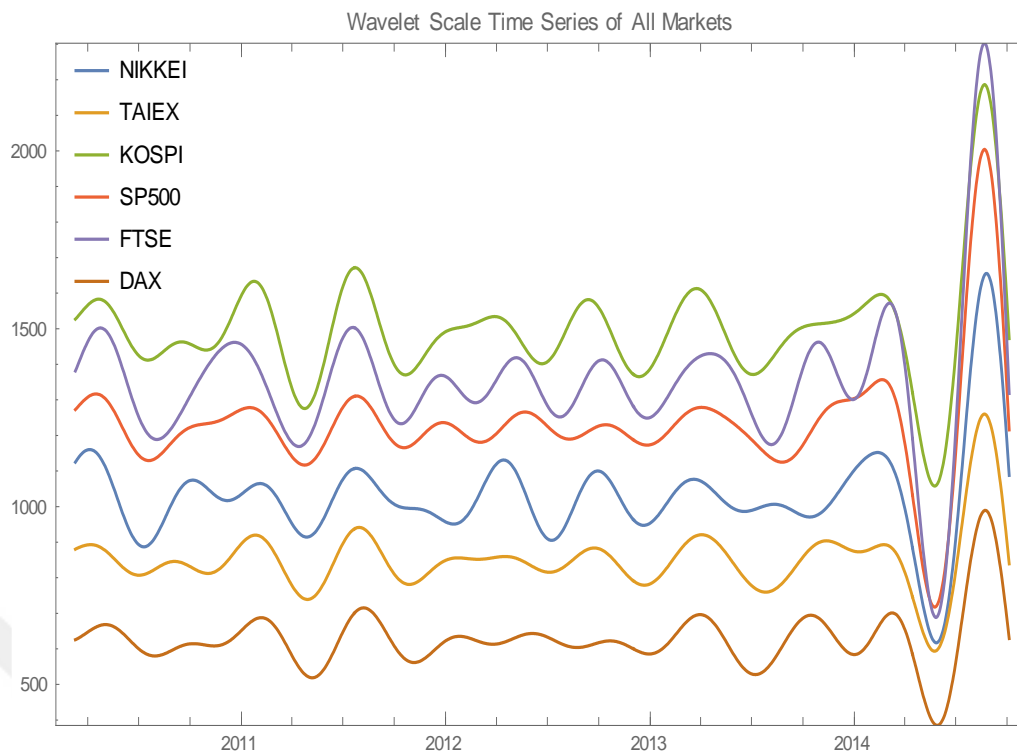


Figure 3.3. *Extracted Values of Indexes (Scale 256)*

When we examine the wavelet coherency of extracted values of Nikkei with each western market, we find out that all series are correlated at 256 day scale as shown in Fig. 4. We now discover that the inversed time series have higher correlation with respect to the raw data as seen in Table 3. In fact we have obtained a time series of Kospi with a correlation value of 91% and more with the rest of the markets. It is also realized that wavelet coherence provides a better tool to investigate the correlation between time series with respect to traditional correlation calculations. Instead of looking at the sole picture alone, wavelet coherence definitely helps locate the interrelated areas in time-frequency space in a broader manner and allows one to explore in much detail.

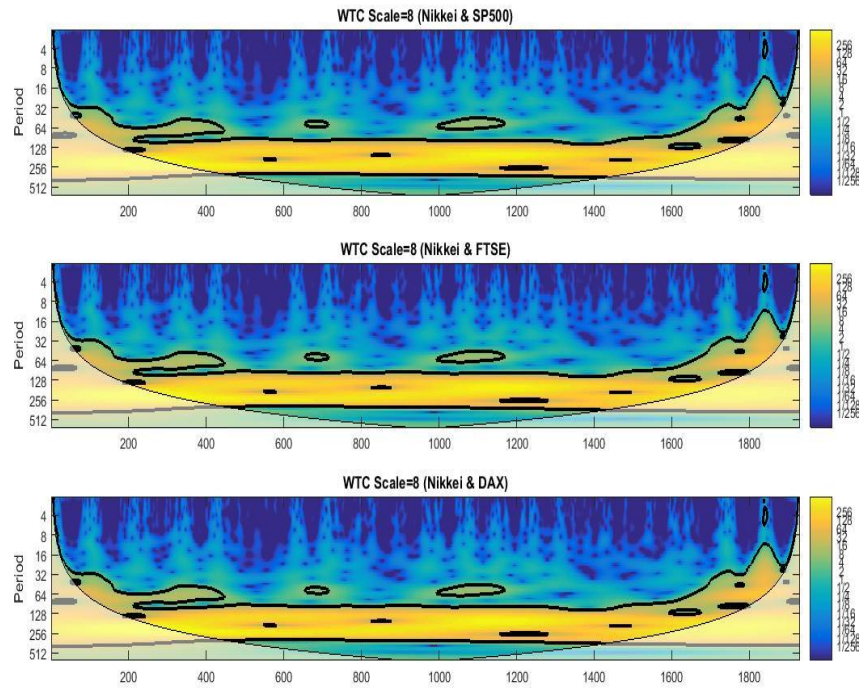


Figure 3.4. Wavelet coherence of inversed time series between Nikkei and each western market at Scale 256

Table 3.2.

Correlation Values of Extracted Indexes (Octave 8)

	SP500	FTSE	DAX	NIKKEI	TAIEX	KOSPI
SP500	1	0.9691	0.9133	0.9514	0.9556	0.9398
FTSE	0.9691	1	0.9138	0.9309	0.9361	0.9259
DAX	0.9133	0.9138	1	0.8862	0.9503	0.9196
NIKKEI	0.9514	0.9309	0.8862	1	0.9398	0.9368
TAIEX	0.9556	0.9361	0.9503	0.9398	1	0.9859
KOSPI	0.9398	0.9259	0.9196	0.9368	0.9859	1

The traditional method for calculating Hurst exponent takes the time series as one time period and provides a single value that indicates the global behavior of the

series. A time series has a long-range dependent (i.e., correlated) structure when the Hurst exponent is in the interval of 0.5–1 and an anti-correlated structure when the Hurst exponent is in the interval of 0–0.5. (Ihlen, 2012). It is our assumption that better forecasting performances are due to the multifractal behavior of the time series obtained. When the time series are multifractal, the data develops long range dependence. When we examine both of the data, raw and inversed, we realize that inversed data still possess the multifractal data properties as well as the raw data itself. Hurst exponent of the series at scale 256 is less than the Hurst exponent calculated for the real data however they are still more or less around 1 as shown in table 4. We found out that after extracting the inversed scale, the biggest Hurst exponent change (~35%) has occurred with SP500 from 1.47 to 0.96.

Table 3.3.

Hurst Exponent of Real and Inversed (Scale 256) Time Series

Hurst Exponents of Wavelet Scale Time Series (Octave 8)						
	NIKKEI	TAIEX	KOSPI	SP500	FTSE	DAX
Hurst Exponent Real Data	1.2398	1.3227	1.4195	1.4781	1.4124	1.3231
Hurst Exponent Scale 256	1.0517	1.0384	1.0637	0.9632	0.9665	1.0156
% Change	15.2%	21.5%	25.1%	34.8%	31.6%	23.2%

We will look at the fractional function series used to calculate the local Hurst exponents. The advantage of local Hurst exponent compared with traditional Hurst exponent is the ability of local Hurst exponent to identify the time instant of structural changes within the time series (Ihlen 2012). In Figure 5 (A-top), inversed wavelet transform data at scale 256 for Nikkei is shown and in Figure 5 (B-bottom), corresponding local Hurst exponents at scale 256 of Nikkei is shown. The inversed

data and corresponding local Hurst exponents of the other markets may be found in appendix B.

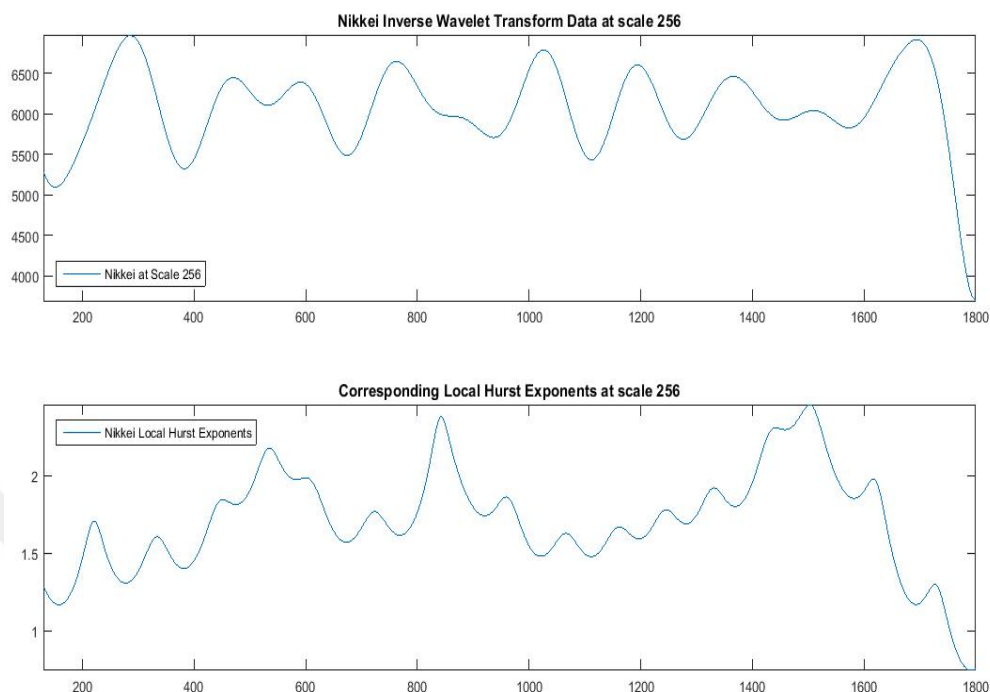


Figure 3.5. *Nikkei Inverse Data (A-top) and Corresponding Local Hurst Exponents at Scale 256 (B-bottom)*

The maximum and minimum local Hurst exponent of Nikkei at scale 256 was 2.4589 and 0.7461, respectively as shown in Table 5. In all the series obtained, the lowest local Hurst exponent belongs to the latest segment of the series, weakening in its long range dependence behavior day by day.

Table 3.4.

Minimum and Maximum Local Hurst Exponents at Scale 256

Min and Max Local Hurst Exponents at Scale 256

	NIKKEI	TAIEX	KOSPI	SP500	FTSE	DAX
Min H_{loc}	0.7461	0.8283	0.8761	0.5462	0.6317	0.7615
Max H_{loc}	2.4589	2.4595	2.6298	2.4161	2.1514	2.4499

In Fig. 6, the fluctuation function series used in the calculation of the local Hurst exponents at scale 256 are shown. The local Hurst exponents are calculated out of values found in fluctuation function.

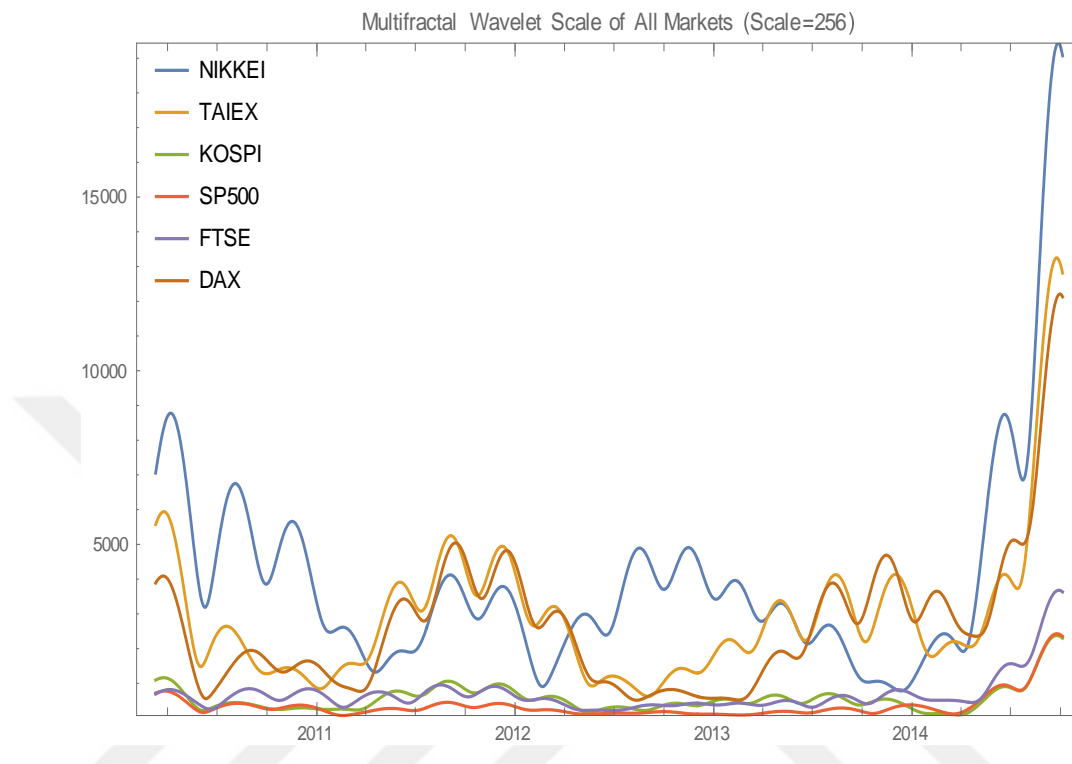


Figure 3.6. *The time series used to calculate local Hurst Exponents at scale 256*

We will be able to use these time series to forecast the prices for the next 30 days but first we needed to rescale them. We found the ratio between the first value of the series and the first value of the raw data and divided the whole series with that ratio. So we obtained a time series closer in ratio. Since the real raw time series data and time series data obtained at scale 256 are both demonstrating multi fractal behavior, we will use autoregressive fractionally integrated moving average (ARFIMA) model with the real data and vector autoregressive fractionally integrated moving average (VARFIMA) model to estimate a process and forecast the price for the next 30 days and compare the results accordingly.

3.5. Forecasting Results

As the dimension of the model increases, the VARFIMA models consider not only the historical data of each series but also other fractionally co-integrated variables in between the series. Hence, multivariate models leads to more accurate results compared to scalar counter models as Lutkepohl and Poskitt (1996) stated. That is why highly correlated data series is important to use in modeling in order to establish efficient estimated process for better forecasting performances. The forecasting performance of the raw data using ARFIMA process will be compared with the forecasting performance of the 2D VARFIMA process.

The data used in VARFIMA is obtained by the following these steps. Firstly, it is extracted out of raw data using scale by scale wavelet transform at scale 256. After the data is verified to be multi fractal, the local Hurst exponents are calculated. In this calculation, a fractional function is obtained with corresponding time series data. Finally, we use these calculated fluctuation function time series data in 2D VARFIMA model.

For each of the eastern market, we have forecasted two trials with each western market for a chosen time interval. The time intervals and their designated figures are listed in Table 5.

Table 3.5.

Dates used to forecast market prices

Forecasting Time Intervals							
		From	Days	Figure	From	Days	Figure
NIKKEI	SP500	12/24/2010	199	Fig. 3.25	12/19/2009	1275	Fig. 3.19
NIKKEI	FTSE	12/24/2010	215	Fig. 3.26	12/24/2010	706	Fig. 3.7
NIKKEI	DAX	11/19/2009	999	Fig. 3.27	11/19/2009	1199	Fig. 3.20

TAIEX	SP500	03/29/2010	385	Fig. 3.28	12/19/2009	803	Fig. 3.21
TAIEX	FTSE	03/29/2010	372	Fig. 3.29	12/19/2009	772	Fig. 3.22
TAIEX	DAX	11/14/2009	501	Fig. 3.39	11/14/2009	1001	Fig. 3.8
KOSPI	SP500	10/15/2010	776	Fig. 3.31	11/19/2011	478	Fig. 3.9
KOSPI	FTSE	07/07/2010	576	Fig. 3.32	03/29/2010	776	Fig. 3.23
KOSPI	DAX	12/19/2009	1176	Fig. 3.33	12/19/2009	875	Fig. 3.24

Even though we have shown that the time series data have long range dependence and multi fractal behavior, ARFIMA results have not resulted with good estimates. The forecasts with VARFIMA on the other hand have given very efficient results. Because of having two vector in the model, the upper and lower bands are given in couples. The highest band in the upper boundary and the lowest band in the lower boundary have been eliminated. In Figure 7-9, one can follow the efficiency of these estimates.

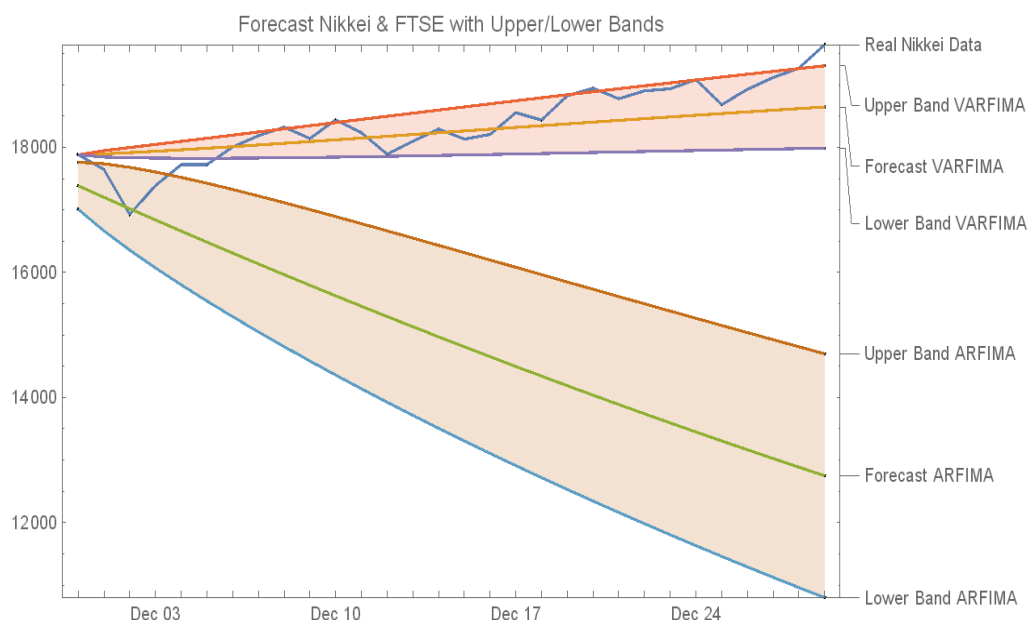


Figure 3.7. *Nikkei with FTSE Forecasting Results for the next 30 days data taken from December 24, 2010 for 706 days*

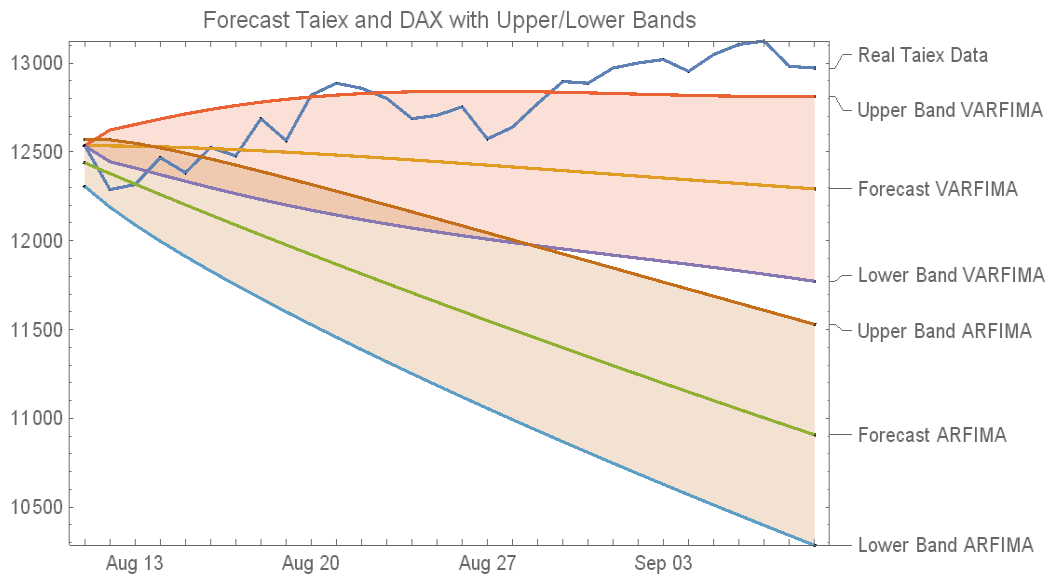


Figure 3.8. *Taiex with DAX Forecasting Results for the next 30 days data taken from November 14, 2009 for 1001 days*

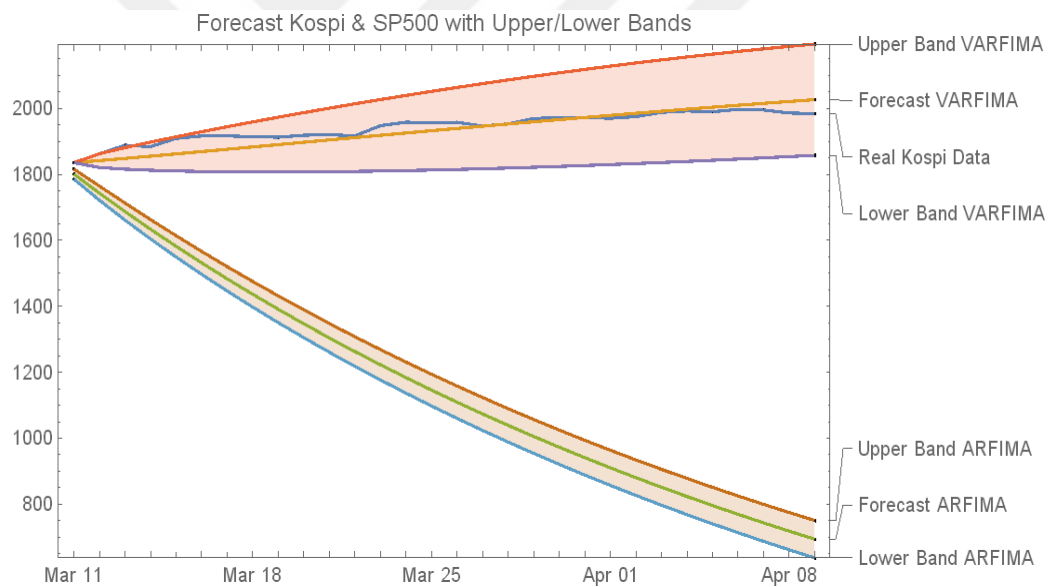


Figure 3.9. *Kospi with SP500 Forecasting Results for the next 30 days data taken from November 19, 2011 for 478 days*

One interesting point to make is that we have used data sets as little as 199 days and as high as 1275 days and we were still able to obtain results with efficient forecasts. This is aligning with the statement made by Dias and Kapetanios (2011) that consistent forecasting results may be obtained in VARMA regardless of the size of the dataset. We have shown that this is also true with VARFIMA process.

Furthermore, as stated by Oral and Unal (2017), the price change direction, either increasing or decreasing trend, have been indicated very efficiently.

3.6. Discussion and Conclusion

We have investigated the co-movement of eastern and western markets using multiple wavelet coherence and multifractal de-trended fluctuation analysis. We have shown that multiple wavelet coherence provides much better resolution with respect to traditional correlation methods to visualize correlation of different time series on various periods and time. As stated in Oral and Unal (2017), multiple wavelet coherence provides better and visual justification of in-phase relation in different states and the correlation between any dataset may be explored more meticulously.

Janakiramanan and Lamba (1998) and Cha and Cheung (1998) states that eastern markets demonstrate more in-phase movement with the western markets of the developed countries with respect to the markets in the eastern part of the world. Our findings also coincides that eastern markets have 90% or more correlation with the western markets. We have also shown that there is long range interdependence between all markets around 256 day period at all times.

Pena and Sanchez (2007) conclude that the multivariate models perform better with respect to the univariate models. We have reached the same conclusion that the forecasting performance of multifractal time series is remarkably increased by using VARFIMA model. These successful results were indifferent to small-size or larger-size data sets used which align with the findings of Dias and Kapetanios (2011).

We have seen that multiple wavelet coherence and continuous wavelet transform may be used to reach time series date sets with higher correlation as indicated by Oral and Unal (2017). Local Hurst exponents of the inversed time series are proven to be multifractal almost at all times. We realized that the lowest local Hurst exponents

values have been calculated during the latest periods for all the markets. It can be concluded that there has been a weakening trend in long range dependence in the markets and possessing less persistent structure. This indicates faster evolving variations in the prices or in other words, periods with large variations as Ihlen (2012) pointed. Furthermore, we have seen that the trend of the price change is also pointed correctly, increasing or decreasing direction. The last but not the least, we have also shown that the time series used to calculate local Hurst exponents can be used to model an estimated process using VARFIMA model and provide substantially better forecasting performance in comparison to its univariate form, ARFIMA.

**Appendix A. Multiple Wavelet Coherence of Real Data and Inversed Data of
Each Market with Western Markets**

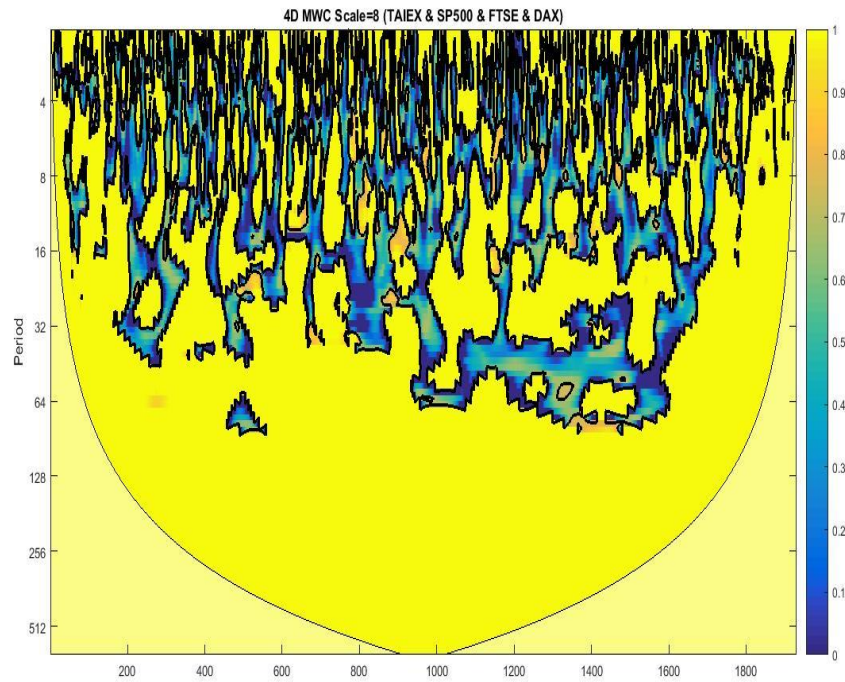


Figure 3.10. Multiple wavelet coherence of Taix with SP500, FTSE and DAX

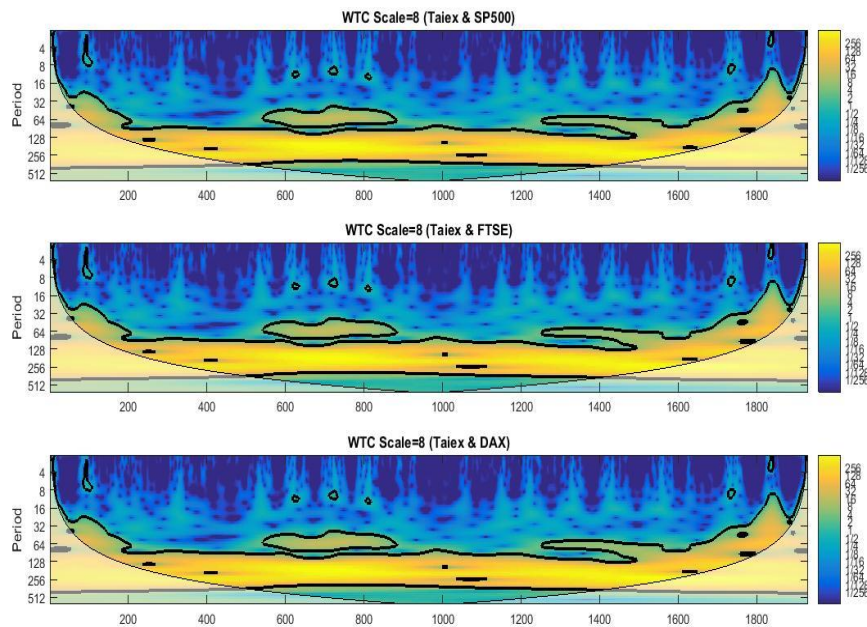


Figure 3.11. *Wavelet coherence of inversed time series between Taiex and each western market at Scale 256*

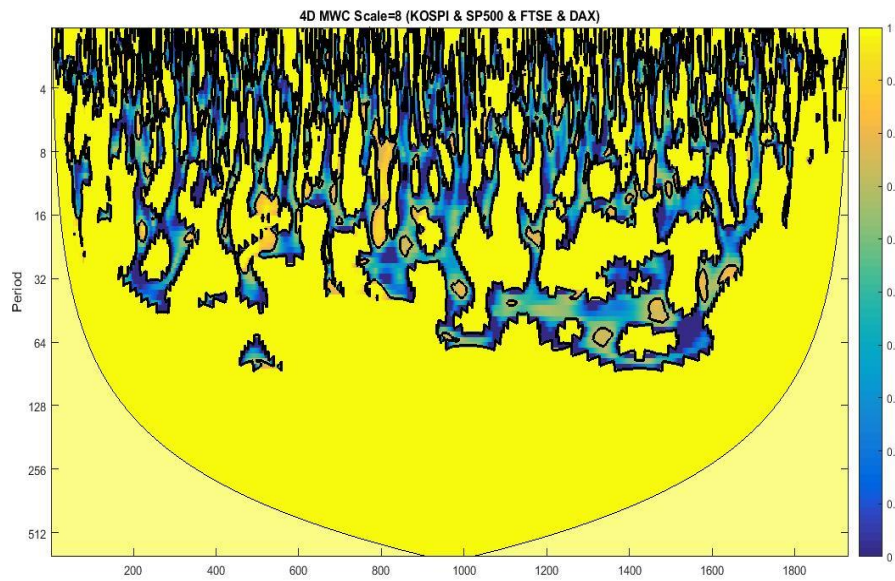


Figure 3.12. *Multiple wavelet coherence of Kospi with SP500, FTSE and DAX*

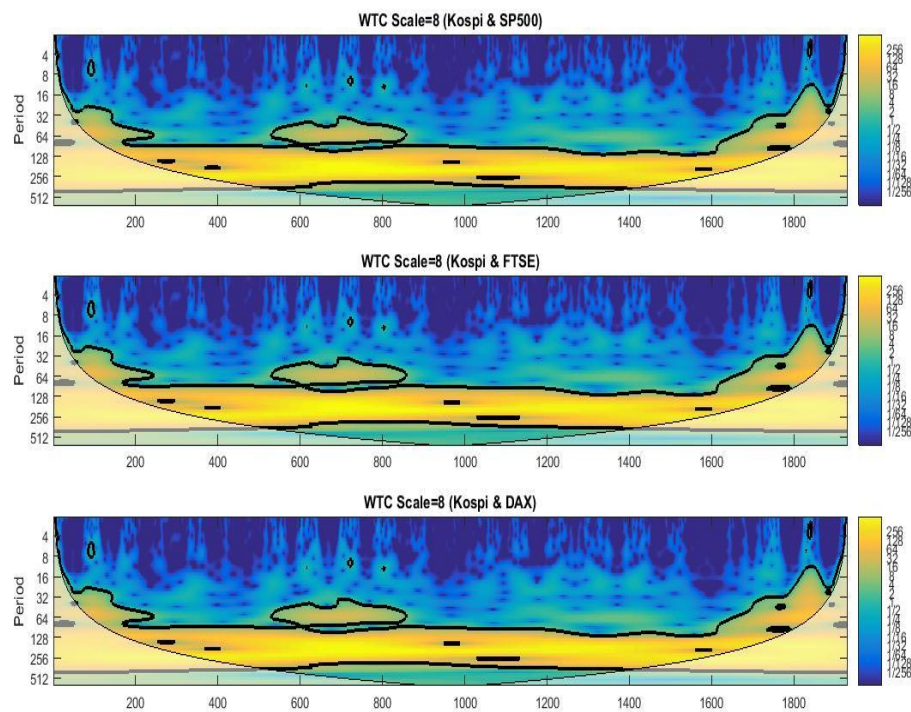


Figure 3.13. *Wavelet coherence of inversed time series between Kospi and each western markets at Scale 256*

Appendix B. Inversed Data and Corresponding Local Hurst Exponents

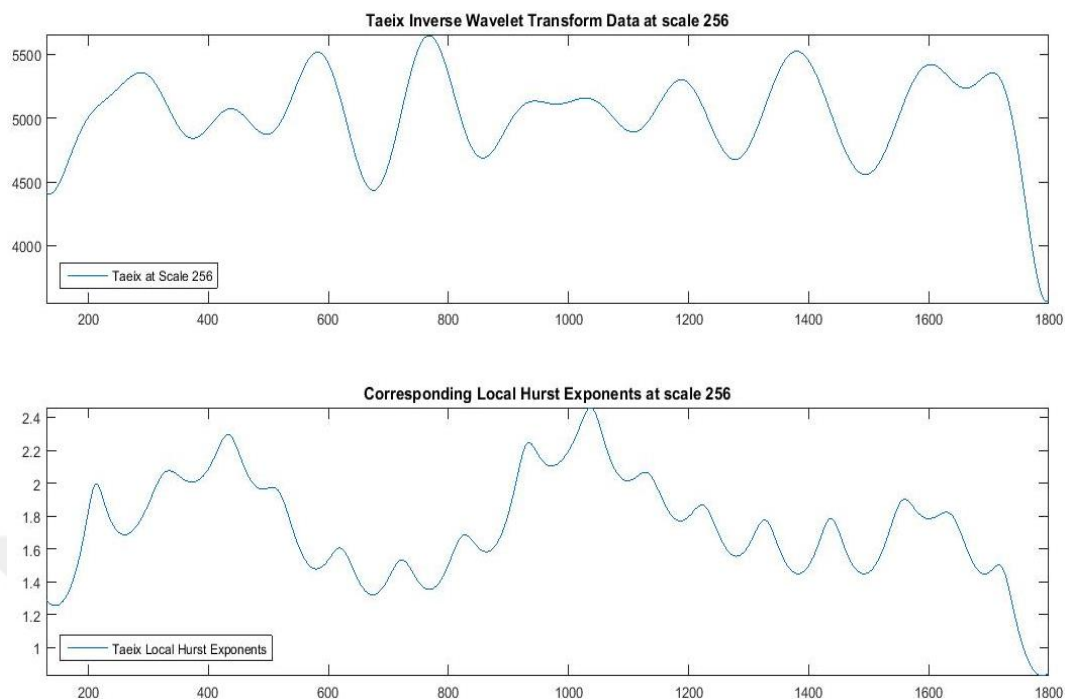


Figure 3.14. *Taiex Inverse Data and Corresponding Local Hurst Exponents at Scale 256*

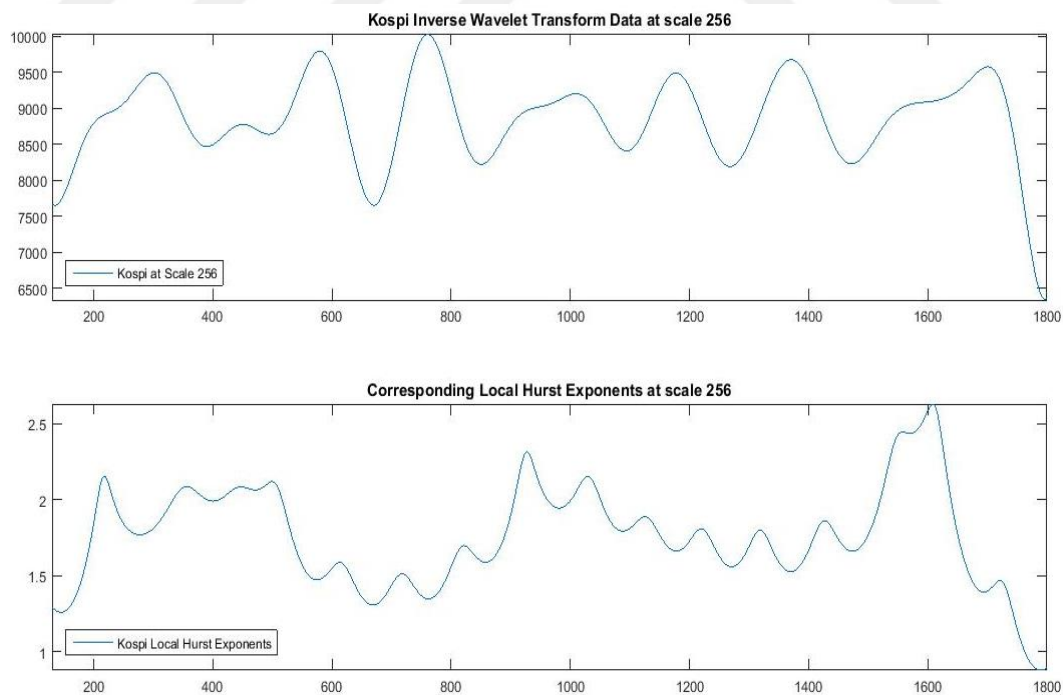


Figure 3.15. *Kospi Inverse Data and Corresponding Local Hurst Exponents at Scale 256*

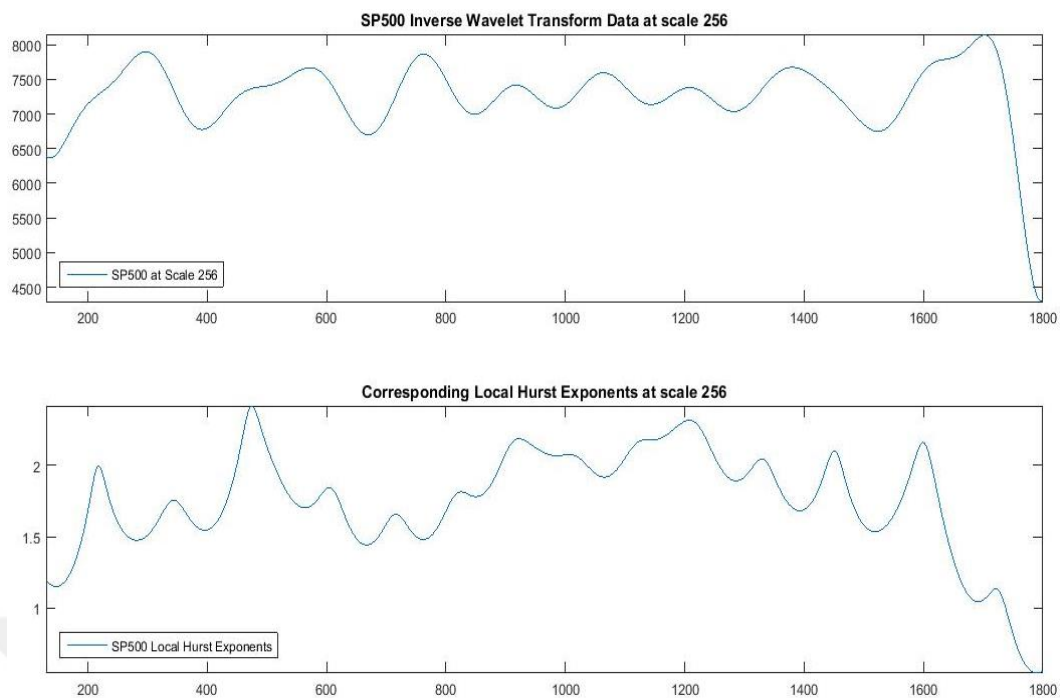


Figure 3.16. *SP500 Inverse Data and Corresponding Local Hurst Exponents at Scale 256*

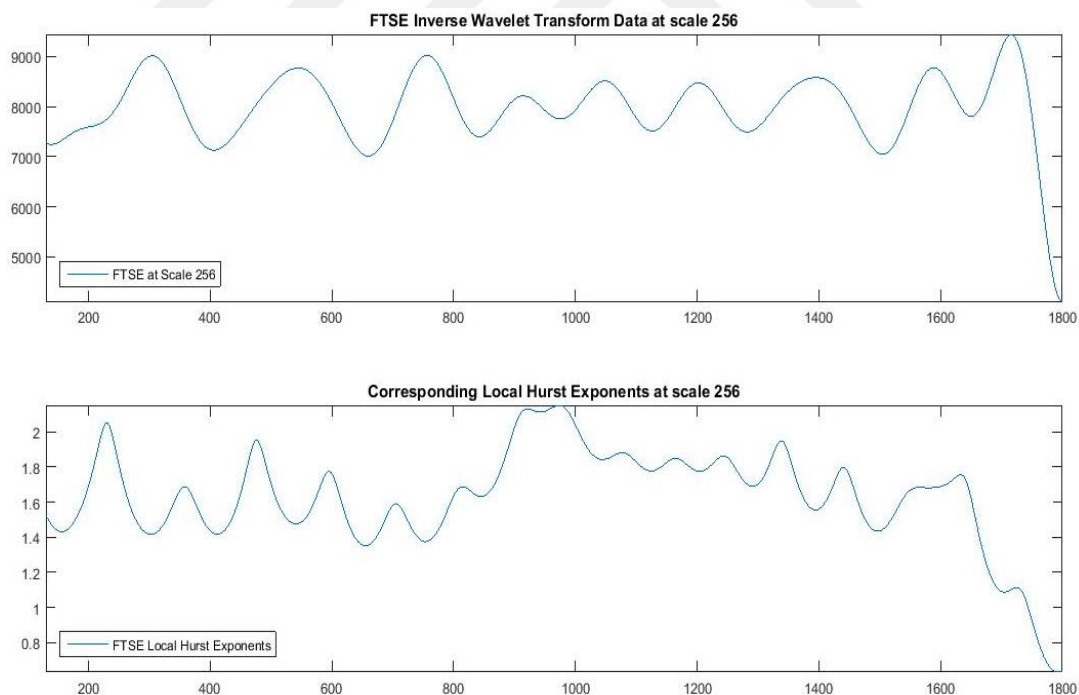


Figure 3.17. *FTSE Inverse Data and Corresponding Local Hurst Exponents at Scale 256*

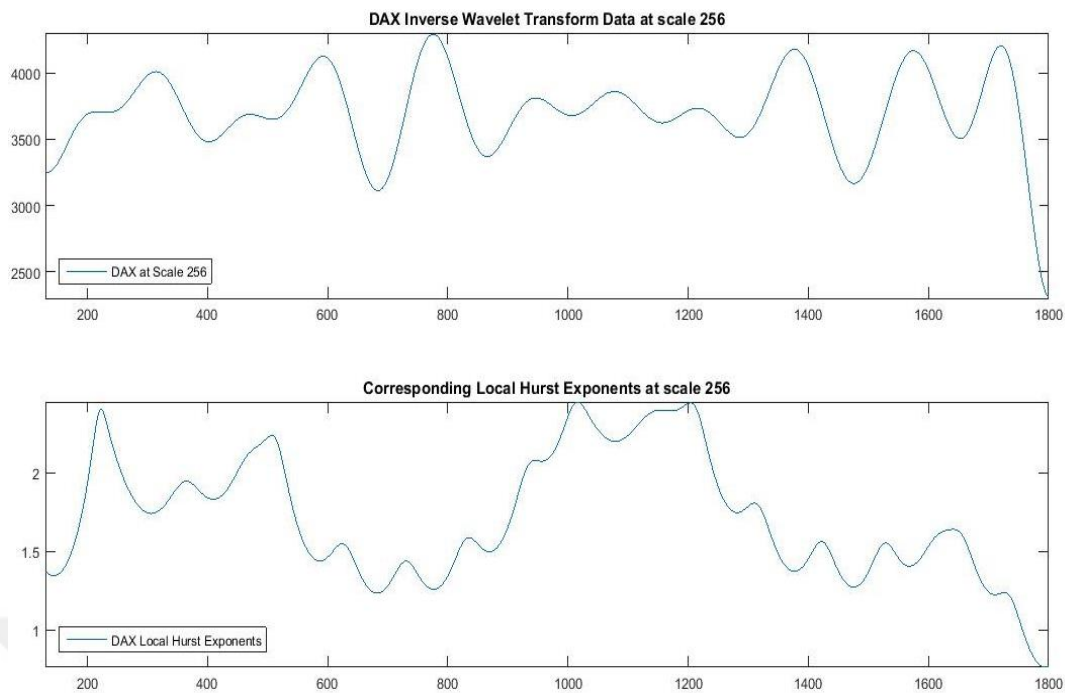


Figure 3.18. *DAX Inverse Data and Corresponding Local Hurst Exponents at Scale*

256

Appendix C. Forecasting Results

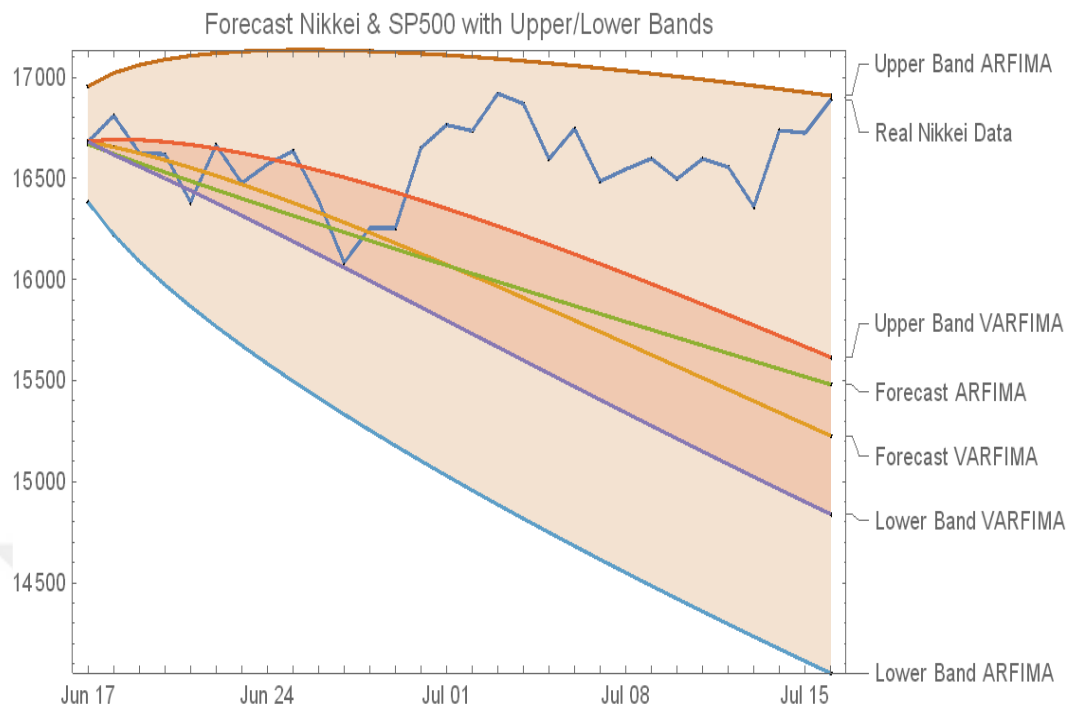


Figure 3.19. *Nikkei with SP500 Forecasting Results for the next 30 days data taken from December 19, 2009 for 1275 days*

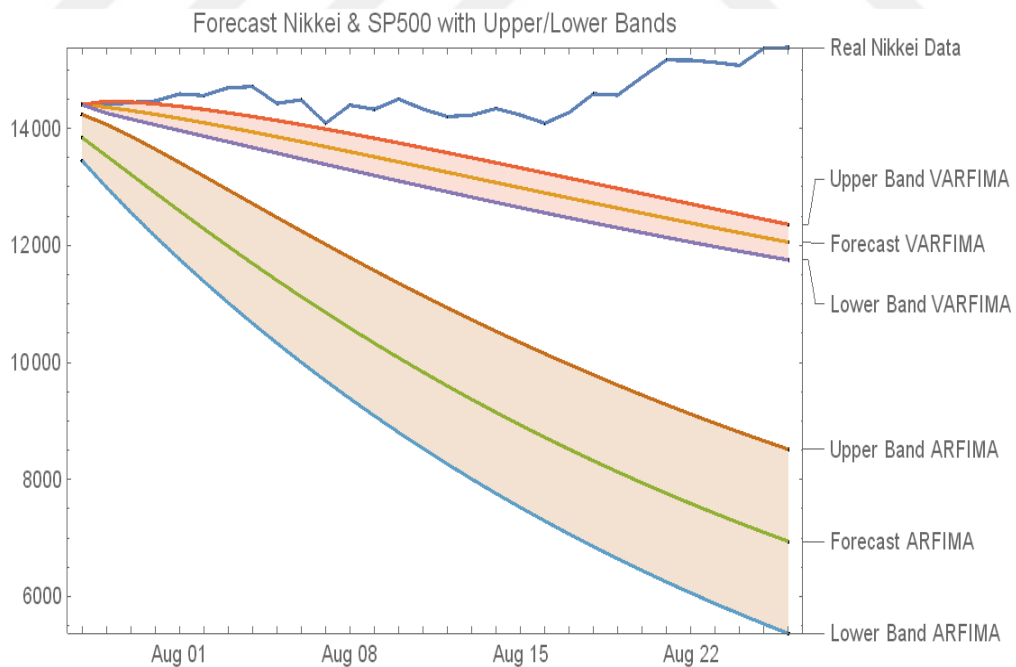


Figure 3.20. *Nikkei with SP500 Forecasting Results for the next 30 days data taken from December 24, 2010 for 215 days*

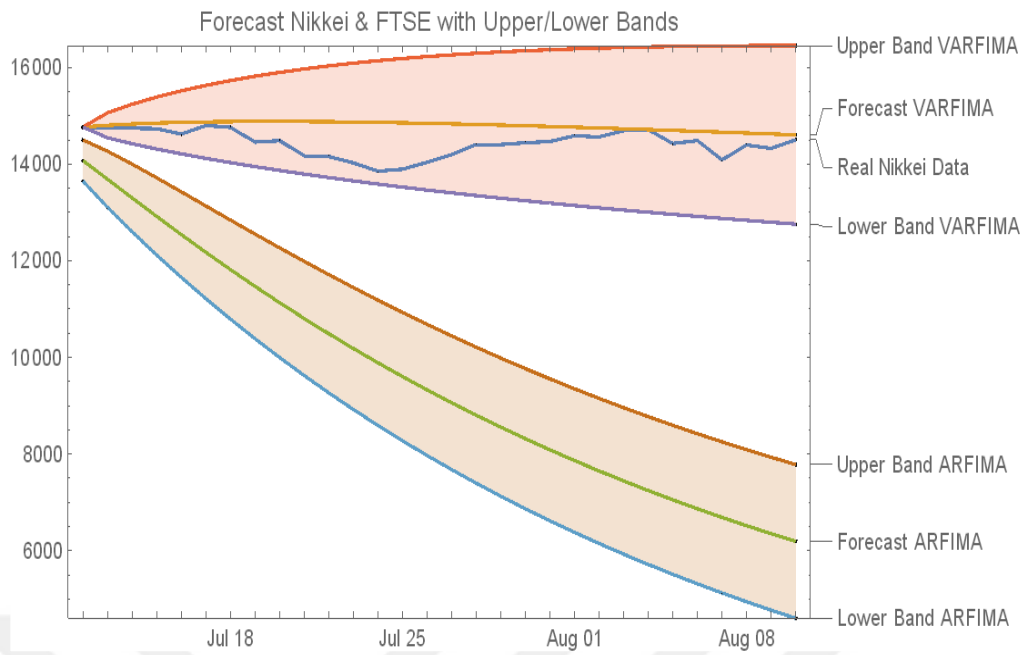


Figure 3.21. *Nikkei with FTSE Forecasting Results for the next 30 days data taken from December 24, 2010 for 199 days*

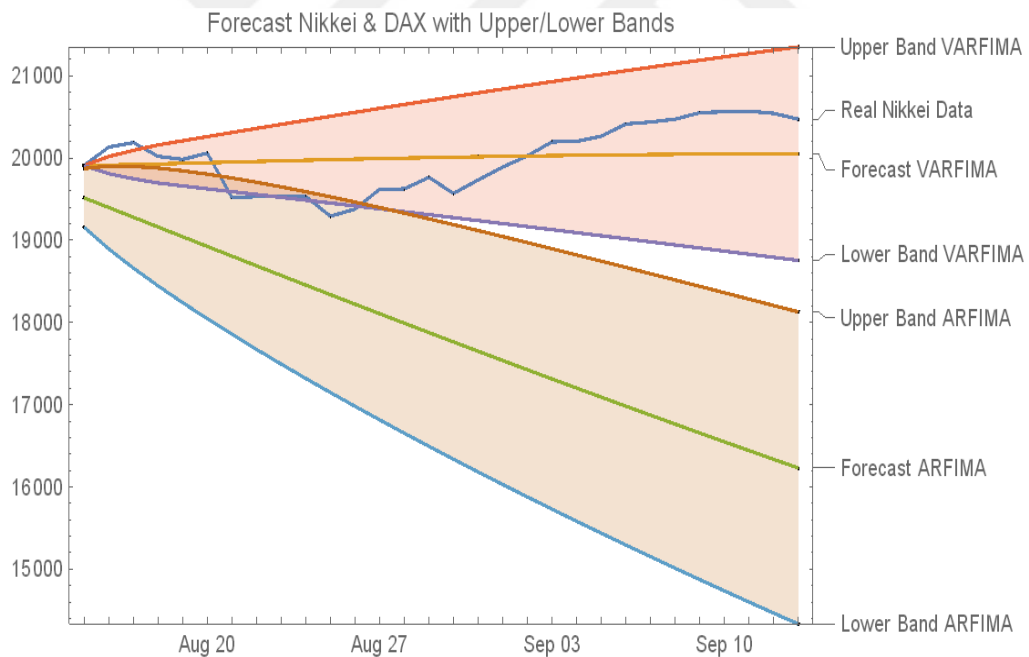


Figure 3.22. *Nikkei with DAX Forecasting Results for the next 30 days data taken from November 19, 2009 for 999 days*

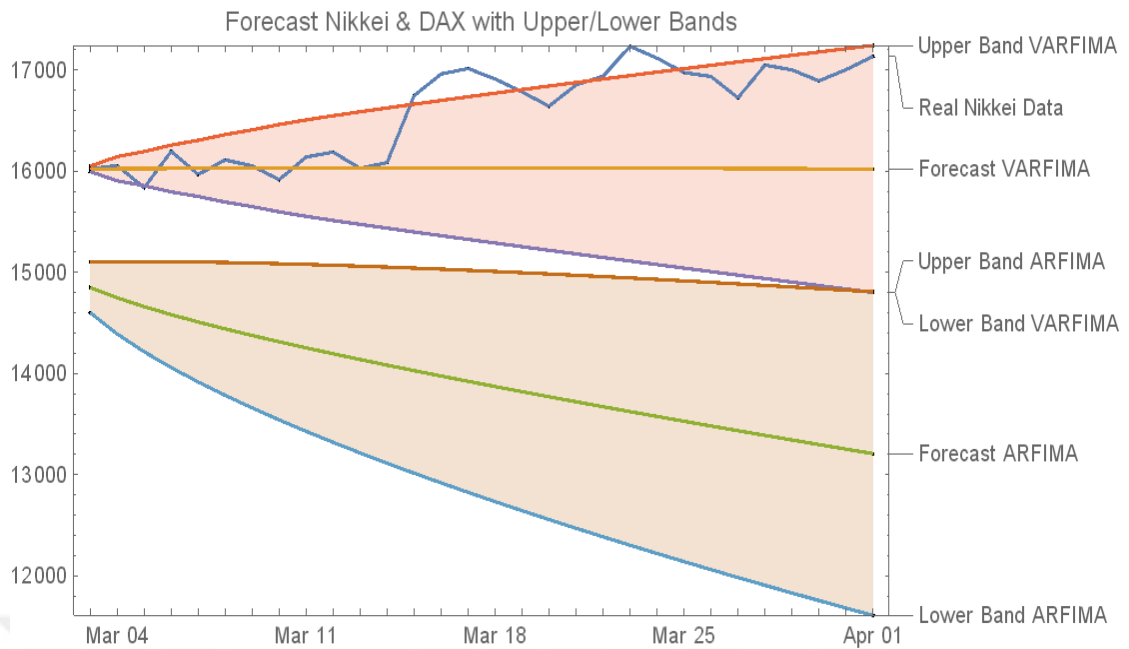


Figure 3.23. *Nikkei with DAX Forecasting Results for the next 30 days data taken from November 19, 2009 for 1199 days*

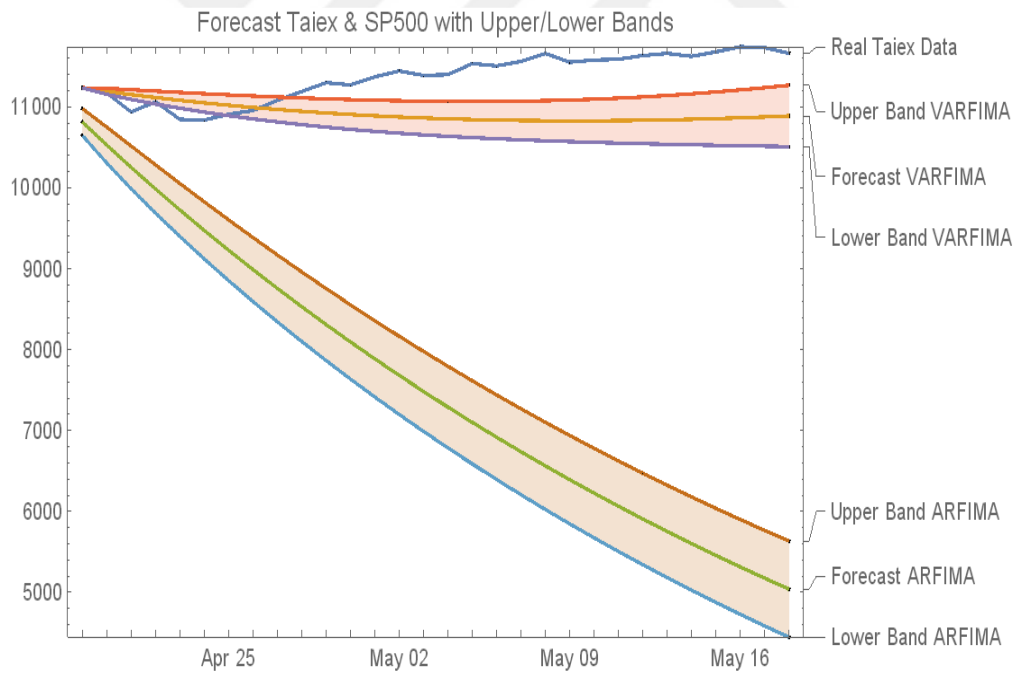


Figure 3.24. *Taiex with SP500 Forecasting Results for the next 30 days data taken from March 29, 2010 for 385 days*

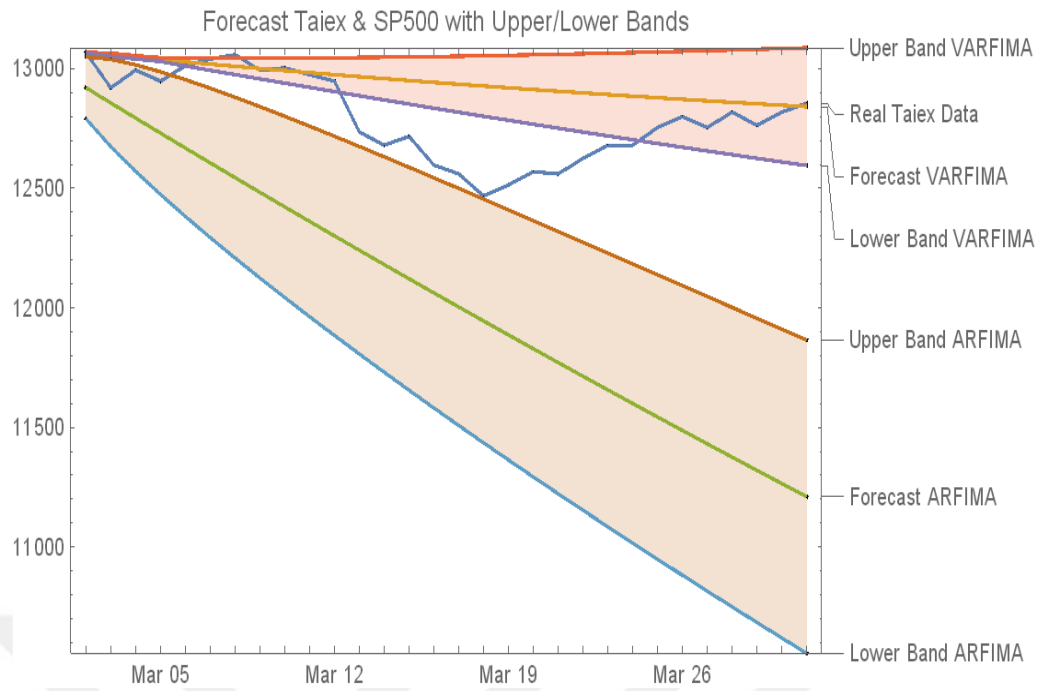


Figure 3.25. *Taiex with SP500 Forecasting Results for the next 30 days data taken from December 19, 2009 for 803 days*

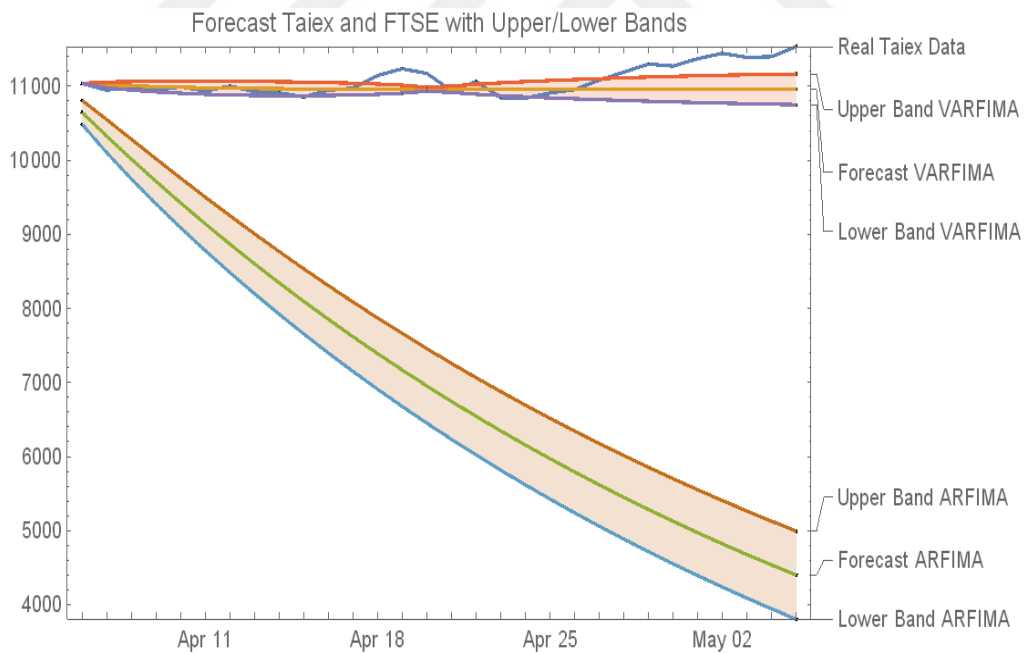


Figure 3.26. *Taiex with FTSE Forecasting Results for the next 30 days data taken from March 29, 2010 for 372 days*

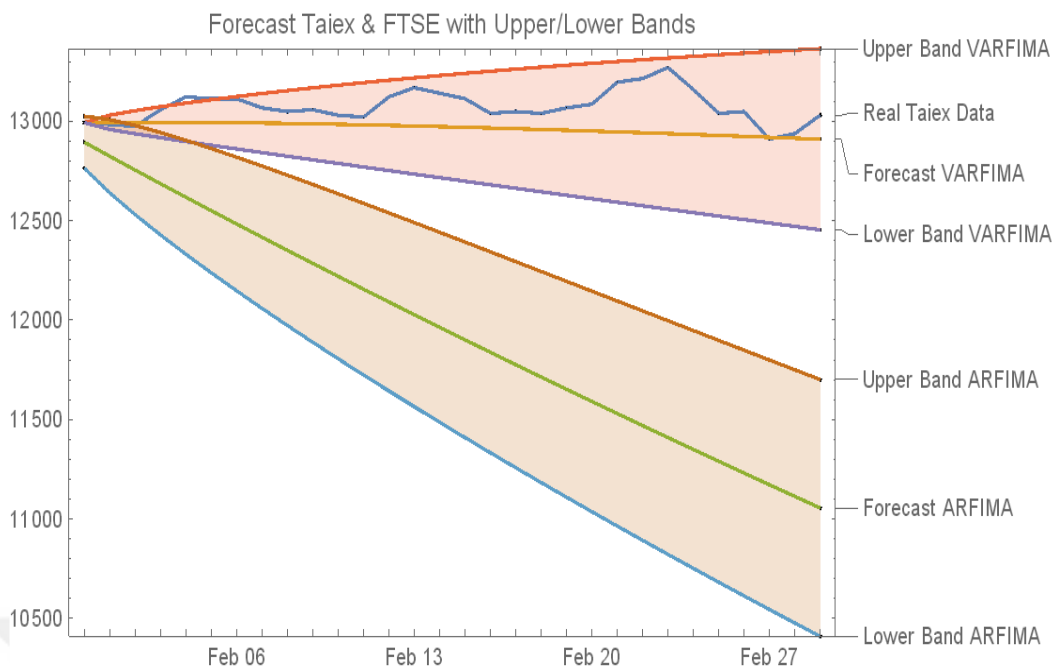


Figure 3.27. *Taiex with FTSE Forecasting Results for the next 30 days data taken from December 19, 2009 for 772 days*

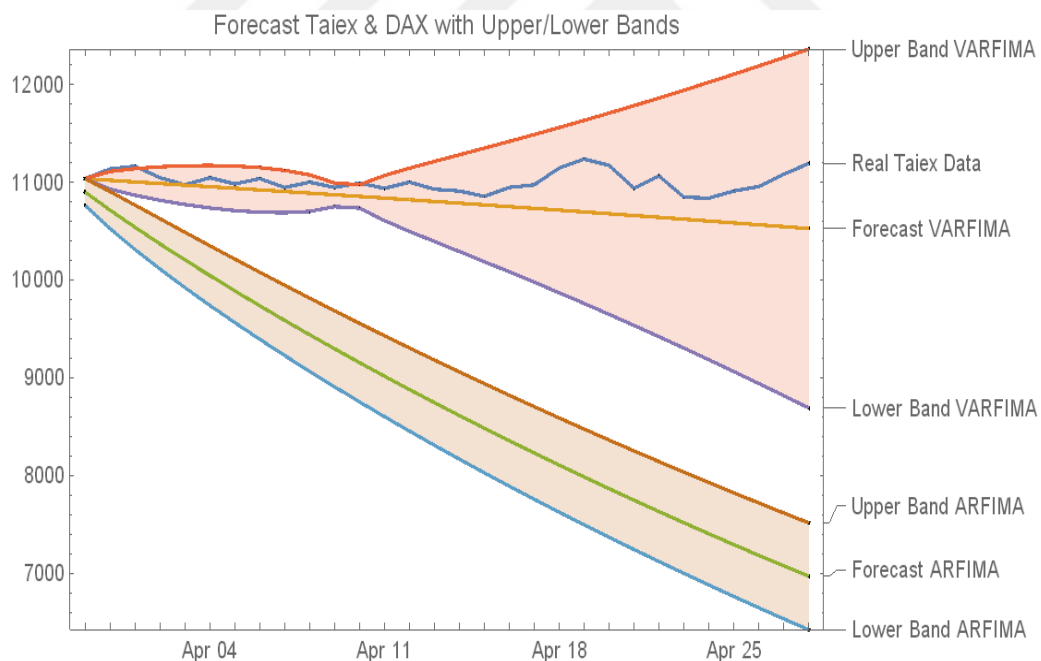


Figure 3.28. *Taiex with DAX Forecasting Results for the next 30 days data taken from November 14, 2009 for 501 days*

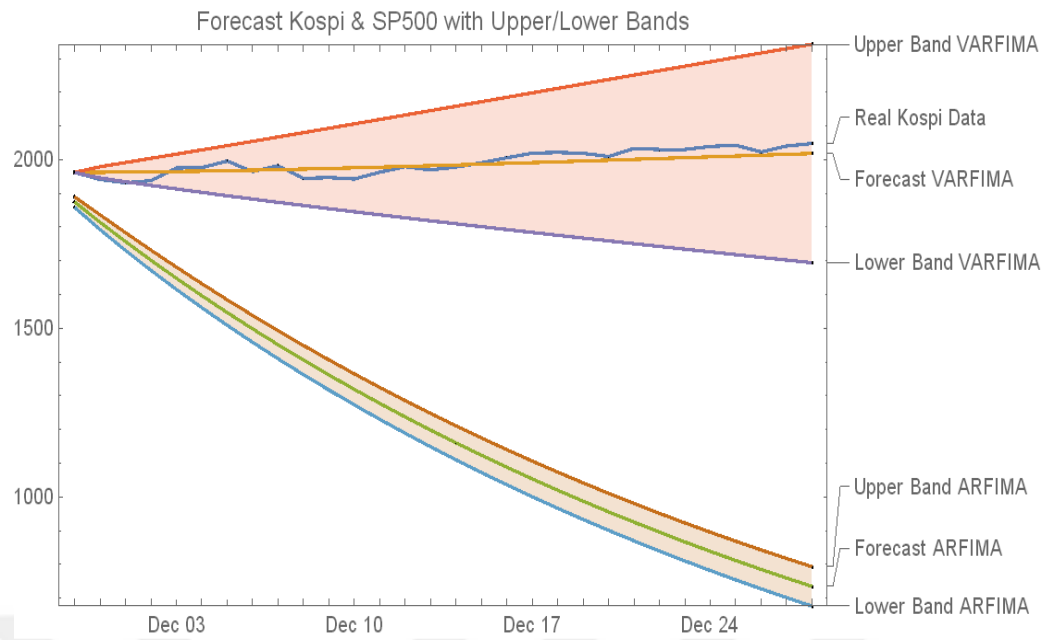


Figure 3.29. *Kospi with SP500 Forecasting Results for the next 30 days data taken from October 15, 2010 for 776 days*

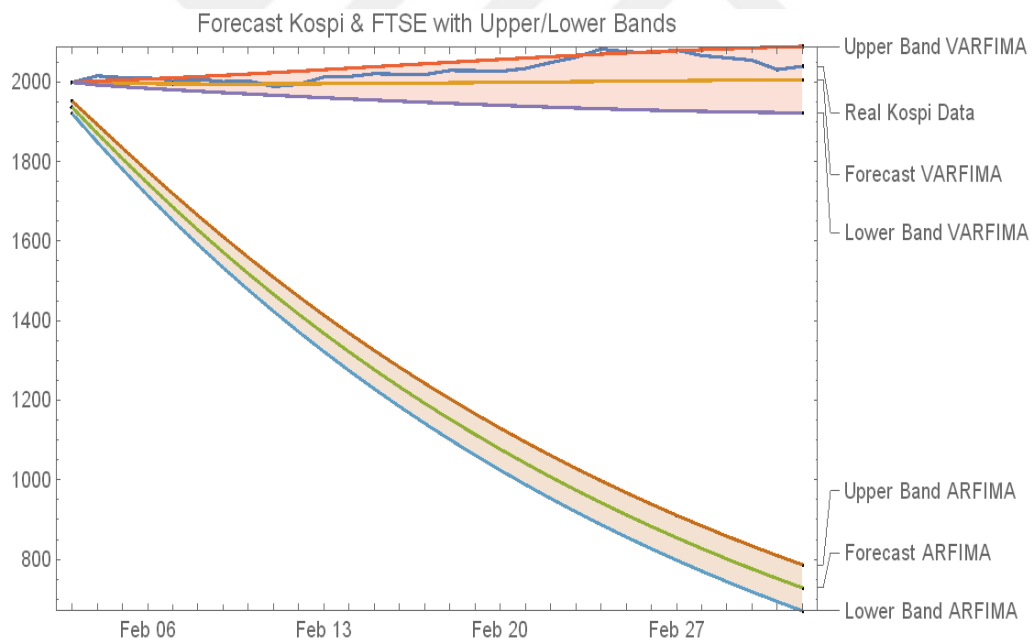


Figure 3.30. *Kospi with FTSE Forecasting Results for the next 30 days data taken from July 07, 2010 for 576 days*

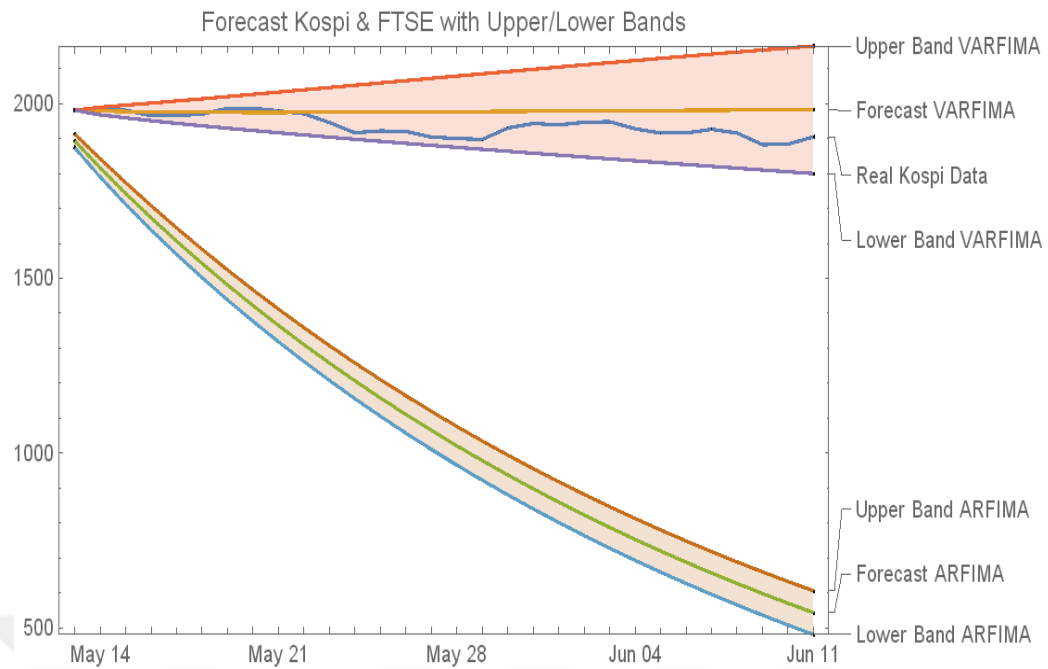


Figure 3.31. *Kospi with FTSE Forecasting Results for the next 30 days data taken from March 29, 2010 for 776 days*

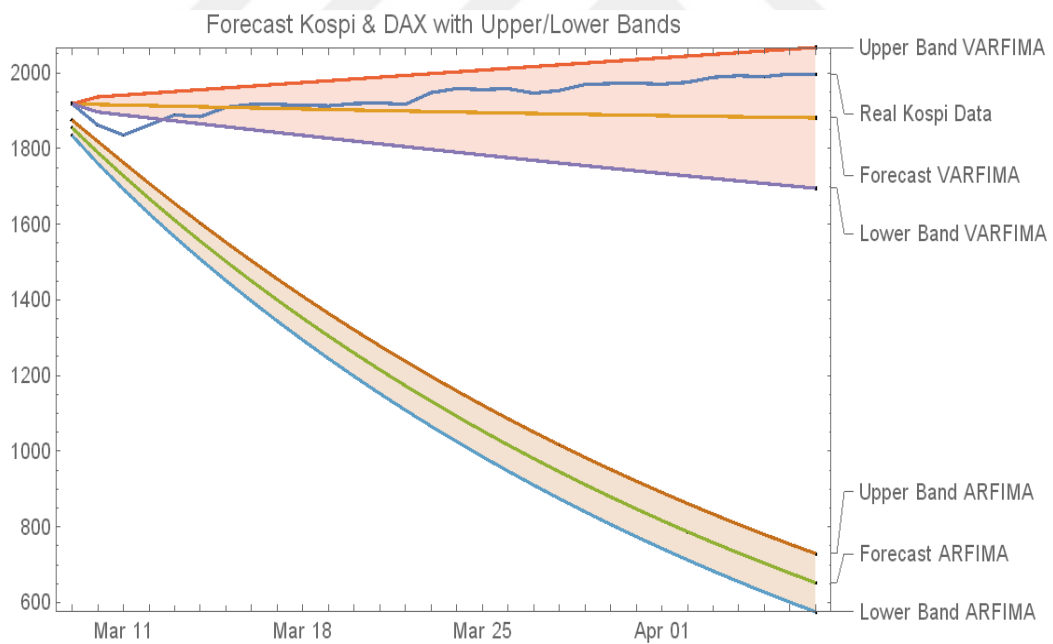


Figure 3.32. *Kospi with DAX Forecasting Results for the next 30 days data taken from December 19, 2009 for 1176 days*

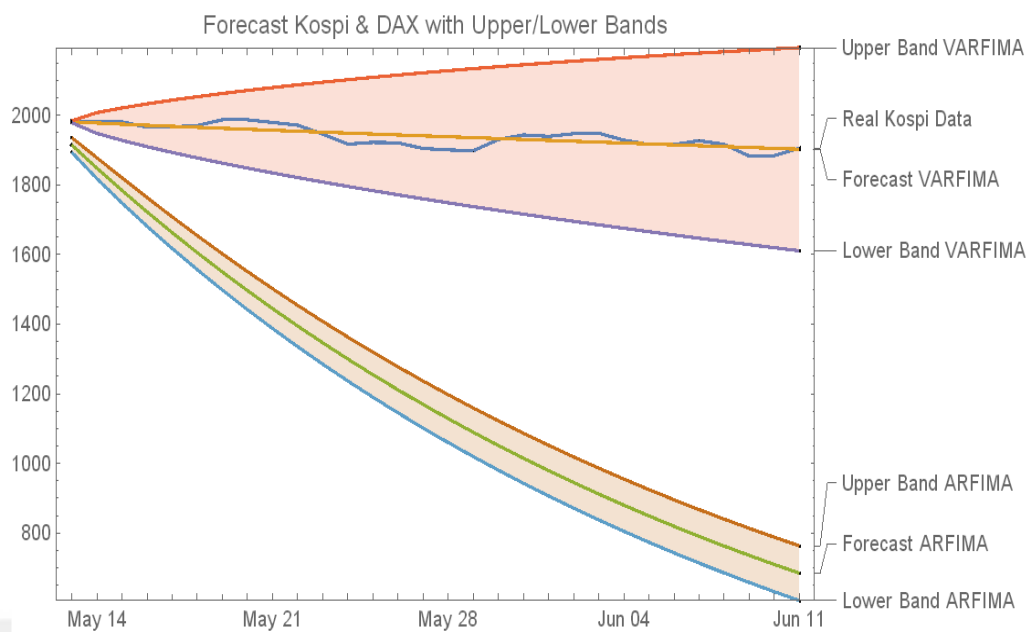


Figure 3.33. *Kospi with DAX Forecasting Results for the next 30 days data taken from December 19, 2009 for 875 days*

CHAPTER 4

MODELING AND FORECASTING TIME SERIES OF PRECIOUS METALS: A NEW APPROACH TO MULTIFRACTAL DATA

Summary

In this chapter, we introduce a novel approach to multifractal data in order to achieve transcended modeling and forecasting performances. The data is composed of ~2000 daily prices of gold, silver and platinum starting from July, 2011. First, the long range and co-movement dependencies on time-frequency space are scrutinized using multiple wavelet coherence analysis. Then, the multifractal behaviors of the series are verified by multifractal de-trended fluctuation analysis and its local Hurst exponents are calculated. Also, root mean squares of residuals at the specified scale are extracted from an intermediate step during local Hurst exponent calculations. These internally calculated series have been used to estimate the process with vector autoregressive fractionally integrated moving average (VARFIMA) model and forecasted accordingly. The results have shown that all metals do behave in phase movement on long term periods and possess multifractal features. Furthermore, the intermediate time series obtained during local Hurst exponent calculations still appertain the co-movement as well as multifractal characteristics of the raw data and may be successfully re-scaled, modeled and forecasted by using VARFIMA model. Conclusively, VARFIMA model have notably surpassed its univariate counterpart (ARFIMA) in all efficacious trials while re-emphasizing the importance of co-movement procurement in modeling.

4.1. Introduction

Multi fractal structure analysis has become more and more popular in financial studies. It is referred as one of the strong and dynamic techniques due to its ability to detect multifractal behavior in non-stationary time series. Especially, local Hurst exponents help point out the discontinuities in the financial time series. Hence, any asymmetric or inconsistent behavior in the time series, such as the failure of any economic system, can be captured. These irregularities are the main reason for the fat tail observations. Local Hurst exponents demonstrate that these irregular behaviors may be organized to be used in various models/methods.

Mandelbrot and Ness has laid the foundations of multifractal analysis by introducing fractional Brownian motions, fractional noises and its applications (Mandelbrot and Van Ness, 1968). Later, multifractal de-trended fluctuation analysis (MF-DFA) has been proposed as an alternative method in analyzing financial time series by Kantelhardt et al. (2002). Heretofore, there have been many researchers using this method in their analysis. Zhang et al. have investigated asymmetric multiscale multifractal analysis of wind speed signals (Zhang et al., 2017). Multifractal and wavelet analysis of epileptic seizures have been studied by Dick and Mochovikova (2011). An in-depth analysis of GE stocks were performed by Thomson and Wilson by contrasting the results with those obtained using multifractal de-trended fluctuation analysis and using conventional time series models (Thompson and Wilson, 2014). Benbachir and Alaoui employed the MF-DFA method in order to explore the multifractal properties of the Moroccan Dirham compared to the US Dollars (Benbachir and Alaoui, 2011). Tas and Unal studied the multifractal character of natural gas daily return using a comparative study of MF-DFA method (Tas and Unal, 2013).

The wavelet analysis is also one of the methods in scrutinizing the time series. Unlike Fourier transform, as Burrus et al. (1998) indicated, wavelet analysis does not need stationarity and is able to look deep into the frequency information of the series at different scales without losing time information (Reboredo and Rivera-Costa, 2014) which helps eliminate the weaknesses in Fourier transform (Gulerce and Unal, 2016). Gencay's study (2002) has become a pioneer work for many researchers using wavelet tools to analyze financial time series in many studies such as Aguiar-Conraria and Soares (2012-2013), Barunik et al. (2013), and McCarthy and Orlov (2012). Multi-scale analysis is accepted as one of the main applications of wavelet methods in finance and economics (Haven, 2012).

There have been many investigations looking into the relation of precious metals using these types of tools. Kucher and McCoskey indicated that the long-run relationships between precious metal prices are strongly influenced by economic conditions using a vector error correction model (Kucher and McCoskey, 2017). A flexible modification of the DCC model that accounts for asymmetry and long memory in variance is applied on precious metals by Klein (2017). He et al. (2017) uses wavelet analysis and ARMA model with higher accuracy to forecast prices of precious metals. The causal relationship among the spot prices of precious metals through mean and variance have been investigated by Bhatia et al (2018) and resulted with a strong causality for the middle quantiles and with significant implications for policy makers, portfolio managers and investors.

In this chapter, we will use a software package for wavelet coherence analysis provided by Torrence and Compo (1998) and Grinsted et al. (2004) and a Matlab tool for multifractal de-trended fluctuation analysis developed by Ihlen (2012). The former will be used to analyze inter relations, co-movement dependencies, frequent and

consistent signals in multiple financial time series of precious metals (gold, silver and platinum). The latter will be used to confirm their multifractal behavior, calculate local Hurst exponents and obtain the fractal function of time series at specific scale determined.

Multiple wavelet coherence will be used to determine the specific time period and scale that possesses common long range dependence out of the time series. With the help of Matlab tool, the multifractal behavior of these time series will be validated and a new series out of local Hurst exponent calculations will be obtained. These new series will be used to model and forecast the prices. It is our assumption that forecasting performances will be better using vector autoregressive fractionally integrated moving average (VARFIMA) compared to autoregressive fractionally integrated moving average (ARFIMA) model.

It is evidently more challenging to estimate the price on the next day due to many different players in the financial world. Thus, developing new methodologies to improve the forecasting performances has become one of the fundamental goals of econophysics as well as financial engineering. There have been univariate as well as multivariate models applied in the past. The first multivariate model has been introduced by Quenouille in 1957 and later improved by Akaike (1974), Dunsmuir and Hannan (1976) and Hannan (1981) in order. Multivariate models are a dynamic system of equations that examine the impacts of fluctuations (shocks) or correlations (interactions) between financial variables as stated by Oral and Unal (2017). Multivariate models provide better forecasting results with higher precision because of using more information out of multiple highly correlated data and having low mean-squared errors compared to univariate models (Oral and Unal, 2017).

Section 2 covers the data and methodology used in this chapter. The main equation of continuous wavelet transform and multiple wavelet coherence, basics of multifractal de-trended fluctuations analysis and vector autoregressive fractionally integrated moving average model will be included as a summary review. In section 3, multiple wavelet coherence will be utilized to detect the highly correlated time periods and frequencies. After the multifractal characteristics of the series are verified, a new series of fractional function will be obtained out of local Hurst exponent calculations at the specified scale. Section 4 will compare and discuss the forecasting results of both multivariate and univariate models. Section 5 will be ended with the discussion of the results. In appendix A will display two forecasting results of each metal couple along with the plot of the data set extracted from the local Hurst exponents' calculations at the specified period.

4.2. Empirical Framework

4.2.1. Data

The daily prices of gold, silver and platinum is acquired from Yahoo Finances! starting from July 2011 which is composed of approximately 2000 daily data.

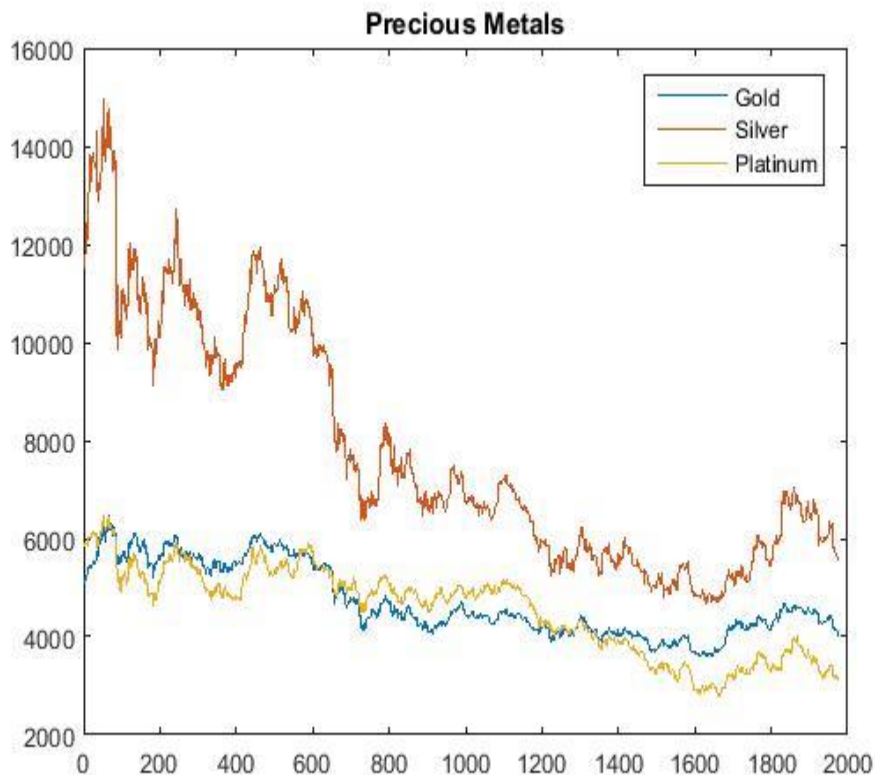


Figure 4.1. *The daily prices of gold, silver and platinum starting from July, 2011 to November, 2016.*

As can be seen from Table 1, silver has the highest mean and standard deviation, thus there is higher fluctuation in the prices of silver with respect to other metals. One thing that draws one's attention is the skewness value of platinum. The negative skewness or negatively skewed means frequent small gains and a few extreme losses. This could indicate platinum a safer investment with respect to gold and silver during economic crisis. On the other hand, positive skewness or positively skewed means frequent small losses but a few extreme gains which is greater for silver due to its higher volatility that we pointed.

Table 4.1.

Daily Data of Precious Metals from July 2011 to November 2016

	Mean	Median	St. Dev.	Kurtosis	Skewness
--	------	--------	----------	----------	----------

Gold	4736.03	4478.74	736.49	1.8535	0.4855
Silver	7805.07	6845.28	2478.29	2.4046	0.7307
Platinum	4574.81	4843.27	872.87	2.0483	-0.2758

When we look at the traditional correlation calculation results of these metals, we realize that there is higher correlation with gold and silver with respect to platinum. Additionally, platinum seems to be in harmony with silver more than gold itself. It is surprising to see 85% correlation with silver and platinum even though the volatility of silver prices is expected to be higher.

Table 4.2.

Correlation of gold, silver and platinum

	Gold	Silver
Silver	0.718556	
Platinum	0.54741	0.8564173

In this chapter, we will look deep into co-movement of metal prices in time and frequency space by using multiple wavelet coherence. Once highly correlated time interval and frequency is determined, the multi fractal behavior of the real series will be validated. A new time series of fluctuation function at the specified scale will be obtained out of its local Hurst exponents calculations. Finally, we will compare and discuss the performance of modeling and forecasting using these series with the help of univariate and multivariate models.

4.2.2. Methodology

4.2.2.1. Continuous wavelet transform (CWT) and multiple wavelet coherence.

An application of wavelet analysis in finance and economics were first presented by Gencay in 2002. Aguiar-Conraria and Soares [2012, 2013], Barunik et al. (2013), Yilmaz and Unal (2016) are some of the many researchers who have utilized these tools in their studies. There are many ways how to sort the types of the wavelet transforms. The division based on the wavelet orthogonality defines two methods, discrete wavelet transform (DWT) for orthogonal wavelets and continuous wavelet transform (CWT) for non-orthogonal wavelets. Nevertheless, CWT performs better to see the signal frequencies evolution during the duration of the signal and compare the spectrum with other signals spectra, thus is used more for feature extraction purposes (Grinsted et al., 2004) to see the results in more humane form. CWT follows the following form in equation (1),

$$CWT_x^\psi(s, \tau) = \langle X, \psi(s, \tau) \rangle = \frac{1}{\sqrt{s}} \int_{-\infty}^{+\infty} X(t) \psi^*\left(\frac{t-\tau}{s}\right) dt \quad (1)$$

Where the transforming function, also known as the mother wavelet, is " ψ ", the translation parameter is " τ " and the scale parameter is " s ". The translation parameter is the time information in the transform domain and the scale parameter is the frequency of the corresponding information.

Wavelet coherence may be evaluated not only in two dimensional data sets but also in multi-dimensional sets of data for the same time and frequency space. Thus, multivariate models where three dimensional multiple wavelet coherence is possible as shown in the following equation (2),

$$C^d = 1 - R_{23}^2 - R_{12}^2 - R_{13}^2 + \rho_{12}\rho_{23}\rho_{31} + \rho_{13}\rho_{21}\rho_{32}$$

$$C^d = 1 - R_{23}^2 - R_{12}^2 - R_{13}^2 + 2R(\rho_{12}\rho_{23}\rho_{31})$$

$$C^d = 1 - R_{23}^2 - R_{12}^2 - R_{13}^2 + 2R(\rho_{12}\rho_{23}\rho_{13}^*) \quad (2)$$

Where C denotes complex coherence, ρ_{ij} is the correlation factor and R_{ij}^2 is squared multiple wavelet coherencies. For details of these methods, the reader may look into the article, “co-movement of precious metals and forecasting using scale by scale wavelet transform (Oral and Unal, 2017).”

4.2.2.2. Multifractal de-trended fluctuation analysis (MF-DFA).

Multifractal de-trended fluctuation analysis (MF-DFA) may be used to analyze financial time series demonstrating volatility clustering or many different forms of irregular behavior. It is in the nature of all financial time series data to have fractal structures and behavior. As Ihlen (2012) pointed, the deviations in fractal structure within time periods with large and small fluctuations may be identified by multifractal analysis. The main advantage of the method is to be able to detect multifractal behavior in non-stationary time series. That is why it is proposed as a robust and powerful technique by Kantelhardt et al. (2002). The aim of the MF-DFA is to find the spectrum of singularities both for stationary as well as non-stationary time series. It is assumed that $X(t)$ is self-similar time series with Hurst exponent $H \geq 0$. For any $c > 0$, we have

$$X(ct) = c^H X(t) \quad (3)$$

According to equation (3), when H is greater than 0.5, the time series data possesses persistent behavior with long range dependence. This persistency indicates practicably the same sign for the next non-overlapping time segment in line. If H is less than 0.5, the time series data will exhibit anti-persistent behavior with short range dependence. This, however, anti-persistent behavior would mean that an increase (decrease) in the process is most likely to be followed by decrease (increase) in the next time segment.

Assume that $X(t)$ is a time series of length N with mean of \bar{x} . Firstly, the accumulated profile $y(i)$ of the time series $X(t)$ for $i=1, \dots, N$ is determined.

$$y(i) = \sum_{i=1}^N [X(i) - \bar{x}] \quad (4)$$

Firstly, a non-overlapping segment of equal length scale s is formed. Then the profile $y(i)$ is divided to the number $N_s = \text{int}(N/s)$ rounding to the nearest integer, $\text{int}()$. The same procedure is repeated starting from the end of the profile in order to include a short part of the end of the profile, doubling the number of segments, $2N_s$.

Each segment is fitted by a polynomial providing a local trend to the data and the variances are calculated by two formulas in terms of segment v . For each segment $v = 1, \dots, N_s$:

$$F^s(v, s) = \frac{1}{s} \sum_{i=1}^s [y((v-1)s + i) - p_v^n(i)]^2 \quad (5)$$

And for each segment from the end of the profile $v = N_s+1, \dots, 2N_s$:

$$F^s(v, s) = \frac{1}{s} \sum_{i=1}^s [y((N-v-N_s)s + i) - p_v^n(i)]^2 \quad (6)$$

$p_v^n(i)$ is the n^{th} order fitting polynomial in the segment order, v . For $n>3$, any order of polynomials can be used, linear, quadratic, cubic or higher. Next, q^{th} order fluctuation functions will be obtained by averaging the variance over all segments.

This calculation is shown in equation (7) as following, for $q \neq 0$:

$$F_q(s) = \left[\frac{1}{2N_s} \sum_{v=1}^{2N_s} [F^2(v, s)]^{q/2} \right]^{1/q} \quad (7)$$

And if $q=0$, the equation is evaluated as in equation (8)

$$F_0(s) = \exp \left[\frac{1}{2N_s} \sum_{v=1}^{2N_s} \ln[F^2(v, s)] \right] \quad (8)$$

Resolving the behavior of the q -dependent fluctuations $F_q(s)$ is the main goal of MF-DFA while taking into consideration the time scale s and various values of q . The equation 5 thru 8 should be run in loop for various values of time scales s . Hence, the multi-scaling behavior of the fluctuation functions $F_q(s)$ may be analyzed. In order to

do that, the slope of log-log plots of $F_q(s)$ with respect to s for different values of q (such as -3, -2, -1, 0, 1, 2, 3) should be estimated. The fluctuation function $F_q(s)$ will demonstrate the following power-law scaling behavior as shown in equation (9) depending on the analysis of long-range power-law correlation as fractal properties,

$$F_q(s) \sim s^{h(q)} \quad (9)$$

For different values of q , $h(q)$ is regressed on the time series $F_q(s)$. The time series is called monofractal, when a constant value for $h(q)$ for all values of q is true.

Conversely, the time series is said to be multifractal, when $h(q)$ is a steadily decreasing function of q . The Hurst exponents of $h(q)$ represent the scaling properties of small (large) fluctuations when the values of q are negative (positive). Ihlen (2012) pointed that the size of local Hurst exponents in the periods of the multifractal time series with local fluctuation of different magnitudes determines the structure of the local fluctuations. Small (large) local Hurst exponents mean large (small) noise like (random walk like) structure of local fluctuations. This is identical with the generalized Hurst exponents for negative and positive values of q , respectively. Regardless, the structural changes within time series are caught instantly with the local Hurst exponents and it is the major advantage compared to generalized Hurst exponent.

4.2.2.3. Vector autoregressive fractionally integrated moving average (VARFIMA).

The efficiency of multivariate time series analysis may be increased by understanding the importance of synchronization of multiple time series. Tsay (2013) stated that the long-run effects as well as the short and long term dynamics characterized by the AR, MA and the fractional differencing parameters may be simultaneously addressed by vector autoregressive fractionally integrated moving

average (VARFIMA) model. Sowell (1989), Durr et al. (1997), Dueker and Startz (1998), Box-Steffensmeier and Tomlinson (2000), Clarke and Lebo (2003) have all used these models in their time series observations. Primarily, the ARFIMA (p, d, q) process can be described by the difference equation in (10)

$$(1 - a_1 L_{|t_n-1|} - \dots - a_p L_{|t_n-p|})(1 - L)^d y(t) = (1 + b_1 L_{|t_n-1|} + \dots + b_q L_{|t_n-p|})e(t) \quad (10)$$

Where $y(t)$ is the state output, $e(t)$ is the white noise input, and L is the shift operator. a_i , and b_j are real coefficient matrices of n by n dimensions, d_i is real integrating parameter between -0.5 and $+0.5$, Σ is the covariance matrix which is symmetric positive definite of dimensions n by n .

The vector ARFIMA process has transfer matrix $t(z^{-1})$ where $t(z)$ function can be defined as (11)

$$t(z) = \left((I_n - a_1 z - \dots - a_p z^p) \cdot (I_n - z)^d \right)^{-1} (I_n + b_1 z + \dots + b_q z^q) \quad (11)$$

where I_n is the identity matrix with dimensions n by n . Equation (11) can now be written in summary notation as

$$A(L)(I - L)^d y(t) = M(L)\varepsilon(t) \quad (12)$$

Where L is the lag operator and $A(z) = (A_0 - A_1 z - \dots - A_p z^p) \cdot (A_0 - z)^d$ and $M(z) = M_0 + M_1 z + \dots + M_q z^q$. Equation (12) can be written as follows:

$$y(t) = M(L)\{A^{-1}(L)(I - L)^{-d}\varepsilon(t)\} = M(L)\xi(t) \quad (13)$$

This means a two-step of calculation for $\xi(t)$ first and then for $y(t)$.

From here, we see that VARFIMA model can be reduced in a straightforward way to a set of n interrelated ARFIMA models. Hence, when we rewrite equation (12), we get

$$y(t) = M(L) \frac{1}{|A(L)|(I-L)^d} A^*(L) \varepsilon(t) \quad (14)$$

Where $|A(L)|$ is the scalar valued determinant of $A(L)$ and $A^*(L)$ is the adjoint matrix. The process becomes

$$|A(L)|(I-L)^d y(t) = M(L)A^*(L)\varepsilon(t) \quad (15)$$

Where a system of n-dimensional ARFIMA process is defined with the common lag operator, L and co-integration fraction, d .

4.3. Wavelet Coherence and Local Hurst Exponents

Wavelet coherence displays the time series data in two dimensional axes of frequency and time space. The time information is displayed on x axis and the frequency information on y axis. The frequency information is also represented as period or scale. However they are inversely proportional where high frequency means low scale or vice versa. The column on the right indicates the correlation scale. The yellow colors in the figure means higher correlation and the blue colors mean no correlation during the specific time and frequency interval. The power of correlation is one at its highest point and zero where there is no correlation. The black lines represent the statistical significance at 5% level against red noise. Since the length of the wavelet may exceed the length of the data on the edges, the discontinuities in the wavelet function is displayed in the faded area [30]. The faded area falls onto the outside of the cone of influence (COI).

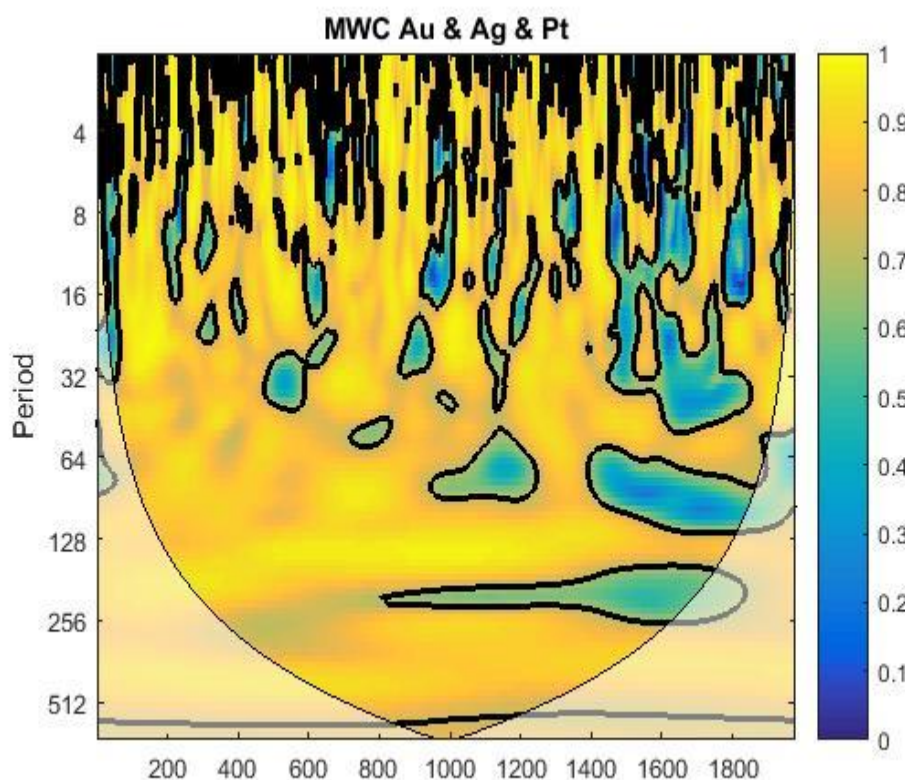


Figure 4.2. *Multiple wavelet coherence of gold with silver and platinum*

Three dimensional multiple wavelet coherence would bring out the effect of two factors together on the commodity itself. As we look at the multiple wavelet coherence of silver with gold and platinum, it shows a strong relation almost at all times and frequencies. There is a weakening relationship at around 32 day period from time to time. All metals are displaying very strong relation along 256 day period at all times. It was also possible to point out that platinum has the lowest amount of coherence with other metals. The traditional correlation calculations have demonstrated themselves in much detail with the wavelet coherence diagrams.

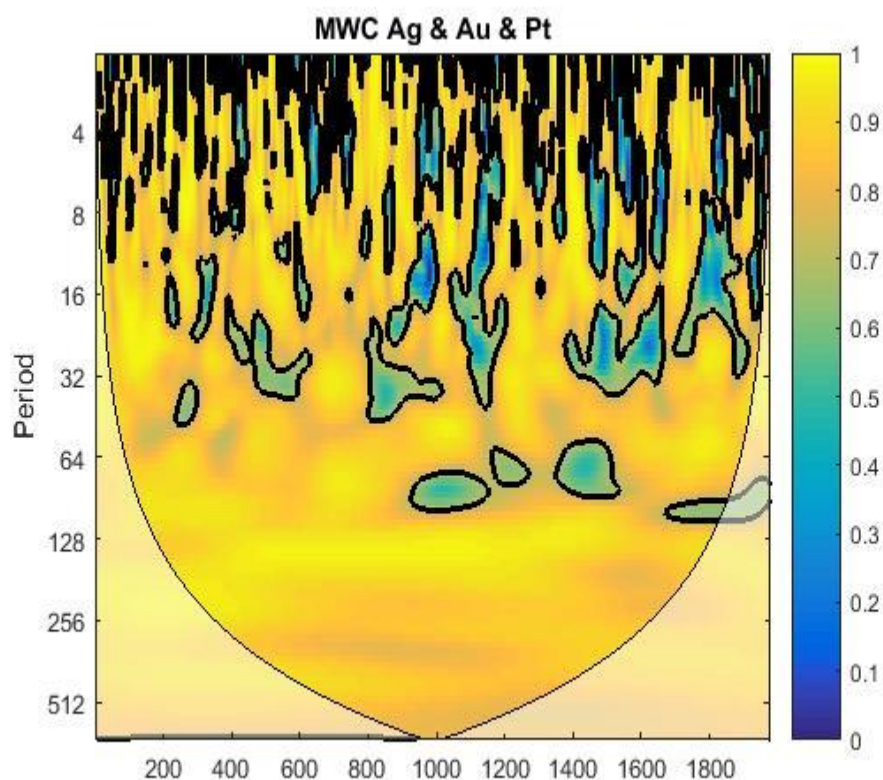


Figure 4.3. *Multiple wavelet coherence of silver with gold and platinum*

It is seen that there are some of the areas colored blue considering long range dependency. The blue areas indicate low interrelation between the metals at the specific time and frequency. These areas are found more in platinum diagram but less in silver diagram. This may be because of reaching equilibrium in prices at different rates during shocks or stresses. Kucher and McCoskey (2017) find in their study that the error correction mechanisms between precious metal prices seem to be asymmetric. This also aligns with our observations and explains some of the weak long run (low frequency / higher periods) relationship over certain periods of time.

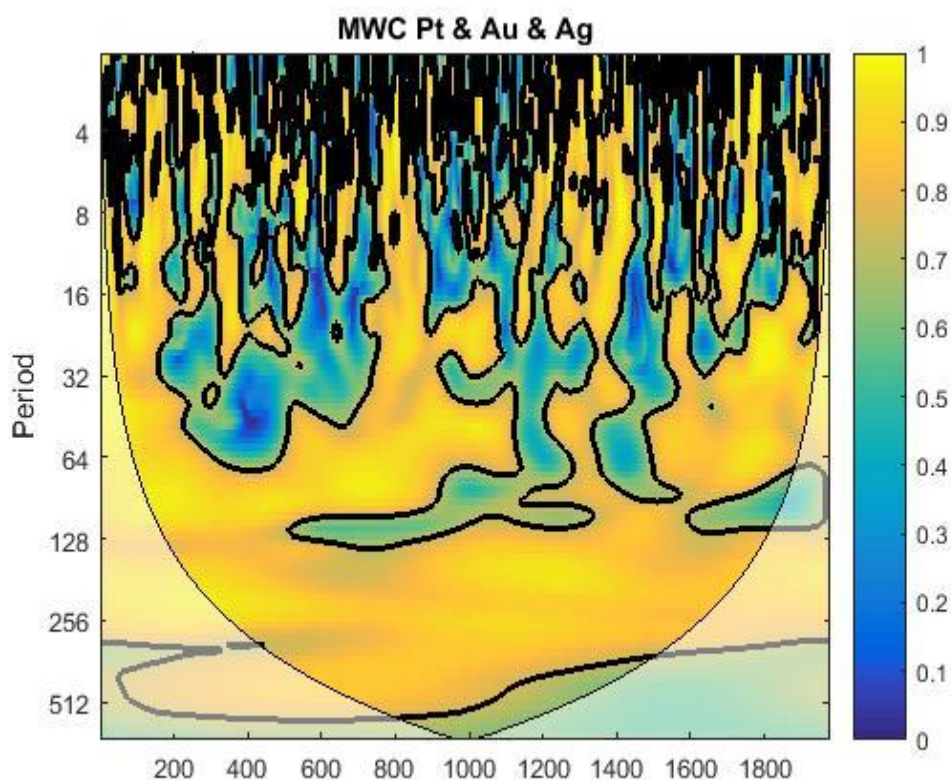


Figure 4.4. Multiple wavelet coherence of platinum with gold and silver

The generalized Hurst exponent considers the time series as a single time period and provides a single value that indicates the global behavior of the series. A correlated (long range dependent) structure is observed when the Hurst exponent is in the interval of 0.5 and 1. An anti-correlated (short range dependent) structure is observed when the Hurst exponent is in the interval of 0 and 0.5. It is expected in this chapter that the better performance of forecasting will be obtained due to the long range dependence and the multifractal behavior of the time series obtained. In table 3 it is shown that the real time series data of all metals have generalized Hurst exponent even greater than 1, indicating a strong long range dependence.

Table 4.3.

Hurst Exponent of Real and Fluctuation function at scale 256

	Gold	Silver	Platinum
--	------	--------	----------

General Hurst Exponents	1.5043	1.4714	1.4927
General Hurst Exponents of Fluctuation Function Time Series at Scale 256	1.3255	1.3237	1.4515
% Change	11.89%	10.04%	2.76%

When we calculated the local Hurst exponents at scale 256, the fluctuation function series obtained at the specified scale are still demonstrating multifractal behavior as strong as the raw data. There is only 10% difference for gold and silver and 2.7% for platinum. The main advantage of working with local Hurst exponents with respect to generalized Hurst exponent is the ability of local Hurst exponent to identify the time instant of structural changes within the time series (Ihlen, 2012).

Table 4.4.

Minimum and Maximum Values of Local Hurst exponents at scale 256

	Gold	Silver	Platinum
Min H_{loc}	1.0342	0.8648	0.8657
Max H_{loc}	1.8254	2.0615	2.133

In figure 5 thru 7, the real data of each metal and their corresponding local Hurst exponents are displayed. In table 4, the minimum and maximum values of local Hurst exponents at scale 256 are listed. Even though gold has the lowest maximum value among all the metals, it does not have weakening long range dependence with the lowest Hurst exponent value of 1.03. Silver and platinum on the other hand have minimum Hurst exponents of 0.86 around the same time interval. This is indicating a weaker persistent behavior in terms of long range dependence. Silver and platinum are demonstrating stable long range dependence in the latest times of the series. However, as shown in figure 5, gold has a continuously increasing value of local

Hurst exponents, suggesting stronger long range dependence with even smaller variations in price.

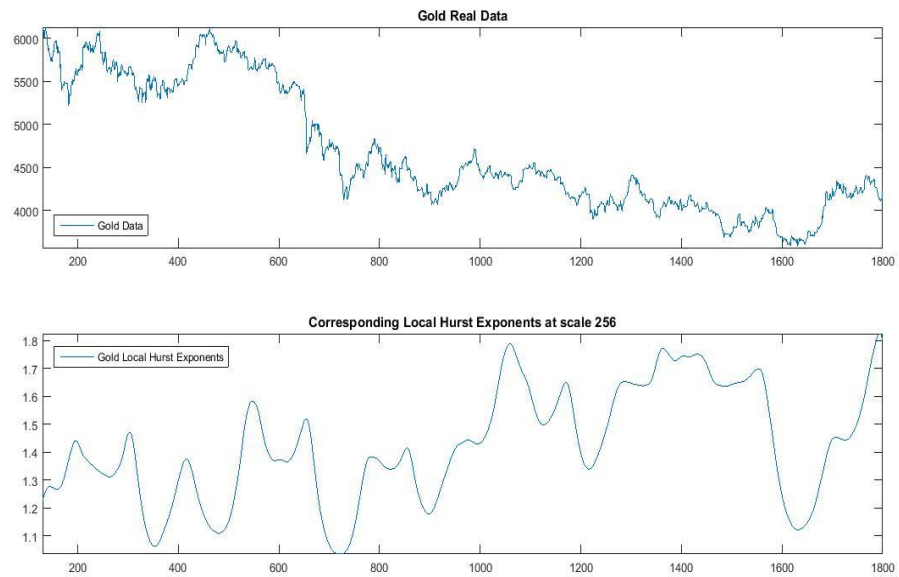


Figure 4.5. *Gold Local Hurst Exponents at Scale 256 day period*

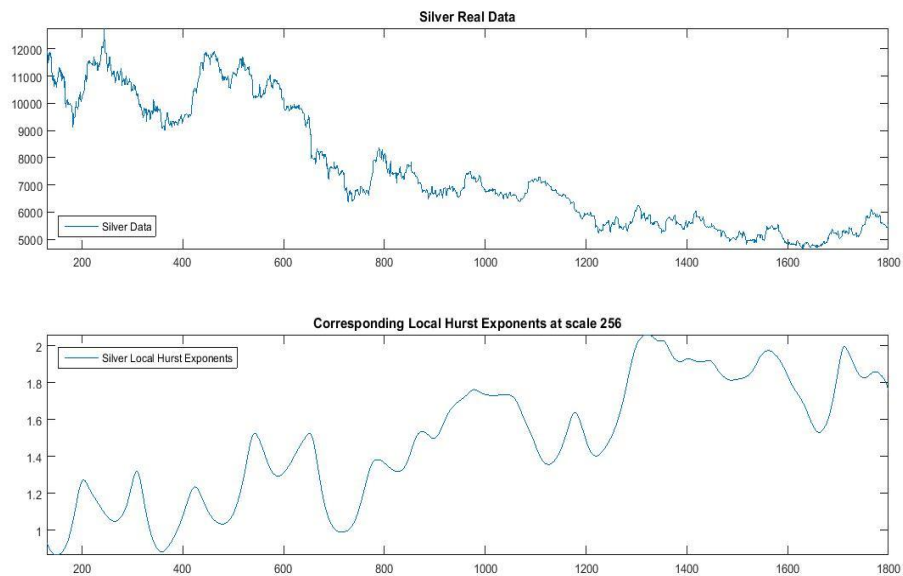


Figure 4.6. *Silver local Hurst exponents at Scale 256 day period*

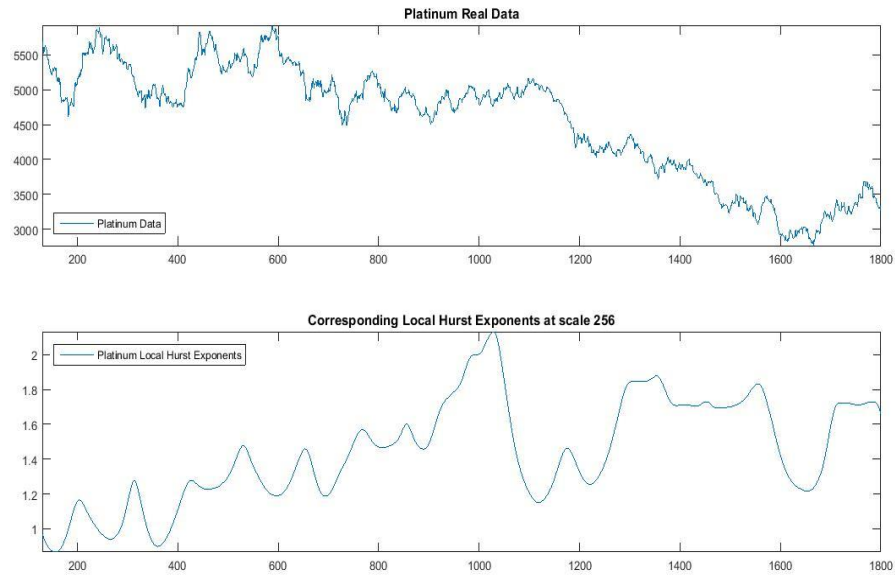


Figure 4.7. *Platinum local Hurst exponents at scale 256 day period*

In figure 8, the fluctuation function time series obtained during the calculation of local Hurst exponents at scale 256 are shown. These time series will be used to model and forecast the prices for the next 30 days. However due to the nature of the calculation, the values need to be rescaled with respect to the raw data. To do so, we calculated the ratio between the mean value of the fluctuation function and the mean value of the raw data. Then we divided the series with that ratio and obtained a new series closer to the real data in value.

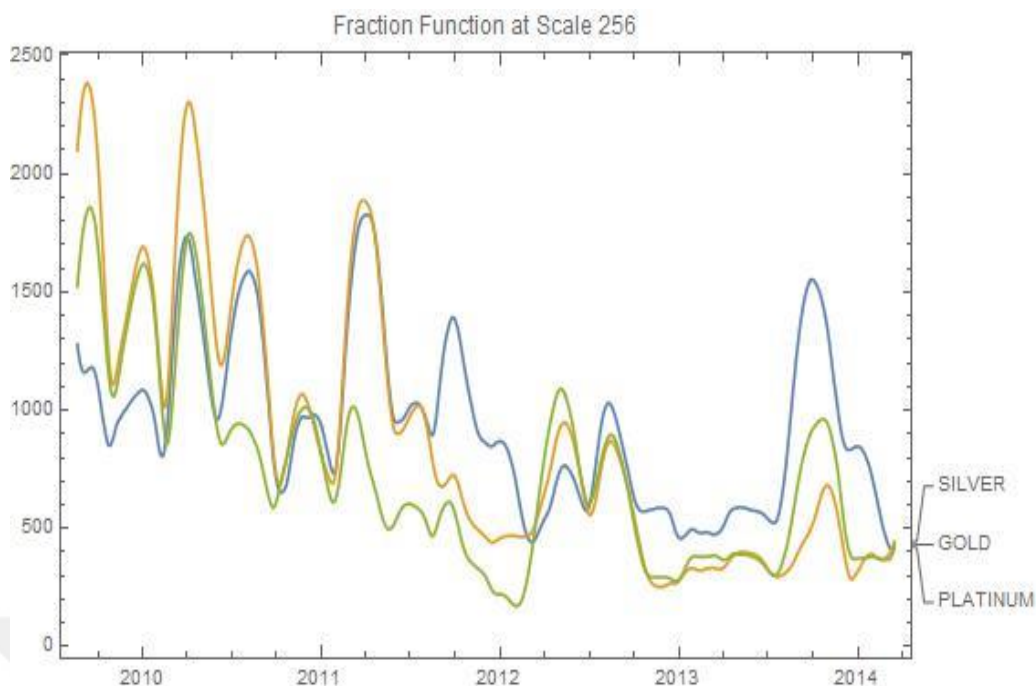


Figure 4.8. *Fraction function at scale 256*

Since we know that both the real data and the fluctuation function data exhibits multifractal behavior, autoregressive fractionally integrated moving average (ARFIMA) model with the real data and vector autoregressive fractionally integrated moving average (VARFIMA) model with the fluctuation function time series will be used to estimate a process and forecast for the next 30 days. Finally we will compare the results accordingly.

4.4. Forecasting Results and Analysis

Multivariate models leads to more accurate results compared to scalar counter models (Tsay, 2013) because not only the historical data of each series but also other fractionally co-integrated variables in between the series are taken into consideration in VARFIMA models. Therefore it is important to set up highly correlated data set. It would help establish efficiently estimated processes with better forecasting results. The raw data and fluctuation function time series data will be picked for the same interval for forecasting purposes. Raw data using ARFIMA process and fluctuation

function data using 2D VARFIMA process will be forecasted and the results will be compared accordingly.

The reader must note that when 2D VARFIMA model are run, the forecasting results are provided with upper and lower limits of two dimensional vectors. In our results, we have eliminated the highest value of the upper boundaries and the lowest value of the lower boundaries displaying the narrowest band possible.

Table 4.5.

Dates and couples used to forecast precious metals

		From	To	Correlation
Gold	Platinum	25.02.2011	11.01.2012	0.7905
Gold	Platinum	19.12.2011	18.04.2012	0.6588
Gold	Silver	25.02.2011	06.01.2012	0.8538
Gold	Silver	06.03.2010	18.05.2012	0.8056
Silver	Platinum	19.04.2010	21.07.2012	0.7189
Silver	Platinum	26.02.2011	11.01.2012	0.8669

In table 5, the dates of time series interval are given for each couple of metals. 6 time interval have been chosen for forecasting purposes. Forecasting for each metal has taken place for the same time interval in VARFIMA for the next 30 days. Figure 9 displays fraction function couple for gold and platinum from February 25th, 2011 to January 11th, 2012. The correlation of these series is approximately 80%. VARFIMA model uses the same time series (gold with platinum and platinum with gold) to obtain the forecasting results of each metal and they are shown in Figure 10 for gold and in figure 11 for platinum. As you can see from both of the results, forecasting

with VARFIMA model have performed extremely well with respect to ARFIMA model of the raw data for the same time frame chosen.

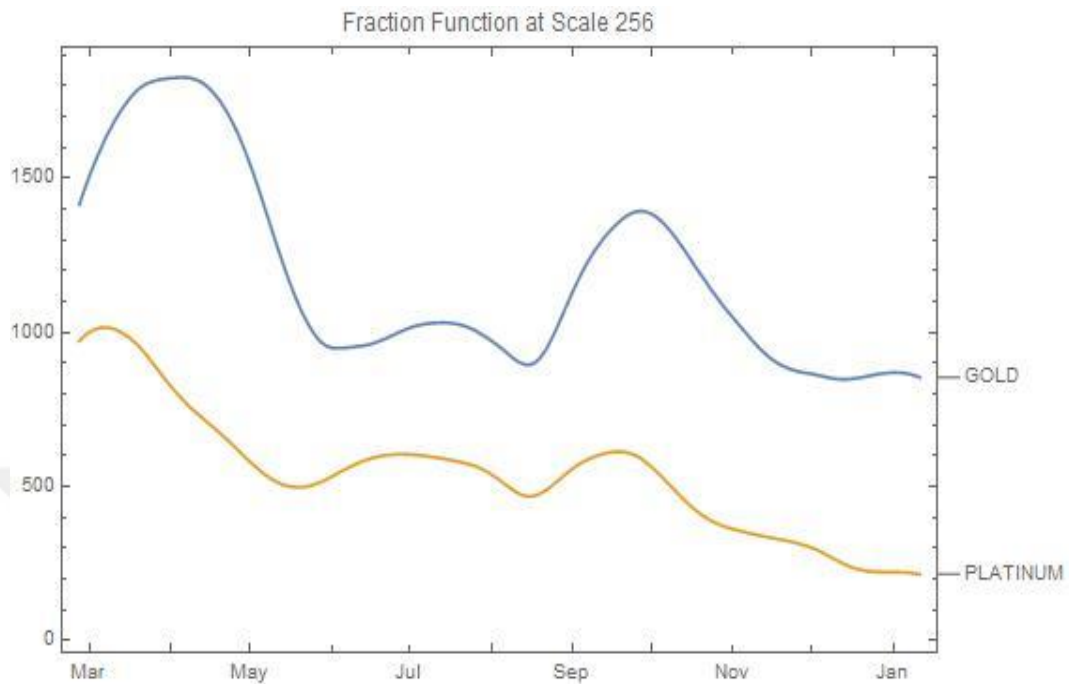


Figure 4.9. Gold and platinum data at Scale 256 from February 25th, 2011 to January 11th, 2012

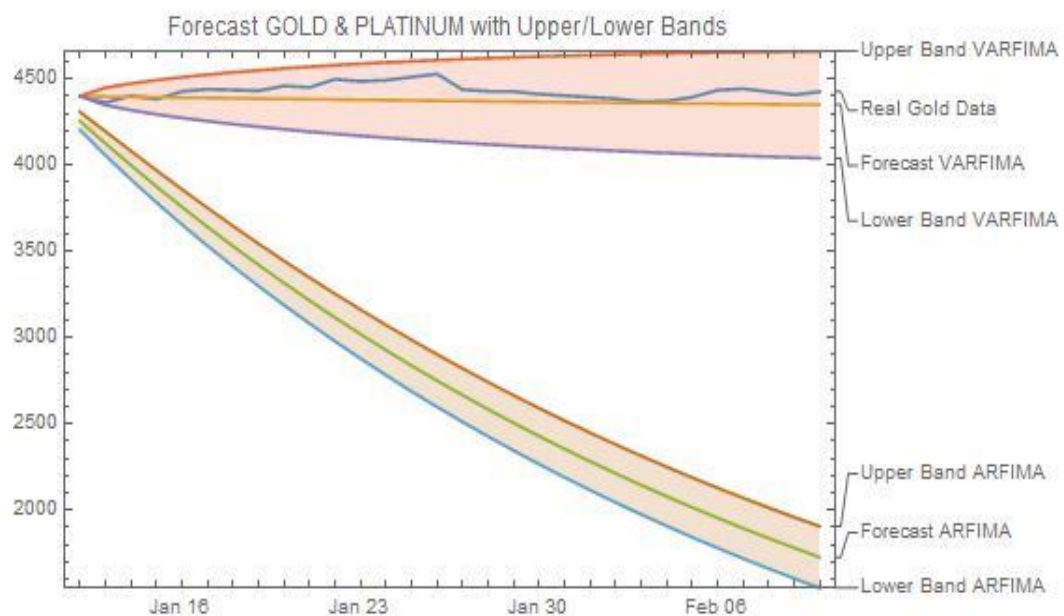


Figure 4.10. Forecasting for gold with platinum starting from January 11, 2012 for the next 30 days

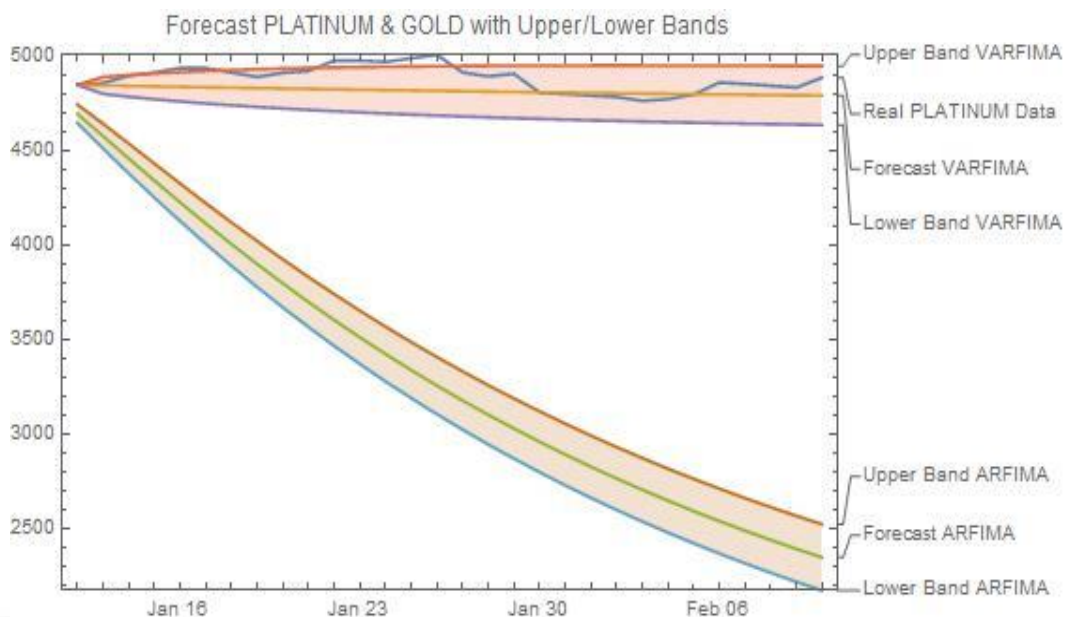


Figure 4.11. *Forecasting for platinum with gold starting from January 11, 2012 for the next 30 days*

This has been the case for all couples chosen. ARFIMA (univariate model) have been used with the raw data itself and VARFIMA (multivariate model) have been used with the fluctuation function time series provided out of local Hurst exponent calculations. It is shown that VARFIMA has provided better forecasting results with respect to its counterpart. Despite of the fact that some of the ARFIMA models have given smaller root mean error values, they were off the charts and still have shown a decreasing trend in all of the results. In all of the forecasting results with the use of VARFIMA model, the estimated function was able to follow an approximate path with the real data. It is also seen that the narrower range of prediction and lower root mean square error in the estimated models are achieved with the increased rate of correlation of the series.

4.5. Concluding Remarks

Multiple wavelet coherence and multifractal de-trended fluctuation analysis (two important tools in the analysis of financial time series) have been employed to explore

the inter dependency and multifractality of precious metals, gold, silver and platinum. Firstly, it is presented that multiple wavelet coherence provides higher resolution to visualize in-phase movement of different time series in time and frequency space compared to any other traditional correlation function analysis (Oral and Unal, 2017). The direct observation allowed us to conclude that all three metals are highly correlated at higher periods throughout the time, especially around 256 day period.

We have observed that long range dependence is weaker over certain periods of time and frequency, which might be due to asymmetric error-correction mechanisms between precious metal prices during shocks or stresses. This could mean that it would take time at different rates for all metal prices to find equilibrium. This is parallel with the findings of Kucher and McCoskey (2017) whom stated that the long run relationships between precious metals are strongly influenced by economic conditions.

Compared to univariate counterparts (ARFIMA), it is depicted that the consistency and performance of forecasting with multifractal time series is remarkably increased with multivariate models (VARFIMA) (Durr et al., 1997). This was also true in spite of the size of the data set chosen (Dueker and Startz, 1998) where we have used set of data from 300 daily prices up to 1100 daily prices.

The generalized Hurst exponents of all precious metals have revealed that daily prices of precious metals do possess long range dependence with persistent structure and demonstrate multifractal behavior in general. Furthermore, local Hurst exponents of precious metals at 256 day period turned out to be multifractal as well. We realized that local Hurst exponents are at the higher portion of the scale during their latest times. It indicates a strengthening trend in long range dependence with persistent

structure (Ihlen, 2012) which in return means that the periods do not experience large variations and the prices are evolving in slower pace.

A new fluctuation function time series is generated during the calculations of local Hurst exponents. These fluctuation function time series are used to model and forecast the data for the next 30 days. Even though both of the methods (ARFIMA and VARFIMA) are adopted to integrate time series into the model fractionally and all series demonstrate multi fractal behavior, ARFIMA model almost never produced forecasting results as successful as VARFIMA model which have outperformed its univariate match conspicuously.

Appendix A. Forecasting results

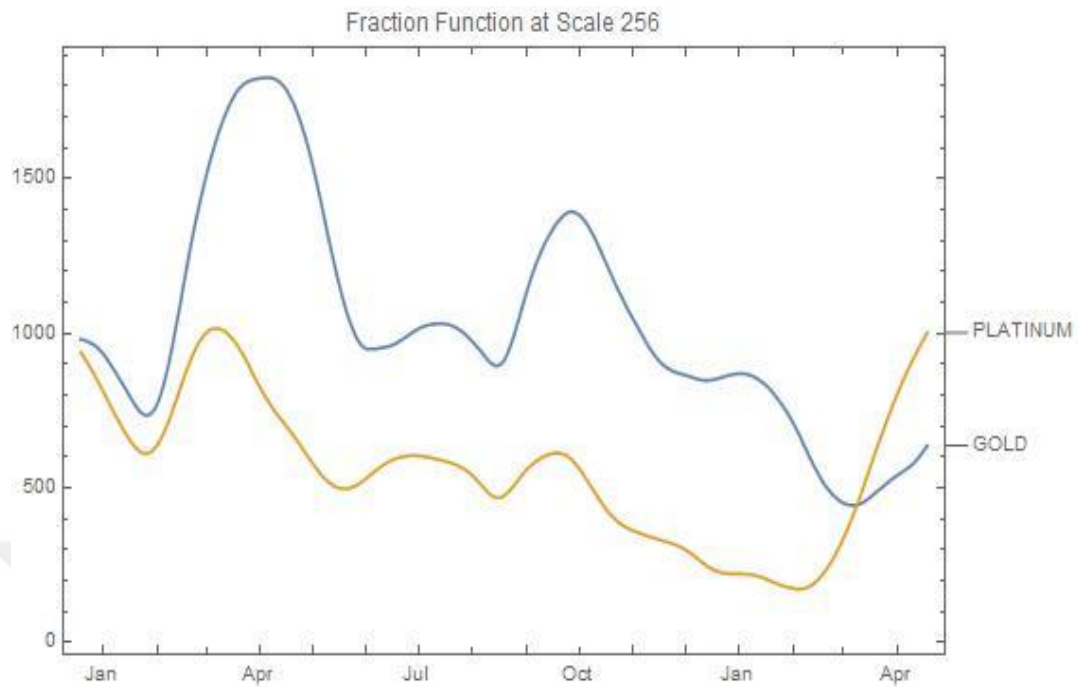


Figure 4.12. Gold and platinum data at Scale 256 from December 19th, 2011 to April 18th, 2012

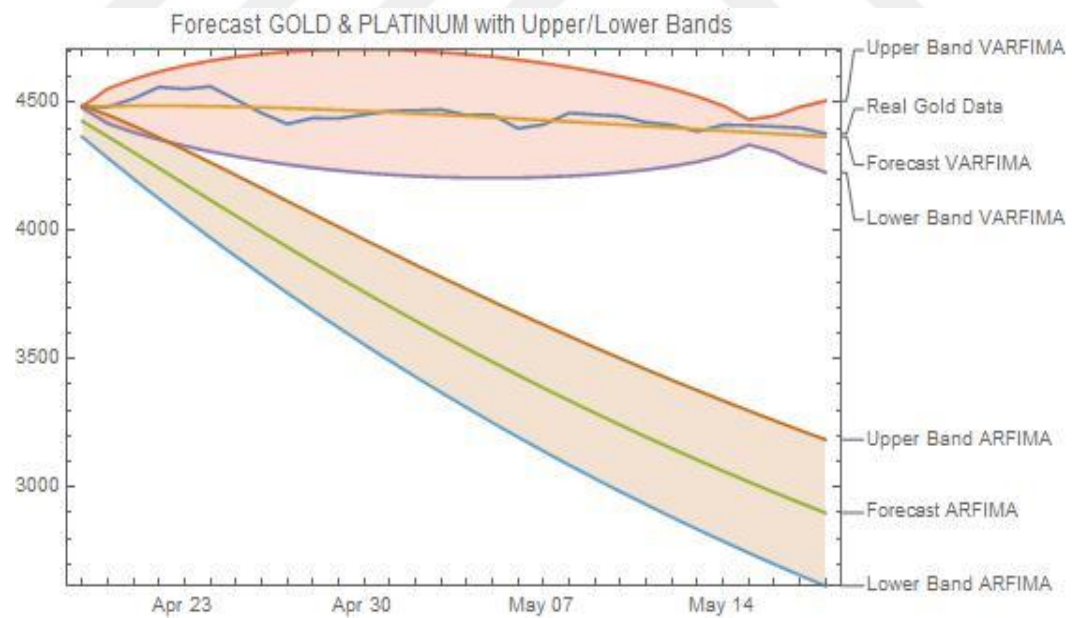


Figure 4.13. Forecasting for gold with platinum starting from April 18th, 2012 for the next 30 days

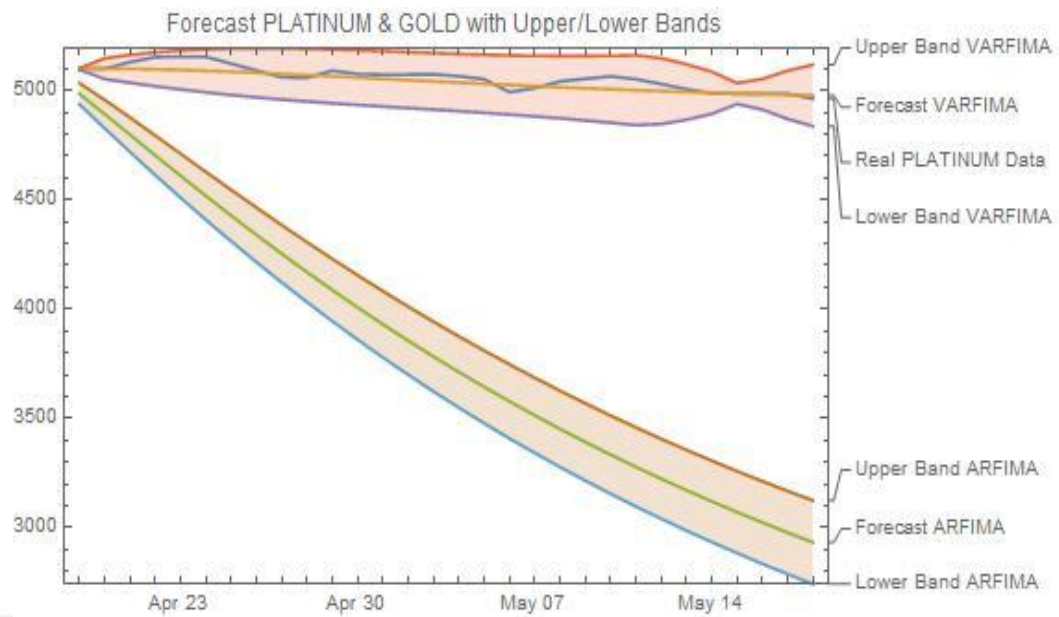


Figure 4.14. Forecasting for platinum with gold starting from April 18th, 2012 for the next 30 days

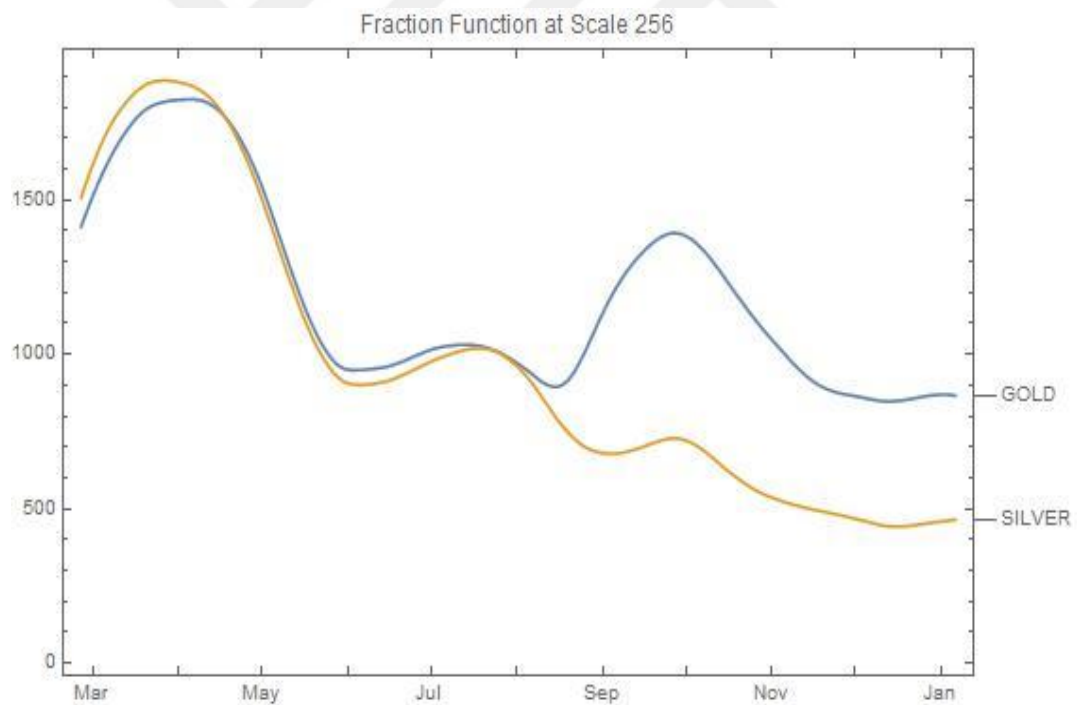


Figure 4.15. Gold and silver data at Scale 256 from 25th February 2011 to January 6th, 2012

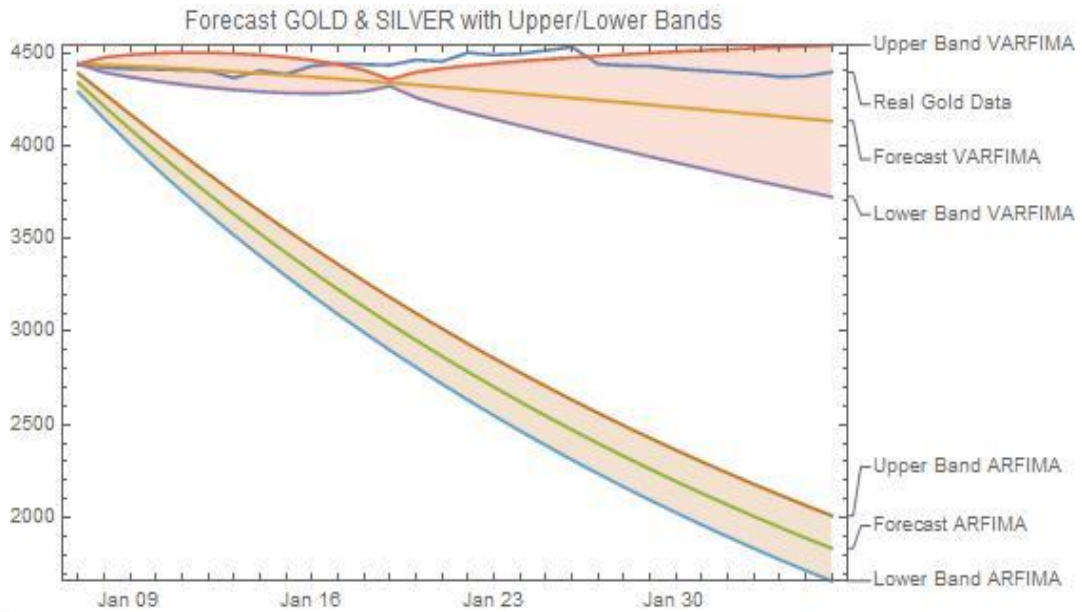


Figure 4.16. Forecasting for gold with silver starting from January 6th, 2012 for the next 30 days

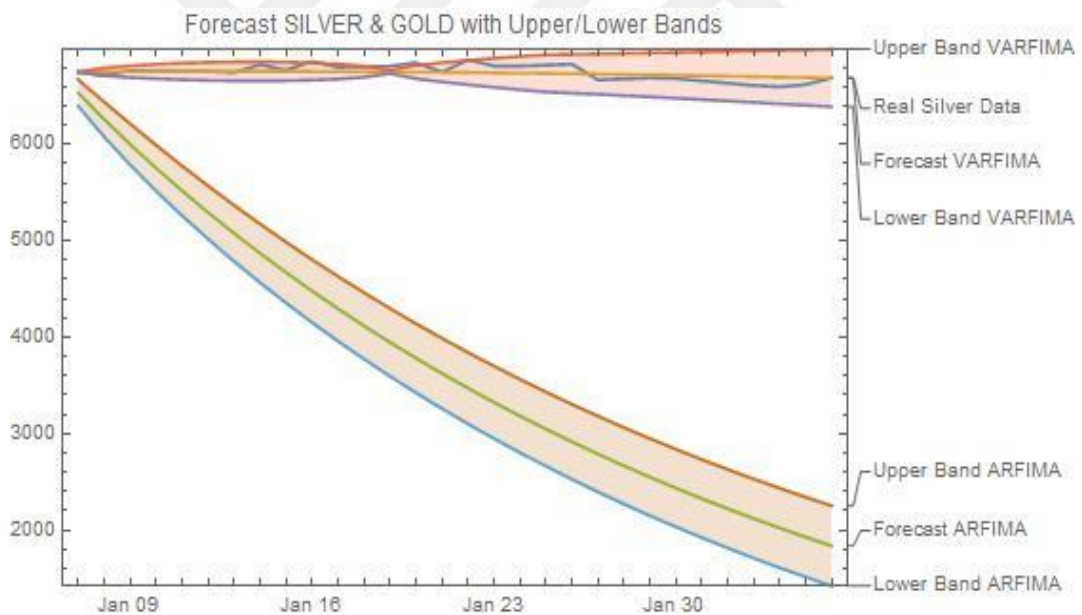


Figure 4.17. Forecasting for silver with gold starting from January 6th, 2012 for the next 30 days

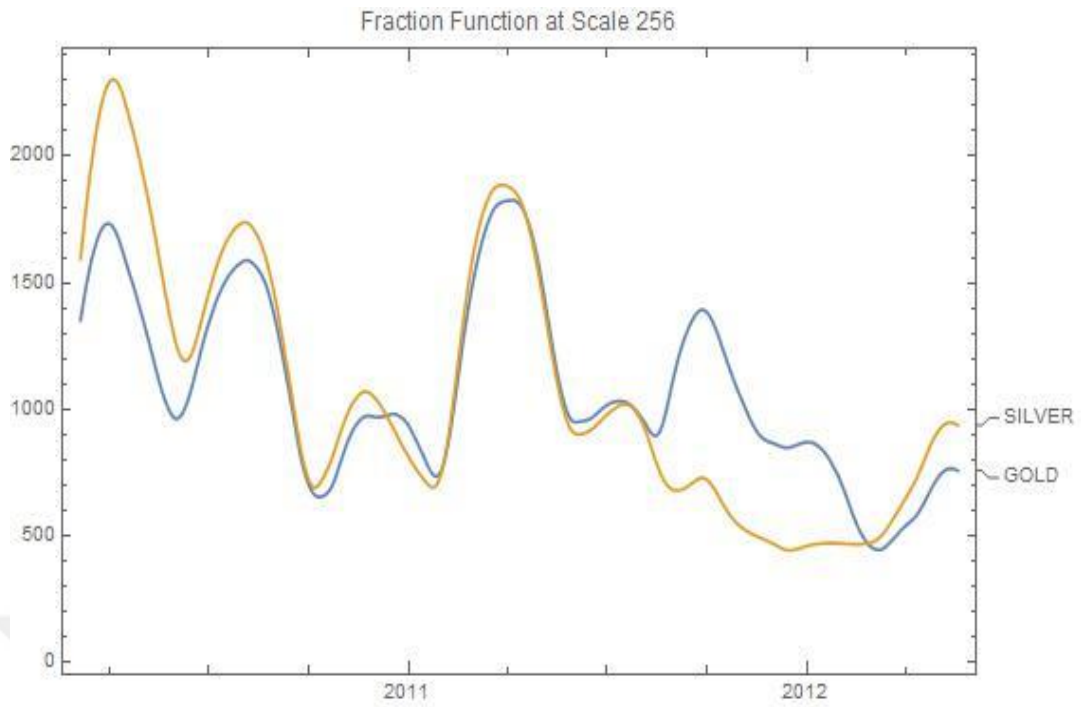


Figure 4.18. Gold and silver data at Scale 256 from March 6th, 2010 to May 18th, 2012

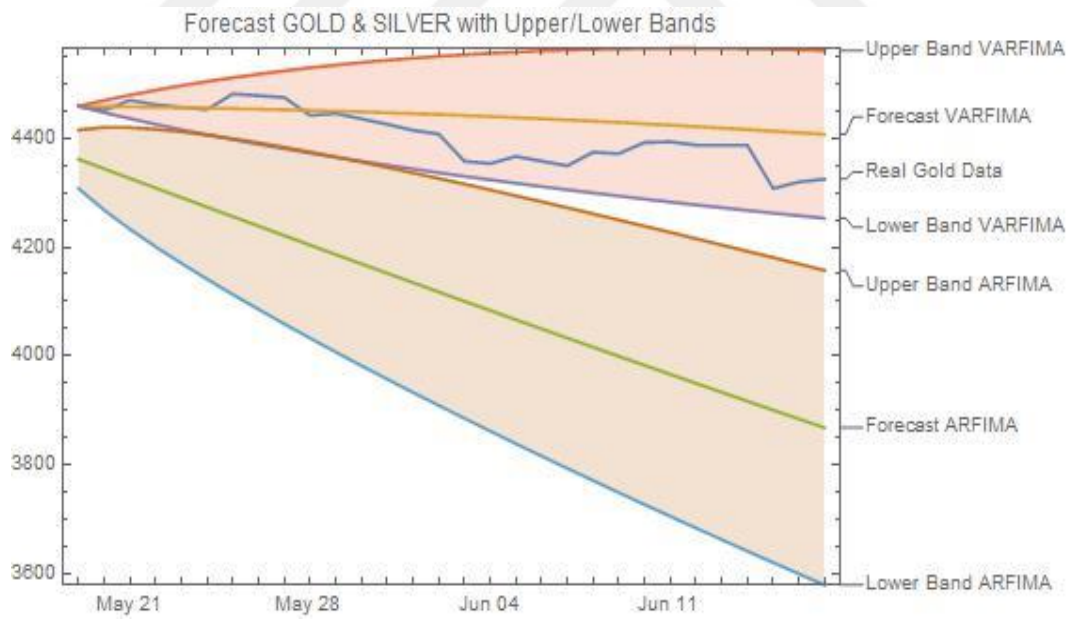


Figure 4.19. Forecasting for gold with silver starting from May 18th, 2012 for the next 30 days

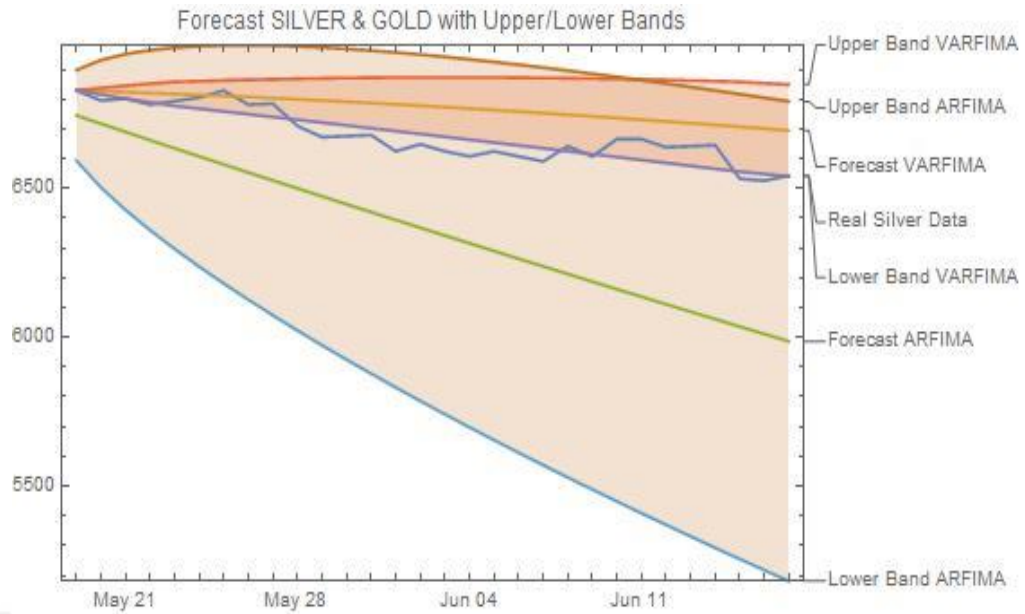


Figure 4.20. Forecasting for silver with gold starting from May 18th, 2012 for the next 30 days

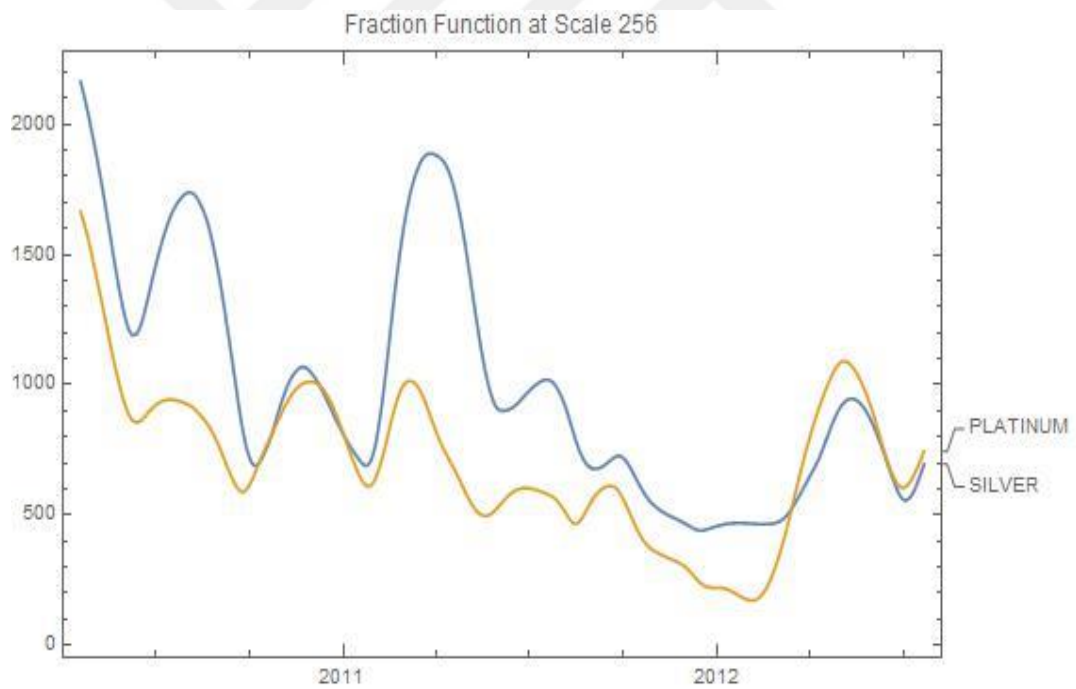


Figure 4.21. Silver and platinum data at Scale 256 from April 19th, 2010 to July 21st,

2012

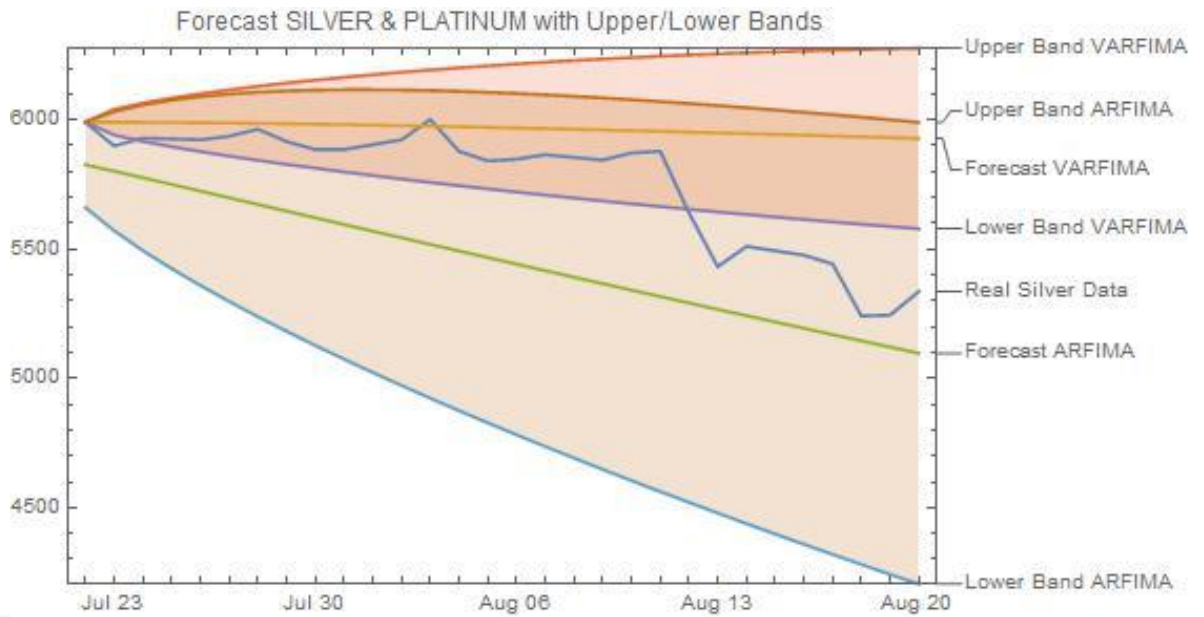


Figure 4.22. Forecasting for silver with platinum starting from July 21st, 2012 for the next 30 days

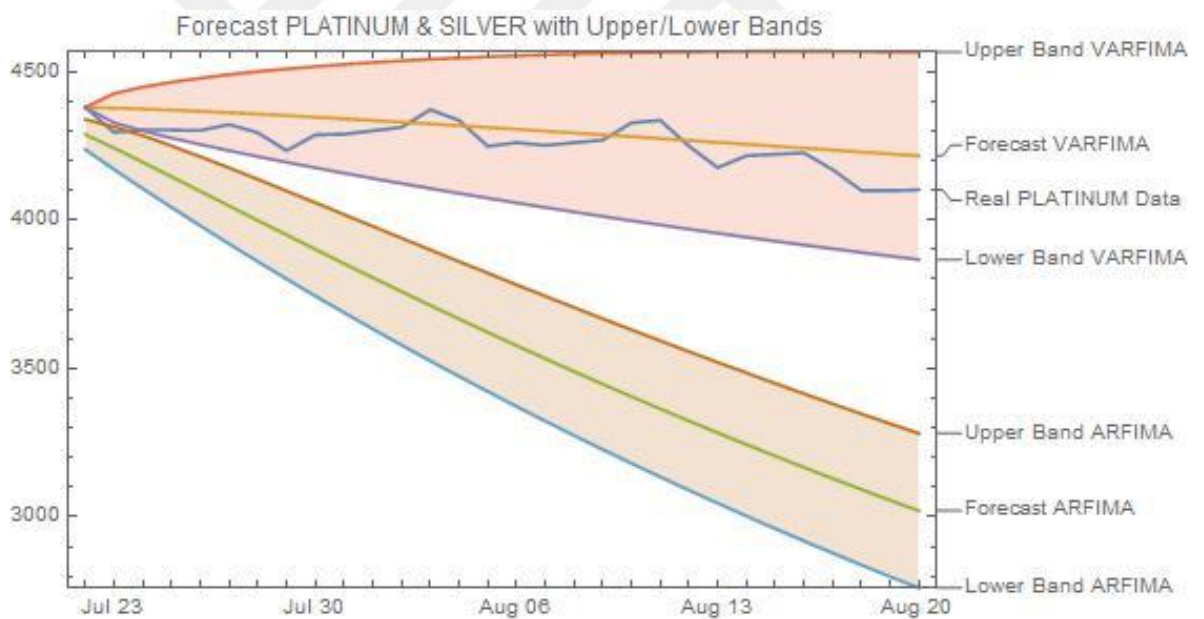


Figure 4.23. Forecasting for platinum with silver starting from July 21st, 2012 for the next 30 days

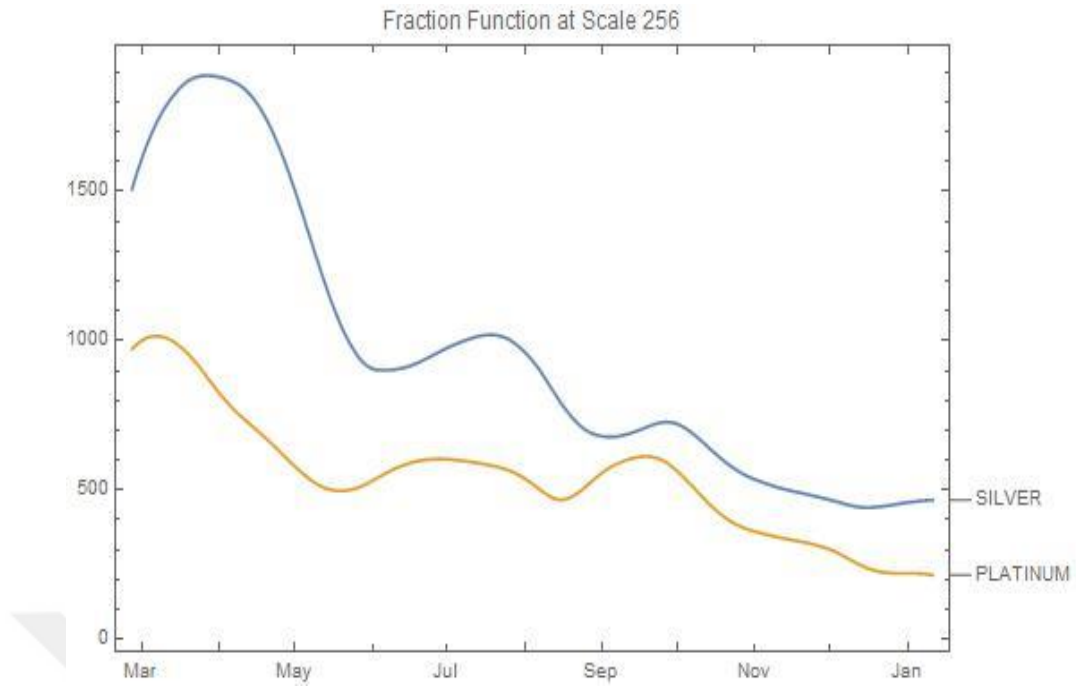


Figure 4.24. Silver and platinum data at Scale 256 from February 25th, 2011 to January 11th, 2012

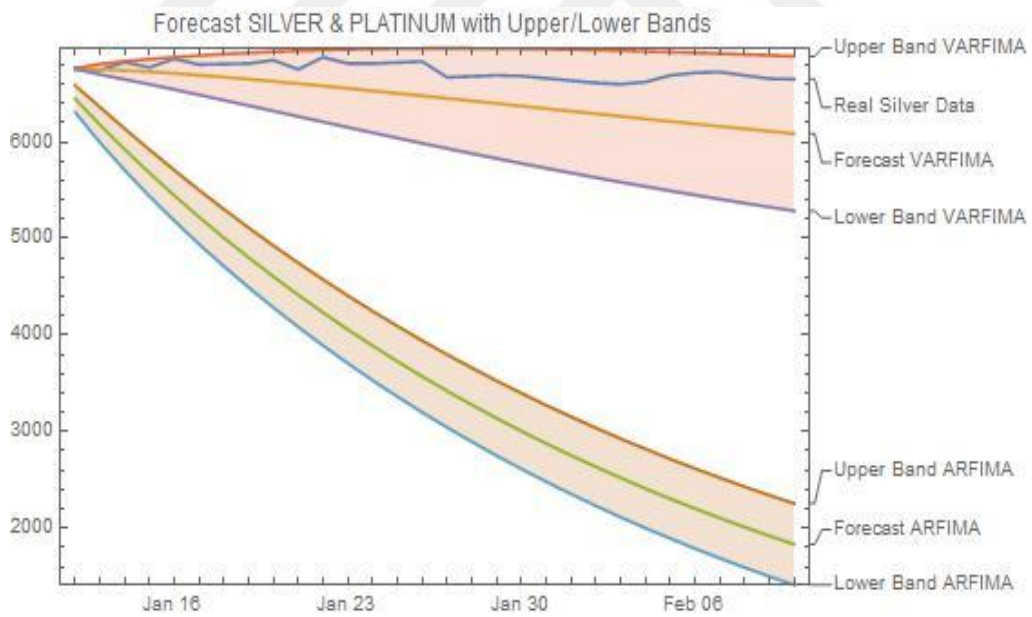


Figure 4.25. Forecasting for silver with platinum starting from January 11th, 2012 for the next 30 days

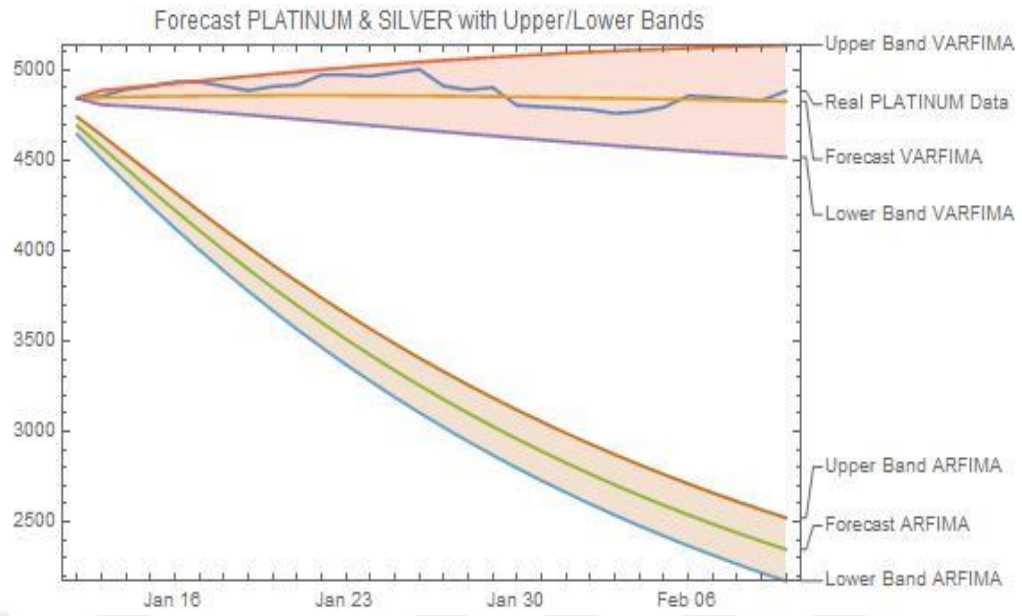


Figure 4.26. *Forecasting for platinum with silver starting from January 11th, 2012 for the next 30 days*

Appendix B. Hurst Exponents for Real and Scale 256 Data

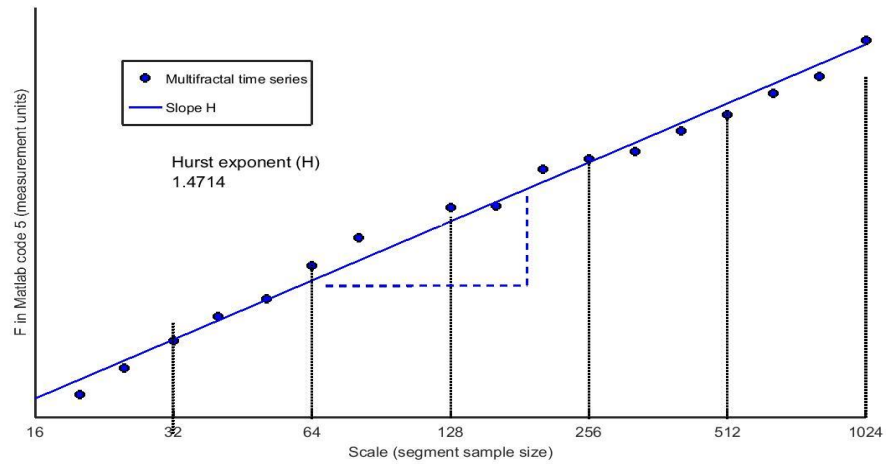


Figure 4.27. Log-log plot of platinum real data ($H=1.4714$)

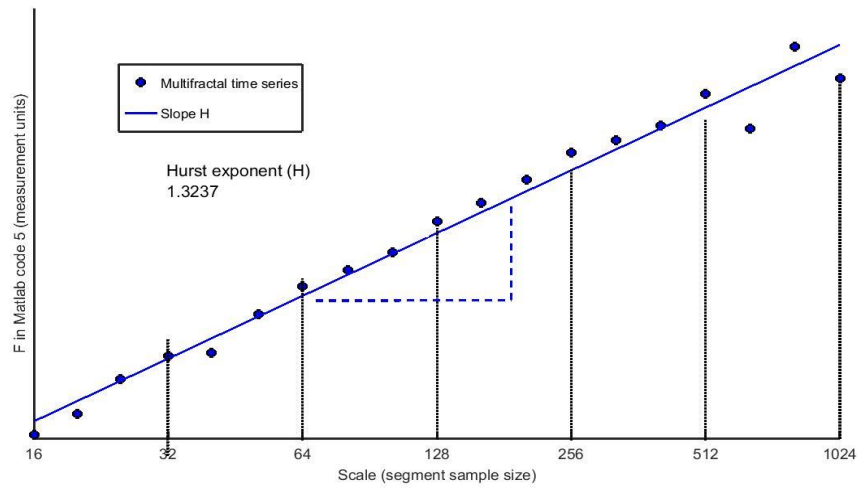


Figure 4.28. Log-log plot of platinum data at scale 256 ($H=1.3237$)

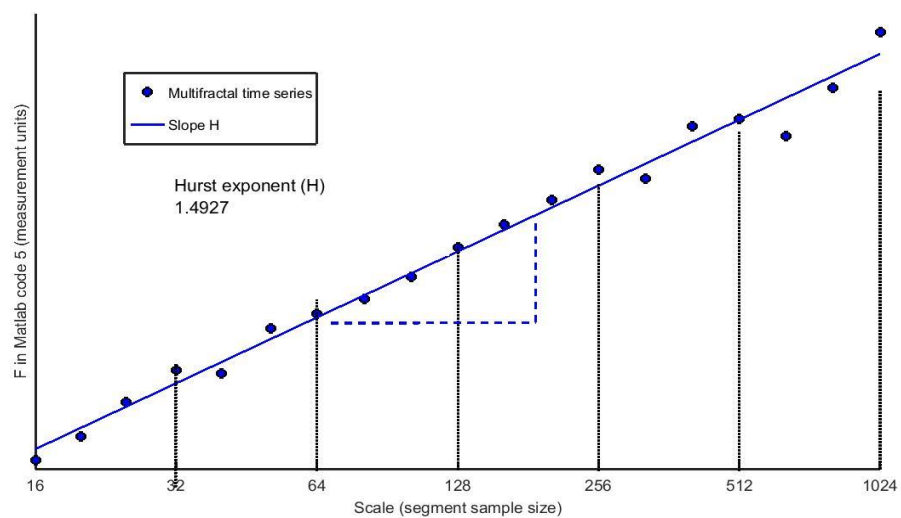


Figure 4.29. Log-log plot of silver real data ($H=1.4927$)

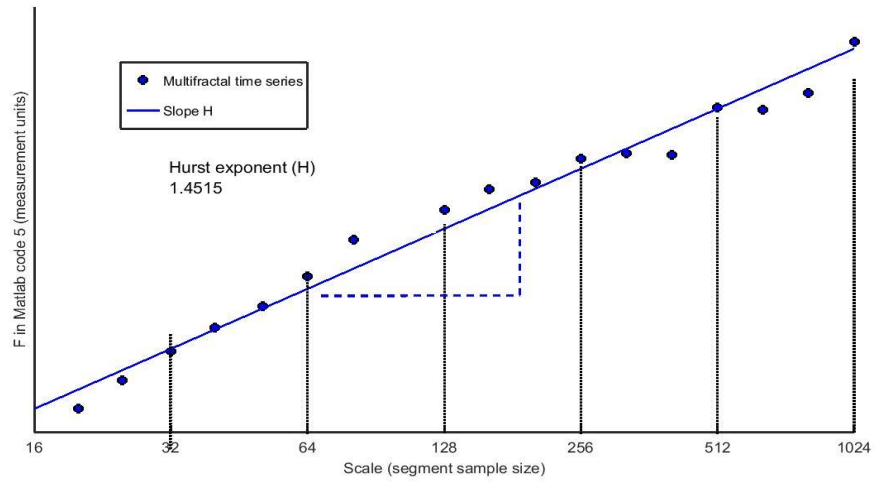


Figure 4.30. *Log-log plot of silver data at scale 256 ($H=1.4515$)*

Appendix C. Local Hurst Exponents

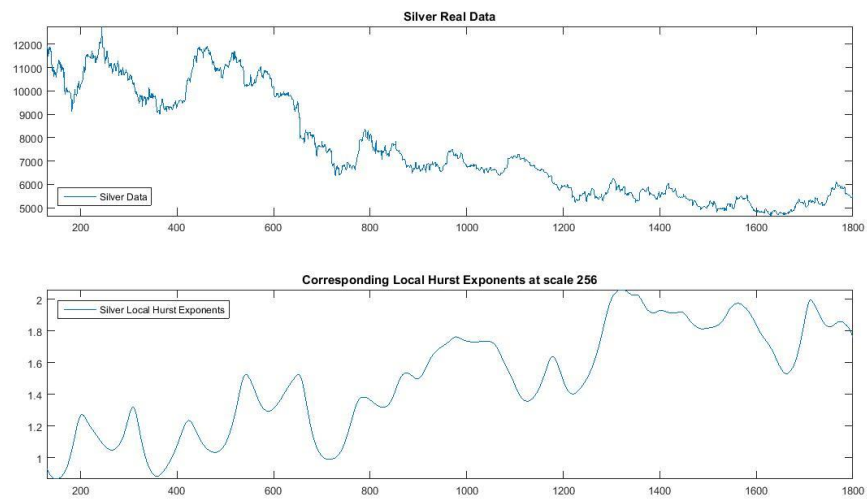


Figure 4.31. *Silver local Hurst exponents at Scale 256-day period*

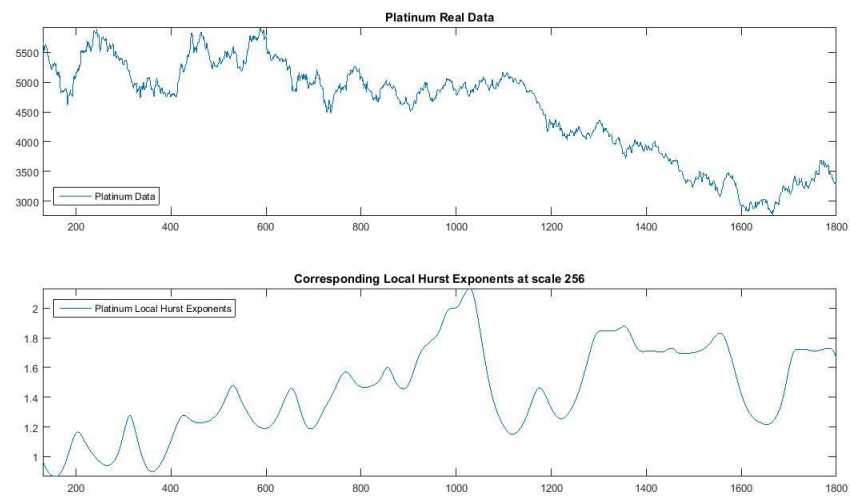


Figure 4.32. *Platinum local Hurst exponents at scale 256-day period*

References

- Aguiar-Conraria L. and Soares M. J. (2012): The continuous wavelet transform: A primer, *NIPE Working Paper No. 16/2011*, University of Minho, 1–43.
- Aguiar-Conraria L. and Soares M. J. (2013): The continuous wavelet transform: Moving beyond uni- and bivariate analysis. *Journal of Economic Surveys*, 28(2): 344–375.
- Akaike H. (1974): Stochastic theory of minimal realization. *IEEE Transactions on Automatic Control*, AC-19: 667-674.
- Athanasopoulos, G. and Vahid, F. (2008). "VARMA versus VAR for Macroeconomic Forecasting". *Journal of Business & Economics Statistics*, April 2008, vol. 26, No.2
- Barunik J., Kocenda E and Vacha L (2013): Gold, oil, and stocks, Preprint, arXiv: 1308. 0210 [q-fin.ST].
- Benbachir S., Alaoui M. H. (2011): A multifractal detrended fluctuation analysis of the Moroccan Dirham with respect to the US dollar. *International Economics and Finance Journal*, 6(2): 287-300
- Bhatia V., Das D, Tiwari A. K., and Shahbaz M. (2018): Do precious metal spot prices influence each other? Evidence from a nonparametric causality-in-quantiles approach. *Resources Policy*, 55: 244-252
- Box-Steinensmeier J. M., Tomlinson A. R. (2000): Fractional integration methods in political science. *Electoral Studies*, 19: 63-76.
- Burrus C. S., Gopinath R. A. and Guo H. (1998): *Introduction to Wavelets and Wavelet Transforms - A Primer*. Prentice Hall, New Jersey.
- Carriero, A., Kapetanios, G. and Marcellino, M. (2008). Forecasting with Dynamic Models using Shrinkage-based estimation ". *Queen Mary University of London – Working Paper no. 635*.
- Cha, B. and Y.-L. Cheung (1998). The impact of the US and the Japanese equity markets on the emerging Asia-Pacific equity markets, *Asia-Pacific Financial Markets*, 5, 191-209.
- Clarke H. D., Lebo M. (2003): Fractional (co)integration and government party support in Britain. *British Journal of Political Science*, 33:283-301.
- Conraria, L. A., & Soares, M. J. (2011). The continuous wavelet transform: A primer. *NIPE Working Paper*, 16, 1-43.
- D. Peña and I. Sánchez, Measuring the advantages of multivariate vs. Univariate forecasts, *J. Time Series Anal.* 28(6) (2007) 886–909.

- De Mol, C., Giannone, D. and Reichlin, L. (2006). Forecasting using a large number of predictors: is Bayesian regression a valid alternative to principal components?". *C.E.P.R. Discussion Paper No. 5829*.
- Dias, GF and G Kapetanios (2011). Forecasting medium and large datasets with vector autoregressive moving average (VARMA) models, *CREATES Research Paper, School of Economics and Management, University of Aarhus*.
- Dick O. E. and Mochovikova I. A. (2011): Multifractal and wavelet analysis of epileptic seizures. *Chaos Theory*, 159-166.
- Doan, T., Littermann, R. and Sims, C. (1984). Forecasting and Conditional Projection using Realistic Prior Distributions". *Econometric Reviews*, 3, 1-100.
- Dueker M., Startz R. (1998): Maximum-likelihood estimation of fractionally cointegration with an application to U.S. and Canadian bond rates. *Review of Economics and Statistics*, 80: 420-426.
- Dunsmuir W. T. M. and Hannan E. J. (1976): Vector linear time series models. *Advances in Applied Probability*, 8: 339-364.
- Durr R. H., Gilmour J. B. and Wolbrecht C. (1997): Explaining congressional approval. *American Journal of Political Science*, 41: 175-207.
- Gencay R. (2002): Discrete Wavelet Transforms, An Introduction to Wavelets and Other. *Filtering Methods in Finance and Economics*.
- Graham, M., Kiviaho, J. and Nikkinen, J. (2012). Integration of 22 Emerging Stock Markets: A Three-Dimensional Analysis. *Global Finance Journal*, 23(1), pp. 34-47.
- Graham, M., Kiviaho, J. and Nikkinen, J. (2013). Short-term and Long-term Dependencies of the S&P 500 Index and Commodity Prices. *Quantitative Finance*, 13(4), pp. 583-592.
- Graham, M. and Nikkinen, J. (2011). Co-Movement of the Finnish and International Stock Markets: A Wavelet Analysis. *The European Journal of Finance*, 17(5-6), pp. 409-425.
- Grinsted J., Moore C. and Jevrejeva S. (2004): Application of the cross wavelet transform and wavelet coherence to geophysical time series. *Nonlinear Processes in Geophysics*, 11(5/6): 561-566.
- Gülerce M. and Ünal G (2016): Using wavelet analysis to uncover the co-movement behavior of multiple energy commodity prices. *International Journal of Wavelets, Multiresolution and Information Processing*, 1650047.
- Hannan E. J. (1981): Estimating the dimension of a linear system. *Journal of Multivariate Analysis*, 11: 459-473.

- Haven E. (2012): De-noising option prices with the wavelet method. *European Journal of Operational Research*, 20121001
- He K., Chen Y. and Tso G. K. F. (2017): Price forecasting in the precious metal market: A multivariate EMD denoising approach. *Resources Policy*, 54: 9-24.
- Hyde, S., Bredin, D., and Nguyen, N., McKenzie, M., and Kim, S.-J. (2007). Correlation Dynamics between Asia-Pacific, EU and US Stock Returns. In *Asia-Pacific Financial Markets: Integration, Innovation and Challenges*, *International Finance Review* Vol. 8, pp. 39-61,.
- Ihlen E. (2012): Introduction to multifractal detrended fluctuation analysis in Matlab. *Frontiers in Physiology*.
- Janakiraman, S. and Lamba A. (1998). An empirical investigation of linkages between Pacific Basin stock markets, *Journal of International Financial Markets, Institutions and Money*, 8, 155-173.
- Kahraman, E. & Unal, G. (2012). Steel Price Modeling with Levy Process. *International Journal of Economic and Finance Studies*, Vol 4, No 2, 2012 ISSN:1309-8055.
- Kahraman, E., & Ünal, G. (2016). Multiple Wavelet Coherency Analysis and Forecasting of Metal Prices. *arXiv preprint arXiv:1602.01960*.
- Kantelhardt J. W., Zschiegner S. A., Koscielny-Bunde E., Havlin S., Bunde A. and Stanley H. E. (2002): Multifractal Detrended Fluctuation Analysis of Nonstationary Time Series. *Physica A*, 316:87-114.
- Klein T. (2017): Dynamic correlation of precious metals and flight-to-quality in developed markets. *Finance Research Letters*, 23: 283-290.
- Kucher O. and McCoskey S. (2017): The long-run relationship between precious metal prices and the business cycle. *The Quarterly Review of Economics and Finance*, 65: 263-275.
- Litterman, R. B. (1985). Forecasting with Bayesian Vector Autoregressions – Five Years of Experience". *Federal Reserve Bank of Minneapolis – Working Paper* 274.
- Loh, L., (2013), Co-movement of Asia-Pacific with European and US stock market returns: A cross-time-frequency analysis, *Research in International Business and Finance*, 29, 1-13
- Lutkepohl, H (2004). Forecasting with VARMA Models, *EUI Working Paper*, Eco No. 2004/25.
- Lutkepohl, H. and Poskitt, D. S. (1996), Specification of echelon-form varma models, *Journal of Business & Economic Statistics*, 14, 69-79.

- Mandelbrot B. B. and Van Ness J. W. (1968): Fractional Brownian motion, fractional noises and its applications. *SIAM Review*, 10(4).
- McCarthy J. and Orlov A. G. (2012): Time-Frequency Analysis of Crude Oil and S&P 500 Futures Contracts. *Quantitative Finance*, 12(12): 1893-1908.
- Ng, E. K., & Chan, J. C. (2012). Geophysical applications of partial wavelet coherence and multiple wavelet coherence. *Journal of Atmospheric and Oceanic Technology*, 29(12), 1845-1853.
- Oral E. and Unal G. (2017): Co-movement of precious metals and forecasting using scale by scale wavelet transform. *International Journal of Financial Engineering*, 4(1): 1750007.
- Oral E. and Unal G. (2017): Dynamic correlation of eastern and western markets and forecasting: Scale-by-scale wavelet-based approach. *International Journal of Financial Engineering*, 4(3): 1750040.
- Peña, D and I Sanchez (2007). Measuring the advantages of multivariate vs. univariate forecasts, *Journal of Time Series Analysis*, 28(6), 886–909.
- Quenouille M. H. (1957): *The Analysis of Multiple Time Series*. London: Griffen.
- Reboredo J. C. and Rivera-Castro M. A. (2014): Gold and exchange rates: Downside risk and hedging at different investment horizons. *International Review of Economics & Finance*, 34: 267–279.
- Rua, A. and Nunes, L.C. (2009). International Comovement of Stock Market Returns: A Wavelet Analysis. *Journal of Empirical Finance*, 16(4), pp. 632-639.
- Simionescu, M (2013). The use of VARMA models in forecasting macroeconomic indicators, *Economics and Sociology* 6(2), 94–102.
- Sowell, F., (1989), Maximum Likelihood Estimation of Fractionally Integrated Time Series Models. Working paper. Carnegie-Mellon University.
- Stock, J. H. and Watson, M. W. (1999). A Comparison of Linear and Nonlinear Univariate Models for Forecasting Macroeconomic Time Series". *International Journal of Forecasting*. Vol. 21, Issue 4, October-December 2005, Pages 781-783.
- Stock, J. H. and Watson, M. W. (2002). \Forecasting Using Principal Components from a Large Number of Predictors". *Journal of the American Statistical association*, 97, No. 460, 1167-1179.
- Tas C. and Unal G. (2013): Multifractal behavior in natural gas prices by using MD-DFA and WTMM methods. *Global Journal of Management and Business Research Finance*, Vol. 13, Issue 11.

- Thompson J. R. and Wilson J.R. (2014): Multifractal detrended fluctuation analysis: practical applications to financial time series. *NC State University*.
- Torrence, C., & Compo, G. P. (1998). A practical guide to wavelet analysis. *Bulletin of the American Meteorological society*, 79(1), 61-78.
- Torrence A C. and Compo G. P. (1998): A practical guide to wavelet analysis. *Bulletin of the American Meteorological Society*, 79(1): 61-78.
- Tsay, R. S. (2013): Multivariate Time Series Analysis: With R and Financial Applications. *Wiley Sons in Probability and Statistics*, Wiley, New York.
- Tsay, W., (2012), Maximum likelihood estimation of structural VARFIMA models, *Electoral Studies*, 31, 852-860.
- Yilmaz A. and Unal G. (2016): Co-movement analysis of Asian stock markets against FTSE100 and S&P 500: Wavelet based approach. *International Journal of Financial Engineering*, 4(4): 1650033.
- Zhang X., Zeng M., and Meng Q. (2017): Asymmetric Multiscale Multifractal analysis of wind speed signals. *International Journal of Modern Physics C*, 28(11):1750137

